HOKKAIDO UNIVERSITY

Title	Studies on the molecular mechanism involved in the second growth of potatoes using microtubers
Author(s)	張, 霞
Degree Grantor	北海道大学
Degree Name	博士(農学)
Dissertation Number	甲第16035号
Issue Date	2024-06-28
DOI	https://doi.org/10.14943/doctoral.k16035
Doc URL	https://hdl.handle.net/2115/92760
Type	doctoral thesis
File Information	ZHANG_XIA.pdf

Hokkaido University Collection of Scholarly and Academic Papers : HUSCAP

Studies on the Molecular Mechanism Involved in the Second Growth of Potatoes Using Microtubers

(マイクロチューバーを用いたジャガイモの二次生長に関わる分子機構の研究)

令和６年度 博士後期課程
北海道大学大学院農学院
農学専攻
生産フロンティアコース
作物生産生物学ユニット
作物生理学研究室
張霞

【Acknowledgments】

This study was conducted in the Laboratory of Crop Physiology at the Hokkaido University Graduate School of Agriculture while the author was a doctoral student in the Department of Crop Physiology, Frontier Production Course, Hokkaido University Graduate School of Agriculture. The author now knows just how important support, critical advice, and professional assistance could be in scientific research such as this study. Here is the list of names of supporters for this study, let the author assure you, that these people have faces covered with sweat because of the help they generously gave to the author. Their support should be reflected in all the help the author received from them.

The author would like to express her sincere gratitude to Dr. Hanako Shimura, a Professor at the Graduate School of Agricultural Science, Hokkaido University, for her kind guidance and assistance in conducting this research. As well as Dr. Yusuke Ohba, Professor; Dr. Yoichiro Fujioka, Associate Professor; Dr. Maho Amano, Specially Appointed Associate Professor; and Dr. Ayaka Kashiwagi, Assistant Teacher, at the Department of Cell Physiology, Graduate School of Medicine, Hokkaido University, who offered helpful advice on the manuscript as it processed and supported the author in a thousand different ways. The staff and associates with the author, Dr. Aya Satoh, Dr. Tomoko Kamazaki, Ms. Takako Saeki, Ms. Chiharu Sakai, Ms. Yue Komatsu, and other seniors at the Department of Cell Physiology, Graduate School of Medicine, Hokkaido University, gave their support not only in academics but also in day life in Japan during the final written working of this study.

Specifically, the instructor of the author, Dr. Kaien Fujino, Professor of the Graduate School of Agricultural Science, Hokkaido University, first convinced the author of the value of this study, enthusiastically suggested the author pursue this research, and helped to sharpen skills of the author. Graciously read early versions of the manuscript and the final manuscript and offered helpful suggestions. Dr. Kaien Fujino deserves the deepest gratitude of the author.

Finally, the author wants to humbly thank her family, close friends, and the students in the Crop Physiology Laboratory for their support, who gave the author the grace to see this study through to the end.

【CONTENTS】

General Introduction 3

Chapter 1 in vitro Induction of Secondary Growth and Secondary Hypertrophy 8

1.1 Introduction 8

1.2 Plant Materials and Methods 9

1.2.1 Plant Materials 9

1.2.2 Micropropagation of Shoot Plantlets 9

1.2.3 Induction of Microtuber Formation 15

1.2.4 Induction of Microtuber Chain Formation 19

1.2.5 Experimental Design and Statistical Analysis 22

1.3 Results 23

1.3.1 Effect of GA on Dormancy-breaking of Axillary Buds 23

1.3.2 Effect of Ancymidol on Formation of Microtubers 25

1.3.3 Effect of Incubation Periods with GA Pretreatment on Formation of Microtuber Chains 28

1.3.4 Effect of Pretreatment with Plant Hormones on Formation of Microtuber Chains 32

1.4 Discussion 36

Chapter 2 in vitro Induction of Secondary Growth and Microtuber Sprouting 38

2.1 Introduction 38

2.2 Plant Materials and Methods 38

2.2.1 Plant materials 38

2.2.2 Preparation of Secondary Growth Microtubers 39

2.3 Results 41

2.3.1 Response of Microtuber to the Exogenous GA Treatment Alone 41

2.3.2 Response of Microtuber to the Exogenous CK Treatment Alone 43

2.3.3 Response of Microtuber to Both GA and CK Treatment 45

2.4 Discussion 47

Chapter 3 Transcriptomic Analyses of Microtuber Sprouting Response to Phytohormone Treatments 50

3.1 Introduction 50

3.2 Plant Materials and Methods 51

3.2.1 Plant Materials 51

3.2.2 Preparation of Secondary Growth Microtubers 51

3.2.3 RNA Extraction and Sample Preparation 52

3.2.4 TPM Value Calculation and Differential Expression 55

3.2.5 Module Construction using WGCNA Package 55

3.2.6 Quantitative Analysis of Candidate Genes Involved in Potato Microtuber Sprouting 56

3.2.7 Quantification and Statistical Analysis 58

3.3 Results 59

3.3.1 Response of Microtuber Sprouting to Phytohormone Treatment 59

3.3.2 Transcriptome Sequencing and de novo Assembly 65

3.3.3 Differential Transcriptome Response to Exogenous Hormone Treatments 68

3.3.4 Weighted Gene Co-expressed Gene Network Analysis (WGCNA) 73

3.3.5 Cytokinin- and Auxin-activated Signaling are Involved in Microtuber Sprouting 80

3.3.6 The Effect of GA on Microtuber Sprouting in the Absence of Nodal Stem 88

3.3.7 The Effect of Nodal Stem on GA-induced Microtuber Sprouting 90

3.3.8 The Effect of CK on Microtuber Sprouting 99

3.3.9 Genetic Analysis of Microtuber Sprouting Response to GA and Both GA and CK 107

3.3.10 Correlations of RT-PCR and RNA-seq Datasets 111

3.4 Discussion 113

3.4.1 Response of Microtuber Sprouting to Phytohormone Treatment 113

3.4.2 Regulation of the Phytohormone Signaling Response to Microtuber

Sprouting 114

3.4.3 Regulation of the Cytokinin Homeostasis Response to Sprouting Growth 116

Chapter 4 Transcriptomic Analyses of Microtuber Sprouting Response to Incubation Periods with Gibberellin Treatment 117

4.1 Introduction 117

4. 2 Plant Materials and Methods 118

4.2.1 Plant Materials 118

4.2.2 Preparation of Secondary Growth Microtubers 118

4.2.3 RNA Extraction and Sample Preparation 120

4.2.4 TPM Value Calculation and Differential Expression 120

4.3 Results 121

4.3.1 Transcriptome Sequencing and de novo assembly 121

4.3.2 Differential Transcriptome Response to GA-incubated Periods 124

4.3.3 Plant Hormone Signal Transduction Pathway Response to Apical Bud Tissues 126

4.3.4 Gene Ontology (GO) Terms Response to Apical Bud Tissues 133

4.3.5 Plant Hormone Signal Transduction Pathway Response to Nodal Stem Tissues 143

4.3.6 Zeatin Biosynthesis Pathway Response to Nodal Stem Tissues 150

4.3.7 Gene Ontology (GO) Terms Response to Nodal Stem Tissues 153

4.4 Discussion 161

General Discussion 163

Summary 166

References 170

【Abbreviation】

MT: Microtuber

stMT: stemmed Microtuber (microtuber with the nodal stem attached)

deMT: Destemmed Microtuber (detached the nodal stem from the stMT, but the junction part remained attached to the MT)

hMT: Microtuber half (cut the MT in half along the equatorial plane and entirely remove the nodal stem, including the junction part with MT)

GA: Gibberellin

CK: Cytokinin

BA: 6-benzyladenine, a synthetic CK

GACK: Both Gibberellin and Cytokinin

NAA: Naphthalene-1-acetic acid, a synthetic auxin

ABA: Abscisic Acid

ABF: ABA-responsive bZIP transcriptional factor

PYL4: Pyrabactin resistance 1-like

PP2C: Type 2C protein phosphatase

SnRK2: SNF1 (sucrose non-fermenting 1) -related protein kinases

IAA: Indole-3-acetic acid inducible

SAUR: Small auxin upregulated RNA

GH3: Gretchen Hagen3

Aux/IAA: Auxin/indoleacetic acid

IPT: Isopentenyltransferase

PGSC: The potato genome sequencing consortium

TPM: Transcript Per Million

KEGG: Kyoto Encyclopedia of Genes and Genomes

GO: Gene Ontology

General Introduction

Potato (*Solanum tuberosum* L), belonging to the *Solanaceae*, is the fourth largest crop in terms of production and one of humankind's most utilized and important non-grain food crops in the world (Ezekiel et al., 2013; Joshi et al., 2016; Zhang et al., 2017), which contains a variety of nutrients, including calcium, starch, crude fiber, vitamin C, and various minerals. Potatoes are a representative crop of Hokkaido and are of global importance. The total potato production worldwide is approximately 400 million tons per year (Celik et al., 2019). The edible part of the potato is the tuber, the enlarged tip of the underground stem.

The process of tuber initiation begins in the subapical zone of the stolon, and the hypertrophy of the tuber occurs progressively in the internodes that existed at the time of initiation. The meristematic activity in the stolon apex ceases as tuber hypertrophy occurs. Potato is propagated in cultivation by nutrients using underground stems (called stolons). Potato tubers undergo endogenous dormancy immediately after harvest, which, in fact, parallels tuber enlargement during formation. The apical and subapical meristems (also known as eyes) of tubers become endo-dormant and cannot sprout due to internal physiological factors. Tubers are physiologically competent to sprout after a certain period, usually for one month or more, and finish endogenous dormancy (Hemberg, 1985; Suttle, 2007). In this article, the term dormancy refers to the endogenous dormant state unless specified otherwise. But before harvest, potato tubers attached to the above-ground part may undergo sprouting called secondary growth, depending on the growing environment. Rising temperatures during tuber growth can cause a temporary break in tuber dormancy (Peivastegan et al., 2019), leading to a temporary tuber-sprouting called secondary growth. When sprouts of secondary growth go dormant again, these sprouts can form secondary tubers, resulting in hump-shaped, malformed tubers, which were defined as secondary hypertrophy (**Figure 1**). Potato tubers can be negatively affected by secondary growth and secondary hypertrophy, especially secondary growth, which is a common issue in potatoes, including sprouting, tuber chaining, and tuber malformations which reduce the tuber starch content, yield, and seed quality, ultimately diminishing commercial value (Jefferies and Mackerron, 1987). Potato is used as an annual crop in agriculture and is usually propagated using seed tubers. Tuber growth-related signaling is

transferred from leaves to underground stolons during tuber development (Bhogale et al., 2014; Zhang et al., 2020).



Figure 1. Representative images of the secondary hypertrophy of tuber in Solanum tuberosum L. ssp. andigena.

This was a case of secondary hypertrophy observed during the 2020 harvest season in our lab. The actual cause of the situation remains unknown, but it is believed to be due to high temperatures during the tuber formation period. Bar = 10 mm.

This is thought to be due to the fact that not only the tuber but also the plant body is influenced by the environment. Transporting signal substances to the tubers, such as gibberellin (GA) which is known as a dormancy-breaking hormone, can terminate dormancy and trigger tuber sprouting (Rappaport, 1956). The exact ways in which viroids cause disease symptoms are not yet fully comprehended, but it has been noticed that they can impact the expression of genes responsible for gibberellin synthesis and homeobox, which regulate meristematic tissues in some cases (Flores et al., 2020; Hammond, 2022). Potatoes infected by viroids are variety-dependent, which cannot maintain dormancy during tuber development, resulting in tuber secondary growth and secondary enlargement significantly.

Tubers are formed by axillary buds in the aboveground part, known as aerial tubers. The tuber-forming ability of the shoot-lateral buds has been reported to provide a simple and virus-free experimental system under laboratory conditions (Struik, 2007). Microtubers (MT) created by conventional tissue culture methods are formed by the part of the shoot whose leaves are cut off node by node so as to include lateral buds in vitro (Leclerc, 1993; Yu, 1998). It is easy to remain virus-free, and there is no time constraint on proliferation. This type of propagule is disease and pest-free, which enhances yields significantly (Ahloowalia, 1994). Microtubers and ordinary tubers have almost no difference in biological characteristics other than dimensions (size) and have characteristics such as virus freeness, high yield, and easy storage. MT formation of potatoes is one of the more efficient methods to increase tubers in vitro (Gixhari, 2018).

Various factors, such as growth regulators, mediums, the mixotrophic system, and various cultivars, have led to difficulties in microtuberization. MTs could be generated in the axillary bud in a node segment cut from the shoot in short-day or dark conditions, with a high concentration of sucrose and low temperature; treatments with plant growth regulators, like GA inhibitors or ABA (Ewing, 1985; Tovar, 1985), are also utilized to suppress the activity of GA so that the development can be focused on the hypertrophy of axillary buds (i.e., microtuber formation) rather than shoot growth of axillary buds (Kolachevskaya et al., 2019a; Nuraini et al., 2018).

The dormancy breakage in potato tubers is accompanied by many physiological changes, such as a balance of catabolism and an increase in net DNA and RNA synthesis.

GA has been known to induce growth, and the endogenous GA level increases rapidly toward the end of tuber spontaneous dormancy and the onset of shoot growth (Suttle, 2004b) by shortening the G1 and S phases of the cells (Turnbull and Hanke, 1985b) and activating DNA and RNA synthesis (Burton, 1948). ABA and ethylene suppress tuber sprouting (Sonnewald and Sonnewald, 2014). Ethylene (ET) inhibits tuber sprouting by influencing carbohydrate metabolism, including increased respiration, glucose, total sugar, and reduced fructose and sucrose (Dai et al., 2016). ABA inhibits DNA and RNA synthesis to maintain tuber dormancy until the GA/ABA ratio reaches a point favoring GA, promoting cell division and sprouting (Claassens and Vreugdenhil, 2000). *StTCP15* was reported to promote potato tuber sprouting by regulating the dynamic balance of ABA and GA (Wang et al., 2022), and a high ABA/GA ratio is correlated with dormancy maintenance. In contrast, a low ABA/GA ratio is consistent with dormancy breakage. A low level (<1 mg L^{-1}) of auxin application has a stimulating effect on tuber sprouting, but a high dose suppresses tuber sprouting (Kumar and Knowles, 1993; Suttle, 2003). Auxin distribution in tuber buds could affect the order of sprout appearance (Sorce et al., 2009). An abrupt increase in the concentration of endogenous zeatin (naturally occurring CK) and a reduction in ABA at the onset of dormancy breakage has been observed (Suttle, 2004a). Both natural (such as zeatin) and synthetic CK (such as kinetin and 6-benzyladenine) applications can rapidly trigger tuber sprouting (Hemberg, 1970; Siregar et al., 2021). Remarkably, Hartmann et al. showed that tubers with a decline in CK levels did not respond to GA application by using transgenic potato plants expressing the catabolic cytokinin oxidase/dehydrogenase 1 (CKX1) in vitro assay; in contrast, tubers with an increased CK content promoted GA-induced sprouting by harboring the isopentenyltransferase (*IPT*) gene, suggesting that CK could stimulate the dormancy breakage of the excised tuber buds and GA-induced sprouting (Hartmann et al., 2011).

Transcriptome profiling offers one way to characterize plant responses. The technologies for Next-Generation Sequencing (NGS) are rapidly advancing and bringing about a significant transformation in the field of biological research (Metzker, 2010; Morozova and Marra, 2008). Technologies for analyzing transcriptomes have been available and widely used since the development of microarray technology. Microarray techniques have limited sensitivity, while real-time PCR is expensive and cannot be used for genome-wide gene expression surveys (Mardis, 2008). While NGS provides

inexpensive and quick high-throughput gene expression profiling, genome annotation, and non-coding RNA discovery (Voelkerding et al., 2009). NGS refers to important technological developments based on the sequencing-by-synthesis (SBS) technology known as pyrosequencing. The transcriptomics variant of pyrosequencing is called sequencing-based transcriptome studies (RNA-seq) or short-read massively parallel sequencing (Denoeud et al., 2008; Marguerat and Bähler, 2010). Over the past few years, RNA-Seq has become the most widely used system for quantitatively profiling the transcriptome (Marguerat and Bähler, 2010; Wang et al., 2008). The genome sequences of both potato (Hardigan et al., 2016) and P. *infestans* have been already published (Haas et al., 2009; Xu et al., 2011a), making RNA-Seq a relatively new approach to studying potatoes and more accessible to potato researchers.

The mechanism controlling tuber dormancy and sprouting formation is crucial in the study of potato physiology. However, potatoes are nutritionally bred, homoploid, and heterogeneous in genetic structure, which makes obtaining genetic variants with a significant phenotypic impact take work. My work reproduced the secondary growth of potatoes using tissue culture and comprehensively analyzed the expression of genes involved in this process. I employed RNA-seq to study the mechanisms that affect gene expression and signal transduction involved in tuber sprouting, which is induced by plant hormones, using in vitro microtubers.

Chapter 1 *in vitro* Induction of Secondary Growth and Secondary Hypertrophy

1.1 Introduction

Potatoes have vegetative propagation on a commercial scale (Morais et al., 2018). However, this type of multiplication makes it easy to accumulate several infections, such as systemic virus infection, provoking degeneration in tuber yield and seed (Nikitin et al., 2018). Removing diseases from potato plants can cause significant damage to the crop. This makes using virus-free propagative material important to ensure its maximum yield potential. Meristem culture is a popular technique for plant propagation (Delgado-Paredes et al., 2021). Plant biotechnological techniques (such as *in vitro* plant tissue culture) developed in recent decades are the most critical tools to manipulate plants to exhibit greater productivity, tolerance to physical and chemical stress, and disease resistance. This allows their wide application not only in propagation but also in genetic improvement.

Since then, biotechnologies have been applied to produce *in vitro* potato tuber called microtuber (MT) (Valencia-Lozano et al., 2022), which has advantages in terms of storage, cultivation, and transport due to its reduced size and weight (Donnelly et al., 2003).

Here, I developed a protocol for MT induction and other necessary materials for later experiments using three potato varieties of *Solanum tuberosum*. L ssp. *andigena*, cv. May Queen and Irish Cobbler. This chapter aims to culture explants (shoots containing axillary buds) and tuberization (including deformed tubers, such as tuber chains) using *in vitro* tissue culture for subsequent studies.

1.2 Plant Materials and Methods

1.2.1 Plant Materials

Virus-free potato tubers of *Solanum tuberosum*. L ssp. *andigena*, cv. May Queen and Irish Cobbler plantlets were kindly provided by the Agricultural Research Center.

1.2.2 Micropropagation of Shoot Plantlets

The tubers were immersed in tap water mixed with a few drops of aqueous sodium hypochlorite solution (effective chlorine concentration: 1% (v/v)) to sterilize the surface for 30 minutes, followed by thoroughly rinsing in running water for 10 minutes to remove the remaining of sodium hypochlorite solution, and then kept in the dark at 10 °C for about 4 weeks until sprouting. The tubers were cut off along the tuber medulla (diameter of 2 cm) containing one eye using a cork borer (2 cm in diameter and 3 cm in length) to obtain the cylindrical pieces of tissue (called plugs) (Make sure that the cork borer did not pierce to the opposite side of tuber and the vascular bundle site was not included).

The obtained plugs were placed in a 250 ml capped jar containing about 100 ml of aqueous sodium hypochlorite solution (effective chlorine concentration: 1%) containing a few drops of Tween 20 (0.05%, a spreading agent). 100 mg L^{-1} of penicillin was then added to prevent necrosis and bacterial contamination during sprouting. Then the jar was shaken upside-down for five minutes. The surface-sterilized plugs were picked and rinsed thoroughly in sterile distilled water in a flow cabinet. Plugs were added a few drops of 0.2 M calcium nitrate and 100 mg L^{-1} of penicillin solution to prevent necrosis and bacterial contamination during sprouting and were incubated in the moist chamber at 25 °C in the dark. After one week, a few drops of 0.2 M calcium nitrate solution were dropped from the apical buds of the plugs in a flow cabinet before pericarp formation. After 3-4 weeks, the etiolated shoots that were elongated about 5-7 cm were collected and cut into nodal shoots for micropropagation, which were employed as a source of shoot explants for research.

Etiolated elongated shoots were cut off with razor form tubers, and the healthy single

node shoots (called shoot explants, containing the lateral primordial buds) about 2 cm were cut out to culture subsequently. The obtained shoot explants were placed in a 250 ml capped jar containing about 100 ml of aqueous sodium hypochlorite solution (effective chlorine concentration: 1%) containing a few drops of Tween 20 (0.05%, a spreading agent) to sterilize the surface for 1 hour. The healthy sterilized plugs were picked and rinsed thoroughly in sterile distilled water in a flow cabinet. Both ends of the shoot explants were then aseptically excised with a razor.

The adjusted shoot explants were then placed vertically and evenly in 400 ml culture bottles containing sterile half of MS medium (**Table 1**) (of which inorganic salts are halved) without burying the lateral bud primordia in the medium and grown at 25 °C in the dark (for 3-4 weeks) (**Figure 2**).

Table 1. The composition of MS medium.

Reagent	**mg L^{-1}**
NH_4NO_3	400
KNO_3	1,900
$MgSO_4 \cdot 7H_2O$	370
KH_2PO_4	170
H_3BO_3	6.2
$MnSO_4 \cdot 4H_2O$	22.3
$ZnSO_4 \cdot 7H_2O$	8.6
KI	0.083
$Na_2MoO_4 \cdot 2H2O$	0.25
$CuSO_4 \cdot 5H2O$	0.025
$CoCl_2 \cdot 6H2O$	0.025
$FeSO_4 \cdot 7H2O$	27.85
$Na_2 \cdot EDTA$	37.25
myo-Inositol	100
Glycine	20
Nicotinic acid	0.5
Pyridoxin HCl	0.5
Thiamine HCl	1
$CaCl_2 \cdot 2H2O$	1,176
Sucrose	25,000
Agarose*	4,000

pH = 5.8

*: Add agarose after adjusting the pH.

Cultivation of Single-node Cuttings:

The shoots developed from the axillary buds of shoot explants were cut out to obtain single-node cuttings (containing the axillary buds) node by node after the leaves were excised with sterile scissors. These nodes were then incubated in the 400 ml culture bottles containing the MS medium (Murashige and Skoog, 1962) supplemented with 25 g L^{-1} sucrose and 4 g L^{-1} agar (referred to as MS subculture medium, **Table 1**), with both plant spacing and row spacing of about 10 mm at 25°C and a cool white light intensity of 15.8 Wat m^{-2} with 16 hours of light photoperiod day period. Each single-node cutting (including the axillary buds) of about 1 cm was subcultured for shoot explants at 4-week intervals in 400 ml culture bottles (8-9 cuttings/bottle) containing approximately 50 ml basal medium to multiply. The multiplication phase was routinely repeated every 4 weeks by subculturing single-node cuttings for the subsequent experiments (**Figure 3**) (El-Sawy et al., 2015). All the media had their pH adjusted to 5.8 and were autoclaved at 121 °C for 20 min before use.

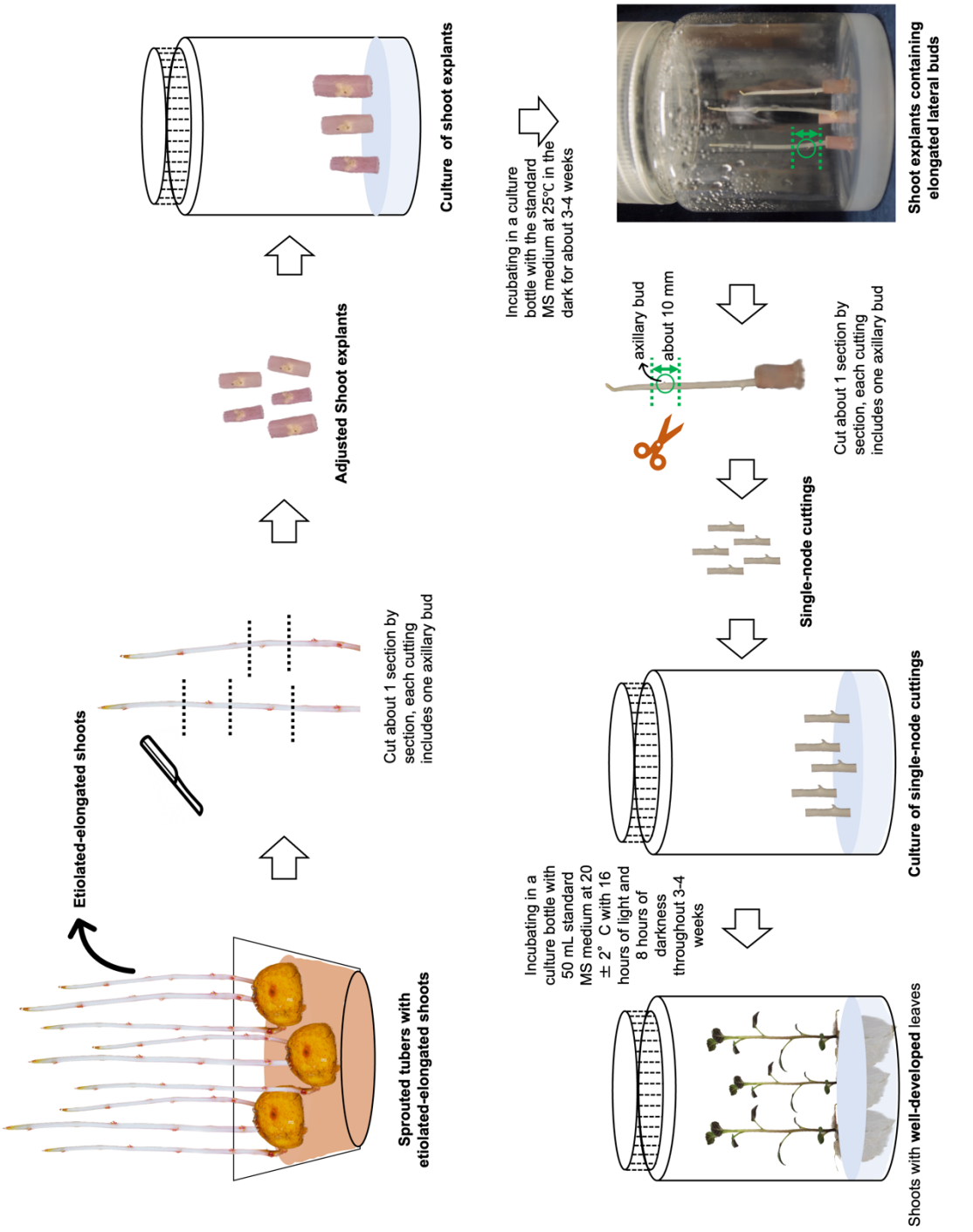


Figure 2. Schematic representation of the process for obtaining in vitro shoots.

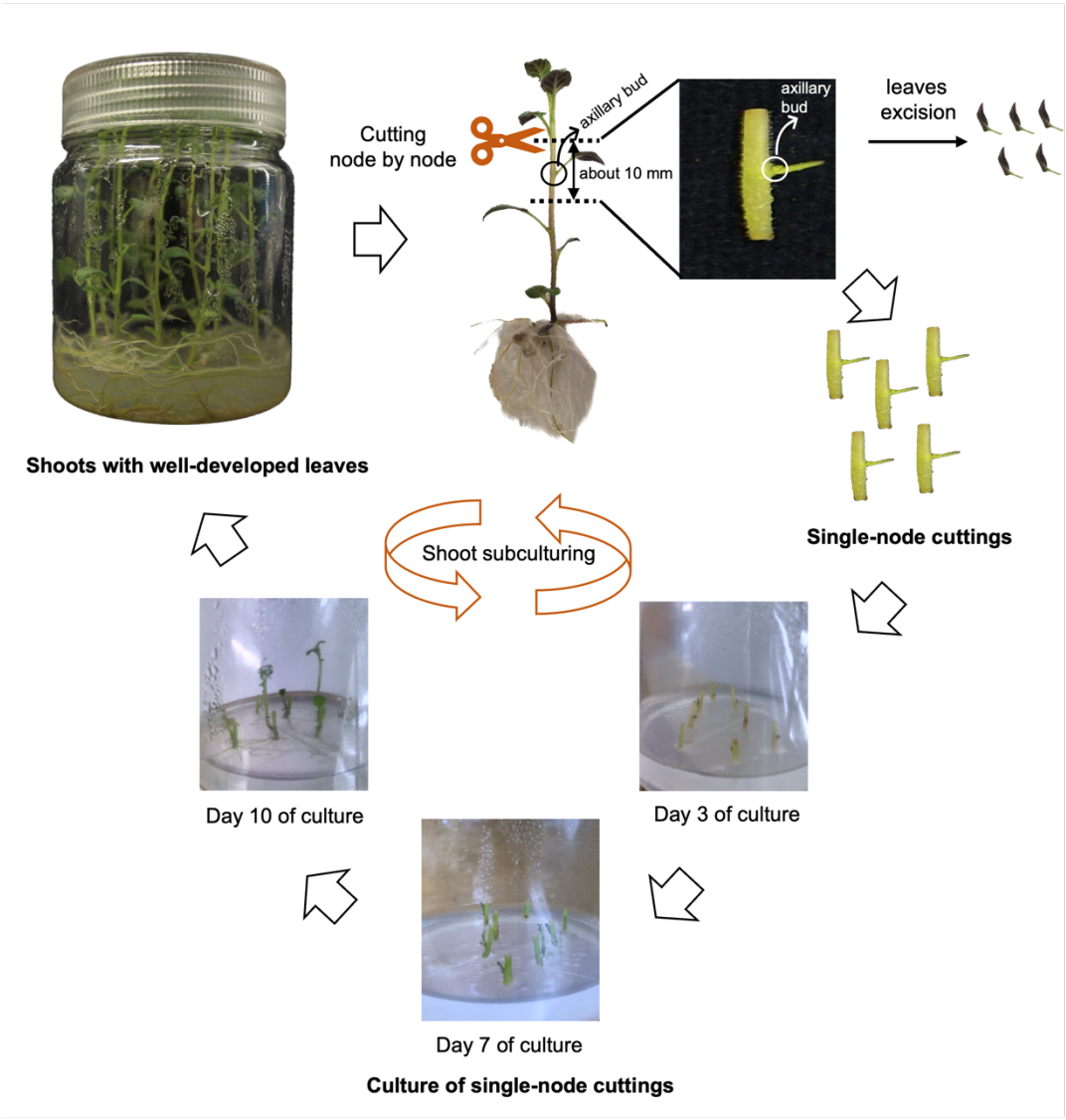


Figure 3. Schematic representation of the process for subculturing in vitro single-node cuttings (shoots) using *Solanum tuberosum*. L ssp. *andigena*, cv. Irish Cobbler and May Queen.

1.2.3 Induction of Microtuber Formation

Microtubers were induced by culturing single-nodal cuttings (ca. 1 cm length) containing one internode and axillary bud, which were cut from 3-week-old shoot explants and then incubated in sterile Petri dishes containing approximately 20 ml basal medium to break the dormancy of the axillary bud, with both plant spacing and row spacing of about 20 mm at 25 °C in the dark for two days. These dormancy-broken single-node cuttings were transplanted and further incubated in sterile Petri dishes containing approximately 20 ml MS tuberization medium (adjusted MS medium) supplemented with 100 g L^{-1} sucrose, 4 g L^{-1} agar, and 20 μM ancymidol (Sigma-Aldrich) (**Figure 4**) to induce the hypertrophy of axillary bud, with both plant spacing and row spacing of about 20 mm at 20 °C in the dark for two weeks.

Dormancy Breakage of Single-node Cuttings:

Single-nodal cuttings (ca. 1 cm length) containing one internode and axillary bud were cut from 3-week-old shoot explants. To confirm the effect of GA on dormancy-breaking of axillary buds, I incubated these single-nodal cuttings in sterile Petri dishes containing approximately 20 ml basal medium (MS medium) supplemented with a factorial combination of 10 μM GA or with nothing (untreated control) with both plant spacing and row spacing of about 20 mm at 25 °C in the dark for four periods (12, 24, 36 or 48 hours).

The following growth characteristics were recorded:

Percentage of sprouting on hour 12, 24, 36, and 48 of culture.

The Induction of Microtuberization:

Single-node cuttings were incubated without hormone treatment for 36 hours to break dormancy. The dormancy-broken single-node cuttings were then transplanted and further cultured in sterile Petri dishes containing approximately 20 ml MS tuberization medium (the adjusted MS medium, **Table 2**) supplemented with 100 g L^{-1} sucrose and 20 μM ancymidol, with both plant spacing and row spacing of about 10 mm at 20 °C under completely dark conditions for 14 days.

The following growth characteristics were recorded:

Percentage of microtuberization on day 3, 7, and 14 of culture.

In addition, to confirm the effect of different levels of ancymidol on microtuberization in this study, I incubated dormancy-broken single-node cuttings in sterile Petri dishes containing approximately 20 ml MS tuberization medium (adjusted MS medium, **Table 2**) supplemented with 100 g L^{-1} sucrose, 4 g L^{-1} agar, and 20 μM, 50 μM or 100 μM ancymidol (Sigma-Aldrich) to inhibit the bud outgrowth of axillary buds and induce the hypertrophy, with both plant spacing and row spacing of about 20 mm at 20 °C in the dark for 14-days using single-node cuttings of ssp. *andigena* (harder for tuberization) and cv. Irish Cobbler (easier for tuberization).

The following growth characteristics were observed:

Size and formation of microtubers on day 14 of culture at the morphological level.

All mediums had their pH adjusted to 5.8 and were autoclaved at 121 °C for 20 min before use. Each sterile Petri dish received 20 ml medium and contained ten single-node cuttings. All the experiments were performed with three replicates using 30 single-node cuttings for each replicate.

Table 2. The composition of adjusted MS medium for microtuberization.

Reagent	**mg L^{-1}**
NH_4NO_3	400
KNO_3	1,900
$MgSO_4 \cdot 7H_2O$	370
KH_2PO_4	170
H_3BO_3	6.2
$MnSO_4 \cdot 4H_2O$	22.3
$ZnSO_4 \cdot 7H_2O$	8.6
KI	0.083
$Na_2MoO_4 \cdot 2H_2O$	0.25
$CuSO_4 \cdot 5H_2O$	0.025
$CoCl_2 \cdot 6H_2O$	0.025
$FeSO_4 \cdot 7H_2O$	27.85
$Na_2 \cdot EDTA$	37.25
myo-Inositol	100
Glycine	20
Nicotinic acid	0.5
Pyridoxin HCl	0.5
Thiamine HCl	1
$CaCl_2 \cdot 2H_2O$	1,176
Sucrose	100,000
Agarose*	4,000

pH = 5.8

*: Add agarose after adjusting the pH.

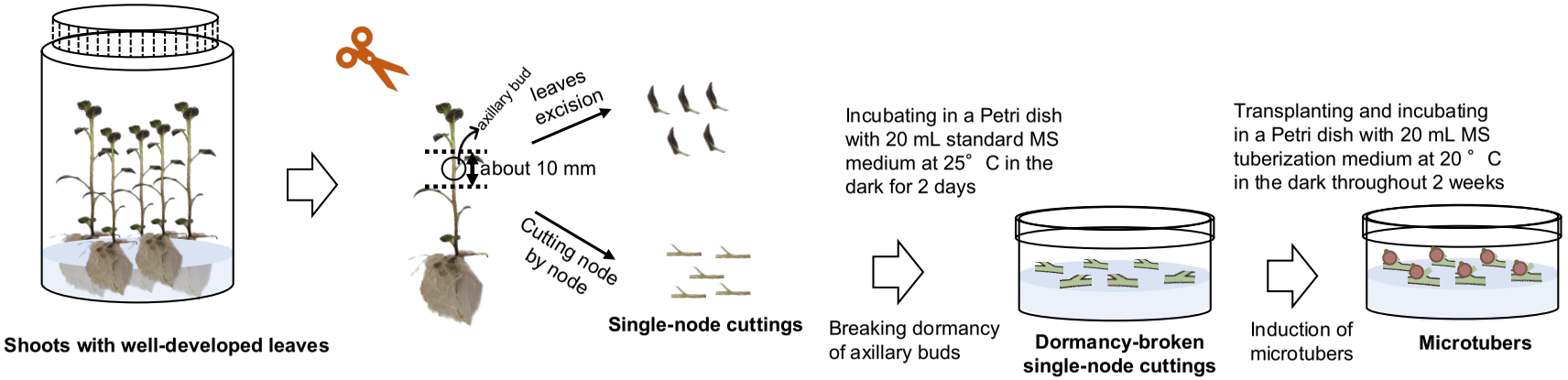


Figure 4. Schematic representation of the process for inducing microtubers using *Solanum tuberosum*. L ssp. *andigena.*

1.2.4 Induction of Microtuber Chain Formation

Microtuber Chains were induced by culturing microtubers attached to the nodal stem, which were cultured for 14 days and then incubated in sterile Petri dishes containing approximately 20 ml MS medium supplemented with 10 μM gibberellin (**Figure 13**) to break the dormancy of microtubers, with both plant spacing and row spacing of about 20 mm at 25 °C in the dark for 12, 24, 36, or 48 hours. These dormancy-broken microtubers were transplanted and further incubated in sterile Petri dishes containing approximately 20 ml MS tuberization medium (adjusted MS medium, **Table 2**) supplemented with 100 g L^{-1}sucrose and 20 μM ancymidol to induce the hypertrophy of buds in microtubers, with both plant spacing and row spacing of about 20 mm at 20 °C in the dark for 14, 21, or 28 days.

Dormancy Breakage of Microtubers:

To confirm the effect of GA, CK, and NAA on dormancy-breaking of microtubers, microtubers attached to nodal stem tissues were cultured to break dormancy before inducing microtuber chain formation in sterile Petri dishes containing approximately 20 ml basal medium (MS medium, **Table 1**) supplemented with a factorial combination of 10, 20, or 30 μM GA, CK, NAA or untreated control with both plant spacing and row spacing of about 20 mm at 25 °C in the dark for 36 hours. The growth characteristic of the length of the axillary bud was recorded:

Percentage of microtuber chain formation on day 14 of culture.

The Induction of Microtuber Chains:

Microtubers were incubated with 10 μM GA for 12, 24, 36, and 48 hours to break dormancy. These GA-treated microtubers were then transplanted and further cultured in sterile Petri dishes containing approximately 20 ml MS tuberization medium (the adjusted MS medium, **Table 2**) supplemented with 100 g L^{-1} sucrose and 20 μM ancymidol, with both plant spacing and row spacing of about 10 mm at 20 °C under completely dark conditions (**Figure 5**). The following growth characteristics were recorded:

Percentage of secondary hypertrophy on day 14, 21, and 28 of culture.

All mediums had their pH adjusted to 5.8 and were autoclaved at 121 °C for 20 min

before use. Each sterile Petri dish received 20 ml medium and contained ten microtubers. All the experiments were performed with three replicates using 30 microtubers for each replicate.

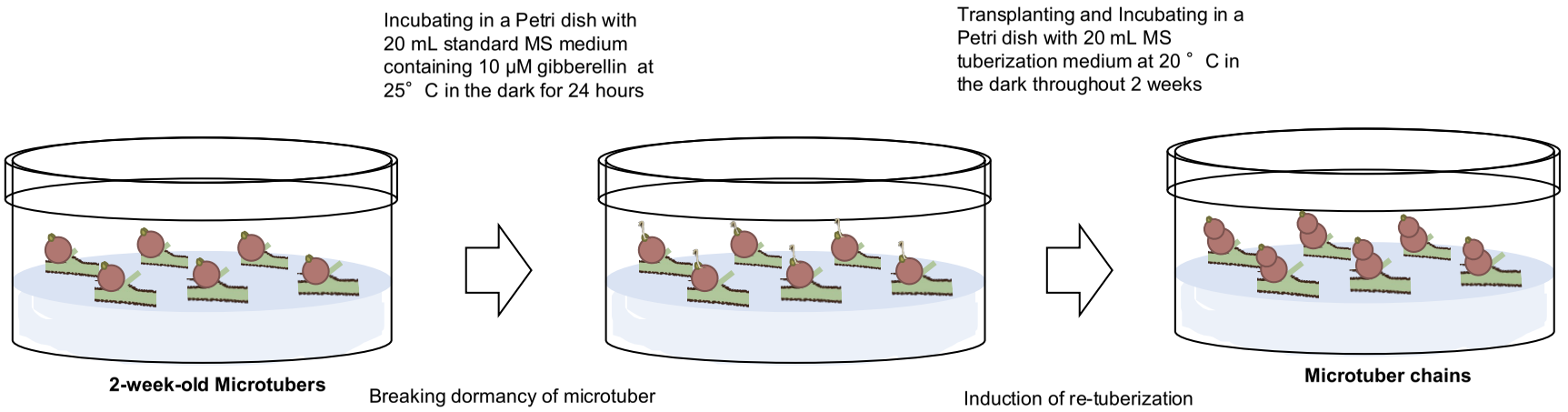


Figure 5. Schematic representation of the process for inducing microtuber chains using *Solanum tuberosum*. L ssp. *andigena*.

1.2.5 Experimental Design and Statistical Analysis

All experiments were set up in a factorial experiment based on a completely randomized design, and data were statistically analyzed by one-way analysis of variance (ANOVA) for testing the differences among treatments using Tukey's multiple comparisons with a 95% confidence level outcome ($p<0.05$) in Prism (version 10). The data from three biological replicates were provided as means (± standard error).

1.3 Results

1.3.1 Effect of GA on Dormancy-breaking of Axillary Buds

The possibility that gibberellin (GA) might be important for breaking the dormancy of axillary buds subjected to correlative inhibition in the intact plantlet was tested using single node cuttings from the shoot explants of *Solanum tuberosum* ssp. *andigena* and cv. May Queen. Applying 10 μM GA_3 (GA) to single-node cuttings growing in agar solidified MS medium enhanced dormancy-breaking on hours 12 and 24 of culture, 36, and 48 hours, respectively. Single-node cuttings incubated on mediums without hormone treatment were set as control (**Figure 6**). GA enhanced the effectivity on inducing bud break on hours 12 and 24 of culture; according to the percentage of dormancy-broken shoots, most single-node cuttings formed on the junction between the leaves and stems, and the numbers of GA-treated single-node cuttings could reach approximately 2 times that of control (**Figure 6B**). However, on hours 36 and 48 of culture, the numbers of dormancy-broken single node cuttings in medium untreated matched with that of GA-treated single node cuttings, and exposure to a temperature of 25°C for 36 hours or up to 48 hours did not alter this phenomenon. This was due to the dormancy of single-node cuttings being almost (>90%) broken on hour 36 of culture. Some single-node cuttings that failed to sprout may be due to their relative distance from the apex of the shoot explants or related to their age and genetics, which remains to be studied. The effect of different species of potatoes on breaking dormancy of single-node cuttings was also examined (**Figure 6**). As expected, the dormancy-broken single-node cuttings reached 56% on hour 24 of culture under GA-treated conditions. However, the dormancy-broken single-node cuttings could reach 85% and 95% on hour 36 and 48 of culture under control conditions (**Figure 6B**). This suggests that the GA application did not enhance dormancy breaking of single-node cuttings on day 2 (24 - 48 hours) of culture in either ssp. *andigena* or cv. May Queen, compared with the control treatment. This may be due to the fact that endogenous GA in single-node cuttings was enough to break dormancy even without exogenous GA application.

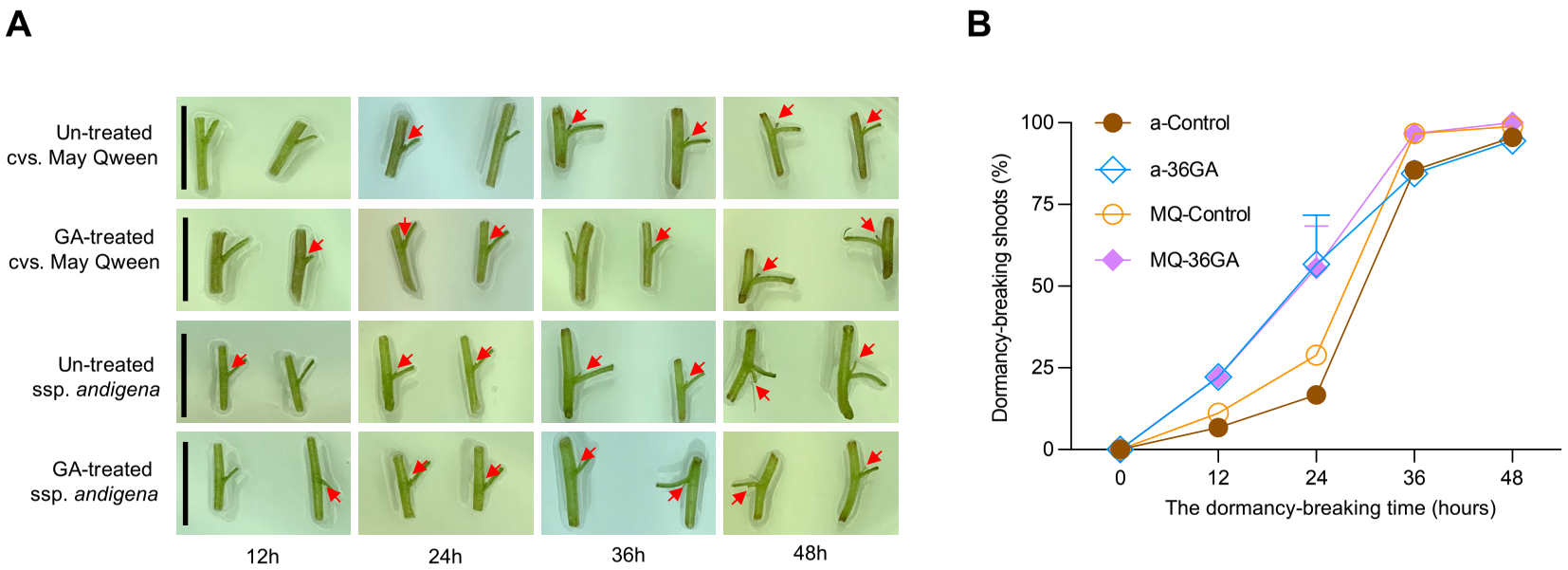


Figure 6. In vitro dormancy-broken single node cutting (shoot) experiments.

(**A**) Representative images of single node cuttings of *Solanum tuberosum* L. ssp. *andigena* (a) and cv. May Queen (MQ) on hour 12, 24, 36, and 48 of culture, respectively. Single node cuttings were cultured in MS medium supplemented with 10 μM GA_3 (GA) or untreated (Control) at 25°C in the dark to break the dormancy. Bar = 10 mm.

(**B**) The percentage of dormancy-breaking shoots.

1.3.2 Effect of Ancymidol on Formation of Microtubers

Removal of the leaf from a shoot explant to make a cutting led to an elongated shoot rather than a tuber, but the application of ancymidol (one GA inhibitor) or abscisic acid (ABA) to the MS medium gave the cutting a tuber which should come from the shoot explants exposed to short days (with 16 hours of light and 8 hours of darkness cycles). Cuttings from shoot explants exposed to long days were hardly able to form tubers. Previous studies in our lab showed that single node cuttings were taken from ssp. *andigena* shoot explants that had received 21 days (i.e., 3 weeks), when cuttings were broken dormancy at 25 °C in the dark for 36 hours, they were then transferred to form microtubers using the MS medium supplemented with 100 g L^{-1} sucrose and 10 μM ancymidol at 20°C in the dark (永山大貴, 2020 修論).

Ancymidol behaved as an anti-gibberellin and played a role in hypertrophy at the apex of the bud. To confirm the effect on the microtuberization of ancymidol, an experiment was carried out to compare the effect on the microtuberization using four levels of ancymidol of Sigma-Aldrich Co. LLC (A9431). However, in my experiments, the reproducibility of microtuberization failed in the adjusted medium supplemented with 10 μM ancymidol using either ssp. *andigena* or cv. Irish Cobbler (**Figure 7**). Interestingly, 20, 50, and 100 μM ancymidol induced buds of single node cuttings hypertrophy, giving rise to its bulk with some bud tissues on the top of microtubers in both ssp. *andigena* and cv. Irish Cobbler. However, the bulk of microtubers induced by 50 and 100 μM was much smaller than that induced by 20 μM, confirming that ancymidol did inhibit the growth and elongation of buds of cuttings, resulting in the microtuberization, but a high level of ancymidol plays a key role in inhibiting microtubers growth (**Figure 7**).

In addition, the observed hypertrophy of the buds of cuttings on day 3, 7, and 14 of culture was also tested using the medium supplemented with 10% sucrose and 20 μM ancymidol in ssp. *andigena* and cv. May Queen. **Figure 8A** showed that this culture condition I used stimulated microtuberization so much that the percentage of well-formed microtubers reached about 80% and 92% **(Figure 8B)** on day 3 and 14 of culture in ssp. *andigena* and cv. May Queen, respectively. These results indicate that no influence was found in inducing microtuberization for species of potatoes in this study.

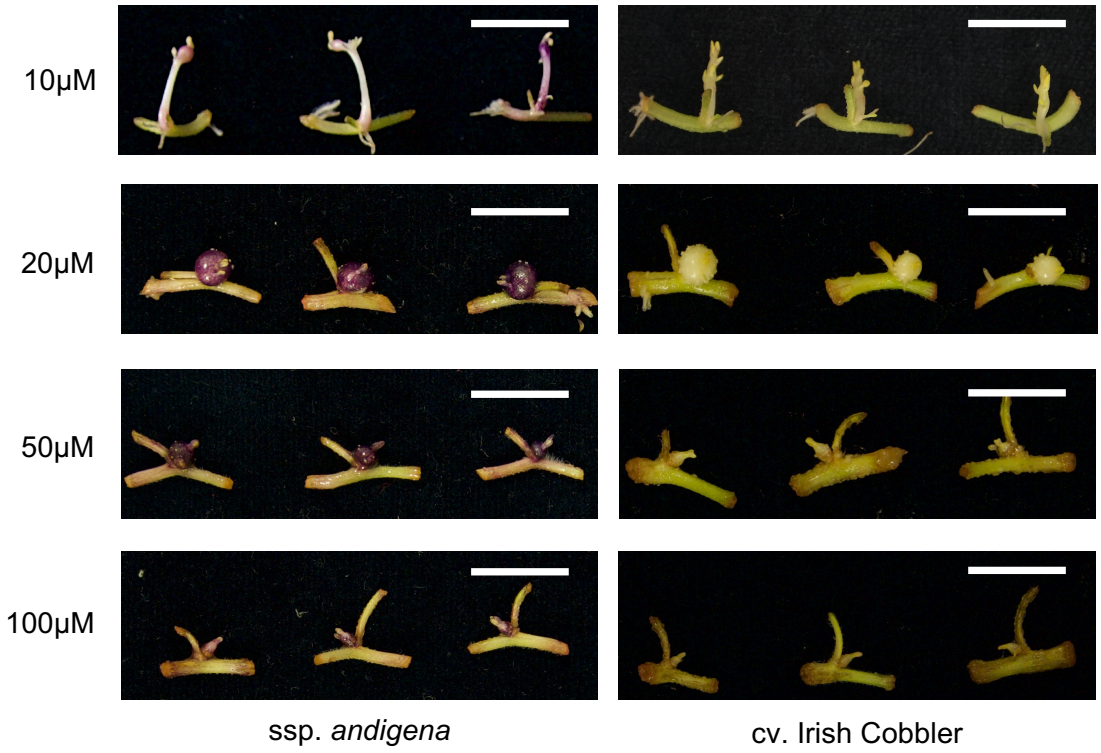


Figure 7. In vitro microtuber (MT) formation experiments over 14 days.

Representative images of the visual MT on day 14 of culture, using single node cuttings of *Solanum tuberosum* L. ssp. *andigena* and cv. Irish Cobbler after incubation with different concentrations of ancymidol of Sigma-Aldrich Co. LLC (A9431) in this study. Bar = 10 mm.

The dormancy-breaking of single node cuttings was executed in MS medium for 36 hours at 25 °C in the dark.

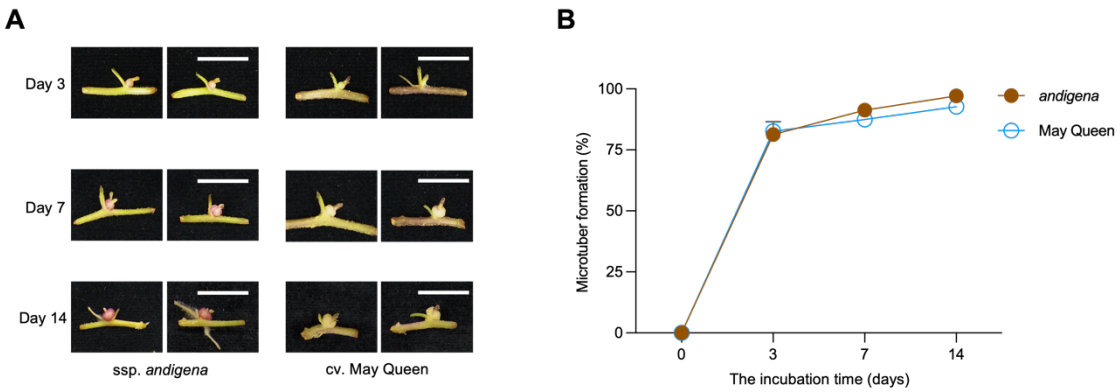


Figure 8. In vitro microtuber (MT) formation experiments over 14 days.

(**A**) Representative images of MTs of *Solanum tuberosum* L. ssp. *andigena* and cv. May Queen on days 3, 7, and 14 of culture, respectively. Bar = 10 mm.

(**B**) Percentage of MT formation.

To break the dormancy of single node cuttings, they were cultured in MS medium supplemented with 10 µM GA_3 (GA) for 36 hours at 25 °C in the dark.

1.3.3 Effect of Incubation Periods with GA Pretreatment on Formation of Microtuber Chains

Single-node cuttings were grown on the adjusted MS medium to form microtubers (**Table 2**) for 14 days. These microtubers were then transferred to the MS medium supplemented with 10 µM GA to break dormancy to induce secondary growth for 12, 24, 36, and 48 hours at 25 °C in the dark. Following GA pre-treatment, these incubated microtubers were then transferred to the adjusted MS medium and grown for 14-28 days. The percentage of microtuber chain formation was recorded on days 14, 21, and 28 of culture.

No microtuber chains (i.e., secondary hypertrophy) were formed by GA pre-treated microtubers of ssp. *andigena*, for 12, 24, 36, or 48 hours after 14 days (**Figure 9A**). However, after 28 days, secondary hypertrophy was observed (**Figure 9C**) and 72%, 79%, 95%, and 92% of microtuber chains were formed in GA pre-treated microtubers of *andigena* for 12, 24, 36, and 48 hours, respectively (**Figure 11**). While in GA pre-treated microtubers of cv. May Queen, secondary hypertrophy was observed and more than 60%, 65%, 73%, and 69% of microtuber chains were formed for 12, 24, 36, and 48 hours, respectively after 14 days (**Figure 10A, Figure 11**).

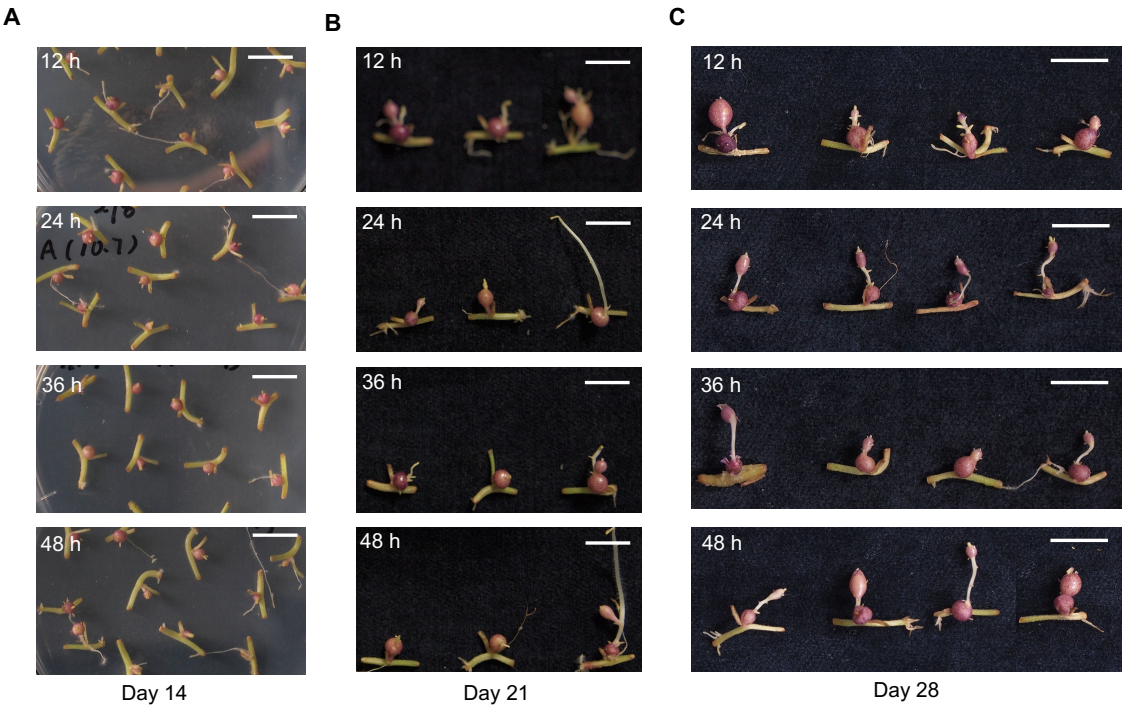


Figure 9. In vitro microtuber (MT) chain formation experiments over 28 days.

Representative images of the visual MT chains on day 14 (**A**), 21 (**B**), and 28 (**C**) of culture, using MTs of *Solanum tuberosum* L. ssp. *andigena* after dormancy-broken with 10 μM GA for 12, 24, 36, or 48 hours, respectively, at 25 °C in the dark. Bar = 10 mm.

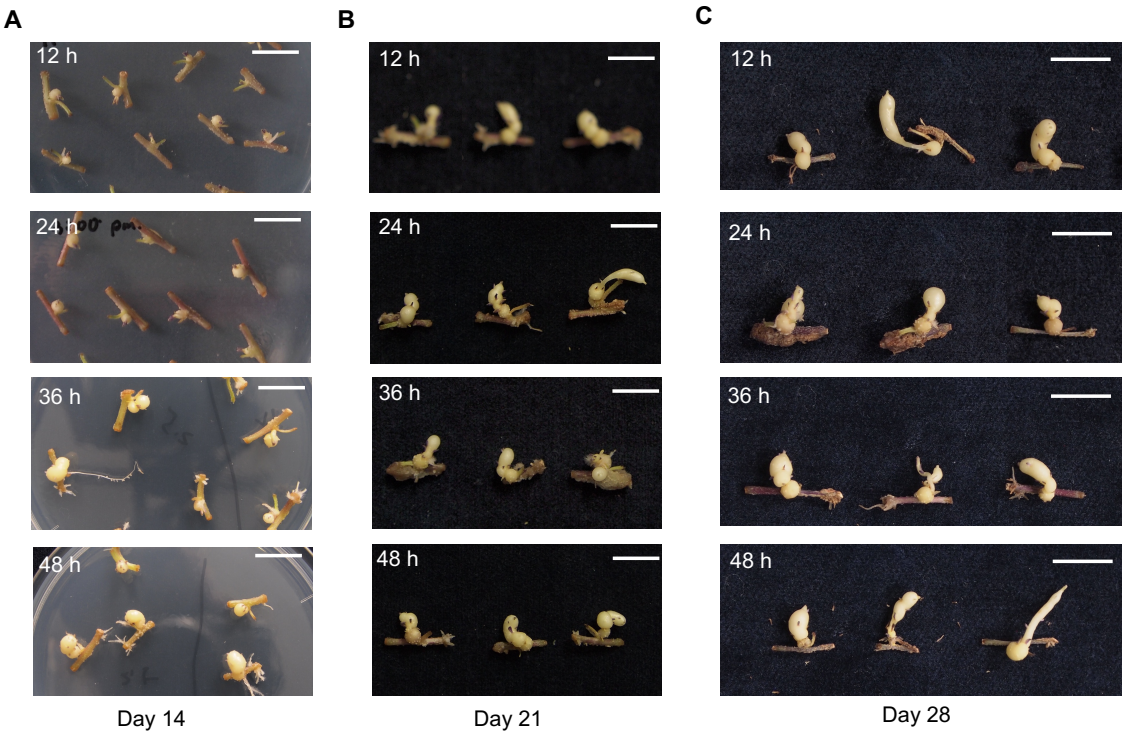


Figure 10. In vitro microtuber (MT) chain formation experiments over 28 days.

Representative images of the visual MT chains on day 14 (**A**), 21 (**B**), and 28 (**C**) of culture, using MTs of *Solanum tuberosum* L. cv. May Queen after dormancy-broken with 10 µM GA for 12, 24, 36, or 48 hours, respectively, at 25 °C in the dark. Bar = 10 mm.

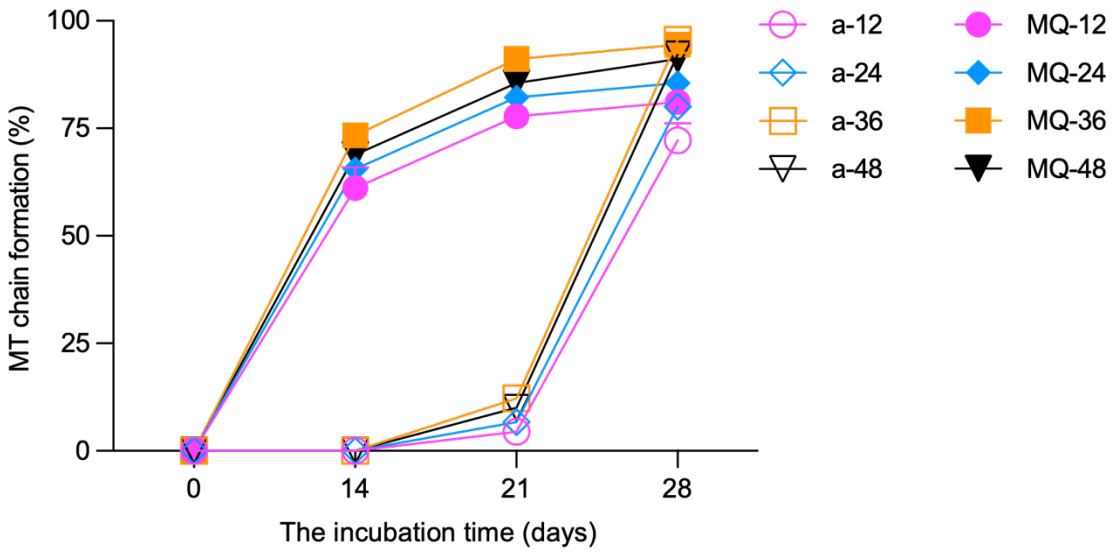


Figure 11. In vitro microtuber (MT) chain formation experiment over 28 days.

The percentage of the MT chain formation on day 14, 21, and 28 of culture, respectively, using MTs of *Solanum tuberosum* L. ssp. *andigena* (a) cv. May Queen (MQ) after dormancy-broken with 10 µM GA for 12, 24, 36, or 48 hours, respectively, at 25 °C in the dark. Bar = 10 mm.

1.3.4 Effect of Pretreatment with Plant Hormones on Formation of Microtuber Chains

In ssp. *andigena*, no formation of secondary hypertrophy was shown after 14 days. The effects of GA, CK, and NAA were analyzed further on breaking dormancy of microtubers, different levels (10, 20, and 30 μM) were also tested in ssp. *andigena* and cv. May Queen. These microtubers were transferred to the adjusted medium supplemented with ancymidol at different concentrations (10, 20, and 30 μM) to test the effect of various ancymidol levels on microtuber chain formation.

Pretreated with GA, CK, or NAA to microtubers of ssp. *andigena*, did not occur secondary hypertrophy at the level of 10, 20, or 30 μM ancymidol (**Figure 12**).

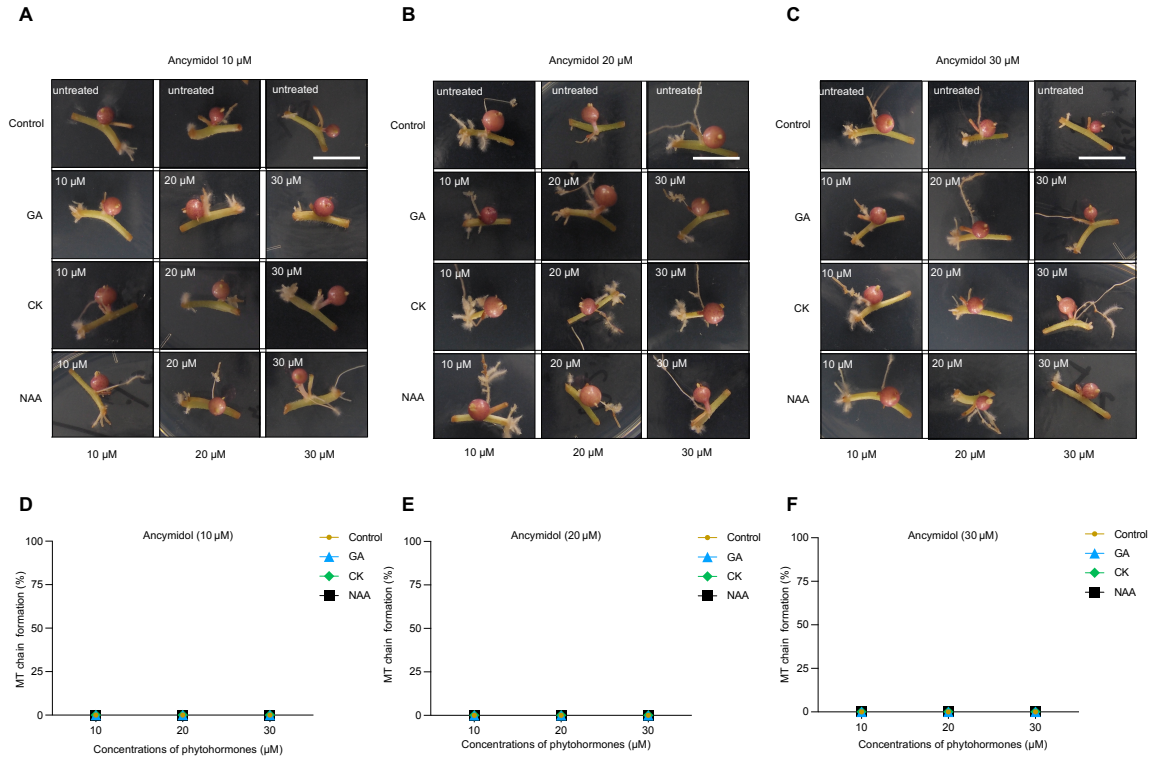


Figure 12. In vitro microtubers (MT) chain formation experiments over 14 days in ssp. *andigena*.

Representative images of the visual MT chains on day 14 of culture, using MT of *Solanum tuberosum* L. ssp. *andigena* after incubated in MS medium supplemented with 10, 20, or 30 μM GA_3 (GA), 10, 20, or 30 μM 6-benzyladenine (CK), 10, 20, or 30 μM NAA, or with no additional plant hormones (untreated control), respectively, for 36 hours at 25 °C in the dark. These hormone-induced MTs were then cultured in the adjusted MS medium supplemented with (**A**) 10 μM, (**B**) 20 μM, and (**C**) 30 μM ancymidol for 14 days at 20 °C in the dark. Bar = 10 mm.

The percentage of formed MT chains cultured in the adjusted MS medium supplemented with (**D**) 10 μM, (**E**) 20 μM, and (**F**) 30 μM ancymidol on day 14 of culture. The percentage of MT chain formation was determined as counts of well-formed MT chains compared with the whole counts of MTs and were calculated every day for 14 days.

However, secondary hypertrophy was observed in microtubers of cv. May Queen (**Figure 13**). Application of plant hormones to microtubers did lead to secondary growth, but the number of microtuber chains produced depended on the concentration and type of hormone used. In addition, the formation of secondary hypertrophy was also concentration-depended on ancymidol. For the application of 10 μM ancymidol (**Figure 13A**), the percentage of microtuber chain formation reached about 43% (**Figure 13D**), 54% (**Figure 10E**), and 34% (**Figure 13F**) under 10, 20, or 30 μM of GA-treated conditions; and it reached about 4%, 3%, and 3% under 10, 20, or 30 μM of CK-treated conditions, which was as the same as that under untreated control condition; in addition, it reached about 13%, 23%, and 12% under 10, 20, or 30 μM of NAA-treated conditions. Suggesting that GA had a more effective role in inducing secondary growth than NAA or CK, and 20 μM level of ancymidol resulted in more microtuber chains than 10 μM or 30 μM level of ancymidol. There was no difference between CK treatment and untreated control, which just resulted in two or three microtuber chains.

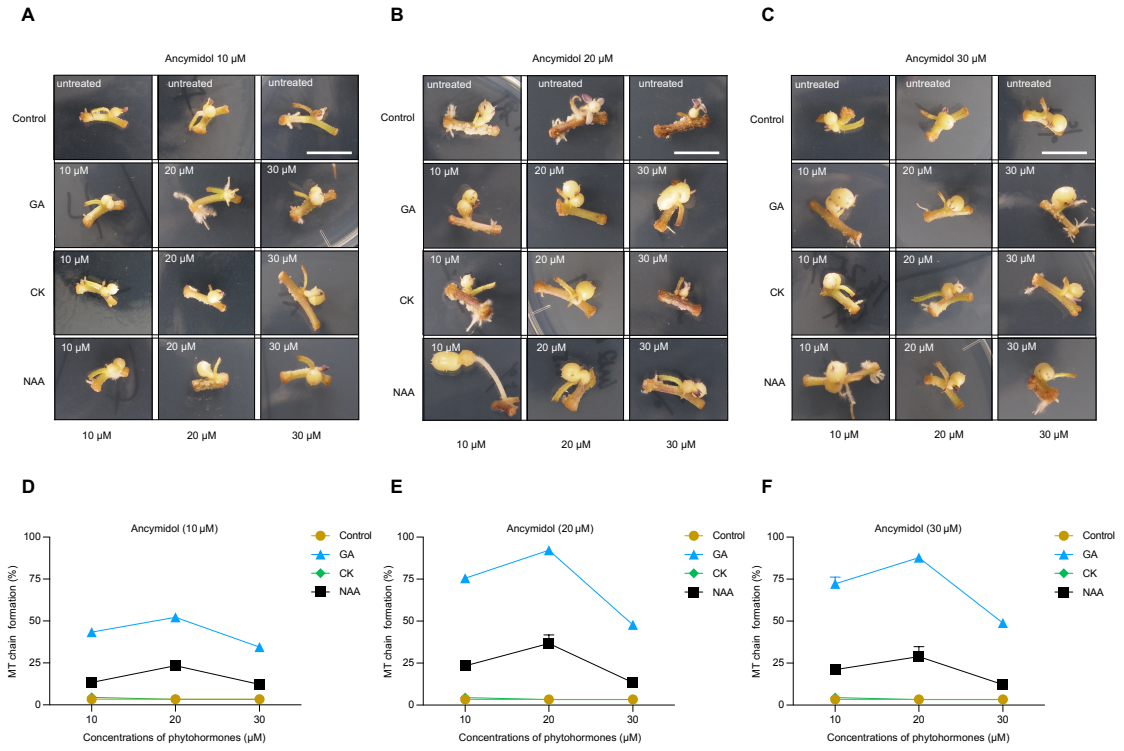


Figure 13. In vitro microtubers (MT) chain formation experiments over 14 days in cv. May Queen.

(**A**) Representative images of the visual MT chains on day 14 of culture, using MT of *Solanum tuberosum* L. cv. May Queen after incubated in MS medium supplemented with 10, 20, or 30 μM GA_3 (GA), 10, 20, or 30 μM 6-benzyladenine (CK), 10, 20, or 30 μM NAA, or with no additional plant hormones (untreated control), respectively, for 36 hours at 25 °C in the dark. These hormone-induced MTs were then cultured in the adjusted MS medium supplemented with (**A**) 10 μM, (**B**) 20 μM, and (**C**) 30 μM ancymidol for 14 days at 20 °C in the dark. Bar = 10 mm.

The percentage of formed MT chains cultured in the adjusted MS medium supplemented with (**D**) 10 μM, (**E**) 20 μM, and (**F**) 30 μM ancymidol on day 14 of culture. The percentage of MT chain formation was determined as counts of well-formed MT chains compared with the whole counts of MTs and were calculated every day for 14 days.

1.4 Discussion

Single-node cuttings are useful for the study of tuberization (Chen et al., 2018; Fischer et al., 2008). A single node with a single small leaf attached to it, cut from a non-induced plantlet, cannot be expected to generate enough endogenous hormones to induce tuberization even under the inductive conditions of continuous darkness. Hence, the behavior of the bud in a single node cutting is dominated by the exogenous components present in the medium. Previous reports have shown that > 8% sucrose in a MS medium was sufficient to induce this process and cause tuberization (Chen et al., 2007; Cheng et al., 2018). Moreover, ancymidol, an inhibitor of gibberellin biosynthesis, was very effective in altering the development of bud meristems from shoot formation to tuber formation, while cytokinin, in this case, was ineffective. This is consistent with the observations (Garcia et al., 2019; Kefi et al., 1997), pointing out that the kinetics of cytokinin accumulation were not compatible with the tuberization response of stem cuttings; it is worth noting that while the effect of gibberellin on the induction of class-I patain gene expression by sucrose was consistent with its inhibitory effect of the tuberization process, kinetin (cytokinin) did not facilitate the sucrose induction of Patatin gene expression (Cardenas, 2021).

Ancymidol is a plant growth retardant that works by inhibiting the ent-kaurene oxidase enzyme from interfering with GA biosynthesis (Coolbaugh et al., 1978; Menzel, 1980), which does not cause abnormal plant growth with long-term use in plant tissue culture (Han et al., 1994). GA content is reduced after plants treated with ancymidol display decreased growth (Shive Jr and Sisler, 1976). In this study, on the basis of the test of three different concentrations (10, 20, and 30 μM) of ancymidol, three potato varieties tubers including diploid and tetraploid were cultured. Results showed that 20 μM ancymidol was a more suitable concentration to form microtubers and microtuber chains at 20 °C in the dark. The results also showed that the adjusted medium supplemented with high concentration of ancymidol had a very serious impact on the formation of microtubers (**Figure 8**), mainly resulting in a large reduction in size. Whether this implies that ancymidol has a greater impact on cell growth than on cell division needs further cytological study.

In order to induce the secondary growth of microtubers, I used GA, CK, and NAA to break the dormancy of microtubers. My results showed that 10 μM GA was a more suitable concentration to break dormancy of microtubers at 25 °C in the dark for 36 hours but not of single-node cuttings. It may be because the endogenous GA is enough to break the dormancy of buds in single-node cuttings since GA has been reported to play an important role in the regeneration of newly lateral bud (Liu et al., 2019). NAA did have a good effect on dormancy-breaking may be due to the fact that auxins do not affect dormancy itself but influence the growth of sprouts after dormancy has been broken (Akoumianakis et al., 2008), although auxins are essential cognate regulators of cell cycle progression in all plant tissues (Francis and Sorrell, 2001). CK can enhance microtuberization and modify tuber dormancy duration depending on cultivars (Wang and Hu, 1985). However, CK-induced microtubers for 36 hours failed to form microtuber chains. This may be because CK was reported to induce cell division and cell expansion in sprouts within 48 hours of CK injection (Turnbull and Hanke, 1985a). Further investigation needs to be conducted to test the effect of CK on different dormancy-breaking-induced periods.

In addition, the results of inducing the formation of microtuber chains showed that secondary hypertrophy was observed in microtubers of cv. May Queen on day 14 of culture using three different plant hormones, while secondary hypertrophy did not occur in microtubers of ssp. *andigena* under the same conditions on day 14 of culture. Moreover, secondary hypertrophy was not observed until day 21 of culture in microtubers of ssp. *andigena* (**Figure 9B**), when using GA induced the breaking of dormancy. Suggesting the microtubers of ssp. *andigena* have a deeper dormancy than microtubers of cv. May Queen. This makes it more worth studying the dormancy and sprouting using microtubers of ssp. *andigena*.

Chapter 2 *in vitro* Induction of Secondary Growth and Microtuber Sprouting

2.1 Introduction

The dormancy breakage in potato tubers is accompanied by many physiological changes, such as changes in the ratios of abscisic acid (ABA)/GA and ABA/cytokinin (CK) (Destefano-Beltrán et al., 2006; Haider et al., 2021). GA has been known to induce growth, and the endogenous GA level increases rapidly toward the end of tuber spontaneous dormancy and the onset of shoot growth (Suttle, 2004b) . CK functions in promoting bud outgrowth emerged decades ago (Dun et al., 2012; Sachs and Thimann, 1967) and are necessary for bud breakage and initiating tuber sprouting (Alamar et al., 2017) by inducing CycD3 genes to function during the cell cycle's G1-S transition (reviewed by Francis, D. et al.) (Francis and Sorrell, 2001). GA and CK were reported to act synergistically to accelerate sprouting (Kolachevskaya et al., 2019b). Remarkably, Hartmann et al. showed that CK could stimulate the dormancy breakage of the excised tuber buds and GA-induced sprouting (Hartmann *et al.*, 2011).

Here, I use three kinds of potato microtubers prepared from single-node cuttings of ssp. *andigena* to observe the effect on the induction of secondary growth with the treatment of plant hormones: GA, CK, or both GA and CK (GACK), meanwhile, to investigate the role the nodal stem plays in plant hormone-induced sprouting in this sprouting induction experiment.

2.2 Plant Materials and Methods

2.2.1 Plant materials

Virus-free potato tubers of Solanum tuberosum. L ssp. *andigena* was kindly provided by the Agricultural Research Center.

2.2.2 Preparation of Secondary Growth Microtubers

To study the effect of plant hormones on the secondary growth of microtubers, I conducted an investigation using 2-week-old microtubers (in vitro induction of microtubers was described as same as in **1.2.3 of Chapter 1**) with treatments of 10 μM GA_3 (GA), 10 μM 6-benzyladenine (CK), or both GA and CK (GACK), or with no additional plant hormone (untreated control). In addition, to eliminate the role of the nodal stem attached to the microtuber on dormancy breaking in microtubers, three treatments of microtubers were adjusted:

1. Stemmed microtuber (stMT): Microtuber attached to a nodal stem.

2. Destemmed microtuber (deMT): Detach the nodal stem from the stMT, but the junction part remains attached to the microtuber.

3. Microtuber half (hMT): Cut the microtuber in half along the equatorial plane to completely remove the nodal stem (including the junction part with the microtuber).

These three treatments of microtubers, stMT, deMT, and hMT, were then cultured on the MS medium supplemented with 10 μM GA_3 (GA), 10 μM (6-benzyladenine) CK, or both 10 μM GA and 10 μM CK (GACK), or with no additional plant hormones (control) for 15 days at 20 °C in the dark (The detailed preparation for in vitro MTs is depicted in the schematic drawing of **Figure 14**). For each condition, 30 microtubers were tested, and 3 biological replicates were collected simultaneously.

In this observation, a microtuber was considered sprouted when it had any sprout > 2 mm in length at the morphological level, given that apical buds may grow temporarily but never elongate more than 2 mm. The percentage of sprout growth (i.e. sprouting) rate was determined as counts of sprouted microtubers compared with the whole counts of microtubers and were calculated every day for 15 days. The apical bud of the dormant microtuber is invisible, surrounded by yellow-green tissues. Once the dormancy is broken, the apical bud (i.e., sprout) emerges from the center of these yellow-green tissues. In addition, the length of sprouting buds was determined as the average length among all sprouting buds of sprouted microtubers and was measured every two days for 2 weeks. The onset of sprouting was characterized at the moment of 5% sprouting rate. All experiments described in this paper were carried out a minimum of three times. Individual

treatment within each experiment was replicated.

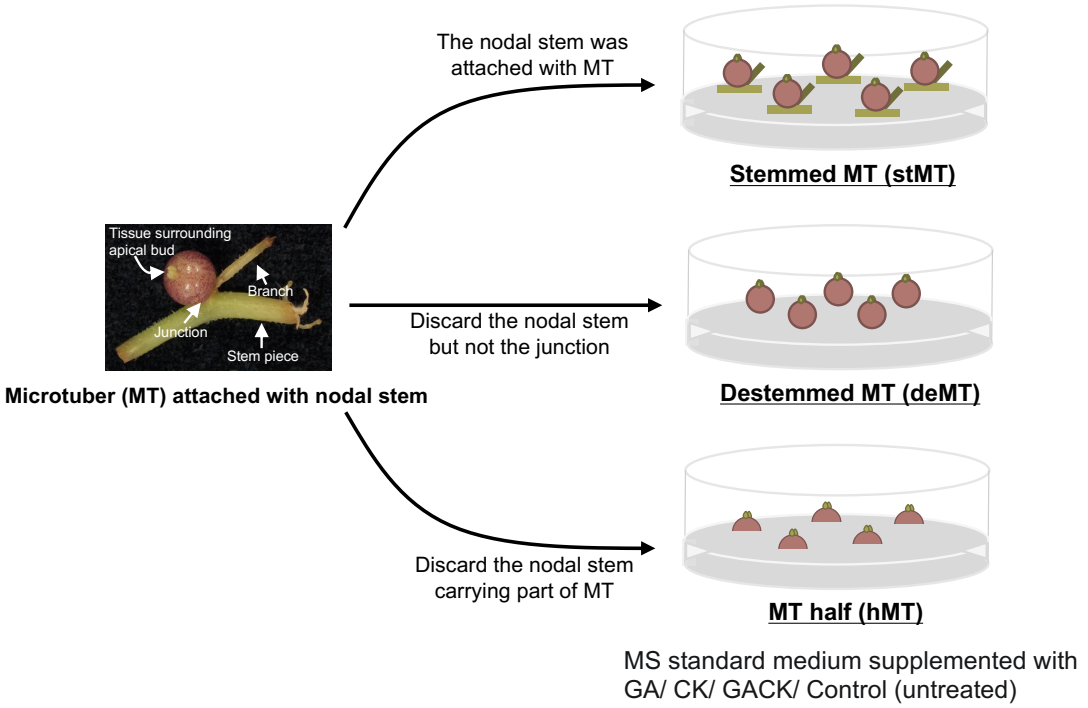


Figure 14. Schematic representation of microtuber (MT) treatment in this study.

Three preparations were used to monitor sprouting: (1) the nodal stem was attached to the MT (stemmed MT, stMT), (2) the stem piece was removed, but the junction remained in the MT (destemmed MT), and (3) the nodal stem was completely removed, including the junction in the microtuber (microtuber half, hMT).

2.3 Results

2.3.1 Response of Microtuber to the Exogenous GA Treatment Alone

stMTs, deMTs, and hMTs (as described in **2.1.2**) were used to study the function of exogenous GA alone treatment in secondary growth and microtuber sprouting. No sign of sprouting among the three treatments of MTs on the control medium was observed until day 15 of culture when about 6% of stMTs sprouted, so I considered 15 days as the rest period for MTs in the dark at 20 ◦C in my study and stopped observing the sprouting behavior after day 15.

On GA applied medium, the sprouting buds of stMTs were visible on day 1 of culture, reaching about 55% and 96% on day 4, and day 12 of culture, respectively (**Figure 15C**), and the length change was significant on day 4, and day 12 of culture (**Figure 15D**). The sprouting buds of deMTs were also visible on day 1 of culture but the sprouting rate reached 34% on day 4 of culture and stopped increasing thereafter (**Figure 15C**). In addition, the sprouting failed to be stimulated in hMTs, and no visible sprouting buds were observed for 15 days, the visual appearance of sprouting on day 10 of culture was shown in **Figure 15**.

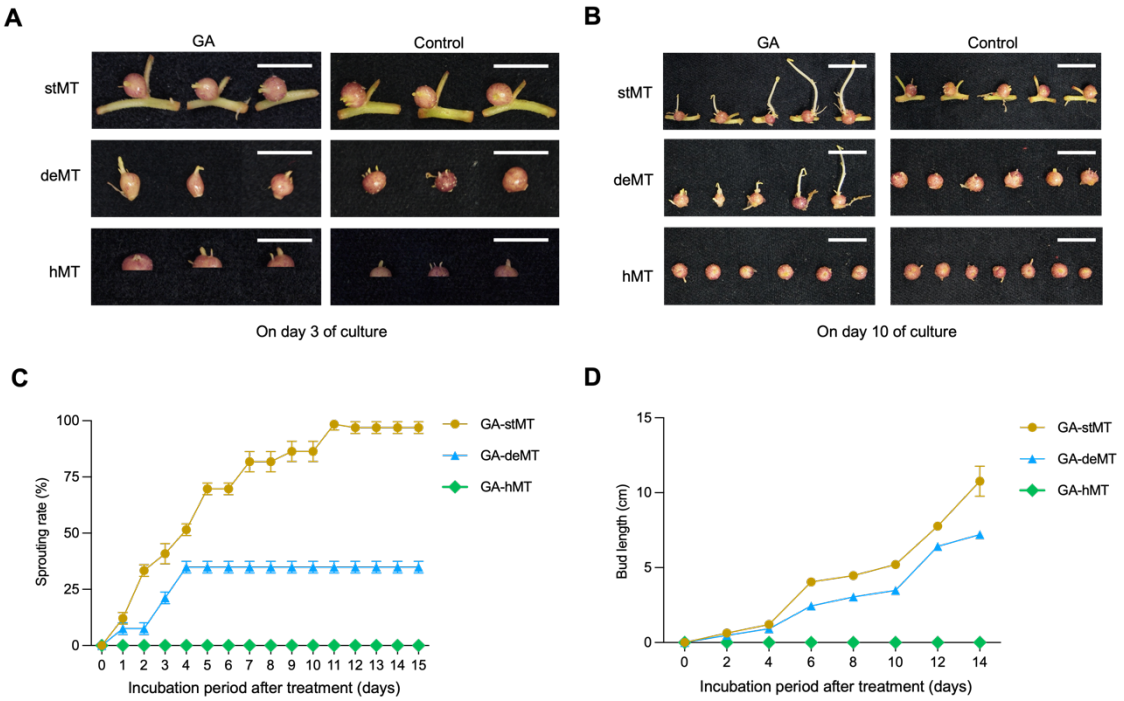


Figure 15. In vitro microtubers sprouting experiment using 2-week-old potato MTs after incubation with gibberellin (GA) treatment for 15 days.

Representative images of the visual appearance of sprouting on day 3 (**A**) and day 5 (**B**) of culture. The percentage of sprouted MTs (**C**) and the bud length (**D**) of stemmed microtubers (stMTs), destemmed microtubers (deMTs), and microtuber halves (hMTs), cultured with 10 µM GA_3 (GA), or untreated (control), respectively. Each value represents the mean ± standard deviation of three replicates (n = 30). Bar = 10 mm.

The percentage of sprouting rate was determined as counts of sprouted microtubers compared with the whole counts of microtubers and were calculated every day for 15 days. The bud length of sprouting buds was determined as the average length among all sprouting buds of sprouted microtubers and was measured every two days for 2 weeks.

2.3.2 Response of Microtuber to the Exogenous CK Treatment Alone

Interestingly, I did not observe any sign of sprouting behavior for 15 days on CK-applied medium, suggesting that CK failed to remove the inhibitory effect of ancymidol and stimulate stMTs sprouting, as were the cases in the deMTs and hMTs (**Figure 16**), and there was no significance among the apical buds in three kinds of microtubers at the morphological level. These observations showed that the exogenous CK alone was not able to trigger microtuber sprouting, regardless of the presence or absence of the nodal stem.

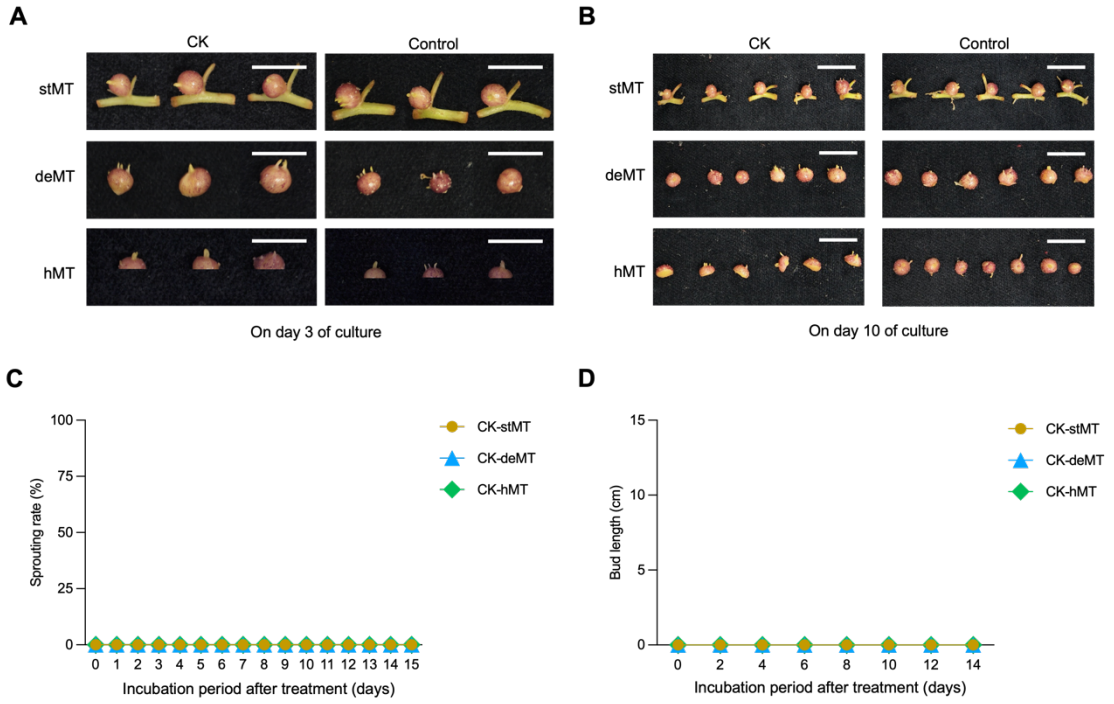


Figure 16. In vitro microtubers sprouting experiment using 2-week-old potato MTs after incubation with cytokinin (CK) treatment for 15 days.

Representative images of the visual appearance of sprouting on day 3 (**A**) and day 5 (**B**) of culture. The percentage of sprouted MTs (**C**) and the bud length (**D**) of stemmed microtubers (stMTs), destemmed microtubers (deMTs), and microtuber halves (hMTs), cultured with 10 µM 6-benzyladenine (CK), or untreated (control), respectively. Each value represents the mean ± standard deviation of three replicates (n = 30). Bar = 10 mm.

The percentage of sprouting rate was determined as counts of sprouted microtubers compared with the whole counts of microtubers and were calculated every day for 15 days. The bud length of sprouting buds was determined as the average length among all sprouting buds of sprouted microtubers and was measured every two days for 2 weeks.

2.3.3 Response of Microtuber to Both GA and CK Treatment

On both GA and CK co-applied medium, the significantly visible sprouting buds were observed for stMTs, and the sprouting rate reached a rate of 86% on day 4 of culture (**Figure 17C**), much more than that in GA alone treatment, indicating that exogenous GA has a significant effect on promoting stMTs sprouting growth and that exogenous CK co-application enhances this sprouting behavior. The length change was significant on day 12 of culture (**Figure 17D**), There was no significant difference in bud length at the morphological level between the GA and GACK treatments.

In addition, for deMTs, microtuber sprouting was also triggered and the visible sprouting buds were observed as in the case with GA alone treatment. More than 67% of microtubers sprouted on day 9 of culture (**Figure 17C**) and about 71% of microtubers sprouted on day 15 of culture, much more than that in GA alone treatment for stMTs but lesser than that in GACK treatment, suggesting that the junction part (between the MT and the nodal stem) remain part of the nodal stem tissue, which is important to support GA-induced sprouting. The length change was significant on day 10 of culture (**Figure 17D**). There was no significant difference in bud length at the morphological level between the GA and GACK treatments.

Interestingly, for hMTs, the sprouting buds were visible on MS medium supplemented with GACK when the nodal stem was excised, suggesting that both GA and CK are essential for MT sprouting. About 14% of hMTs were observed sprouting on day 1 of culture (**Figure 17C**), and the length change was significant on day 14 of culture (**Figure 17D**). When treated with GACK, there were noticeable differences in shoot morphology between stMTs and hMTs on day 10 of culture (**Figure 17B**), however, this difference disappeared on day 15 of culture (**Figure 18C**).

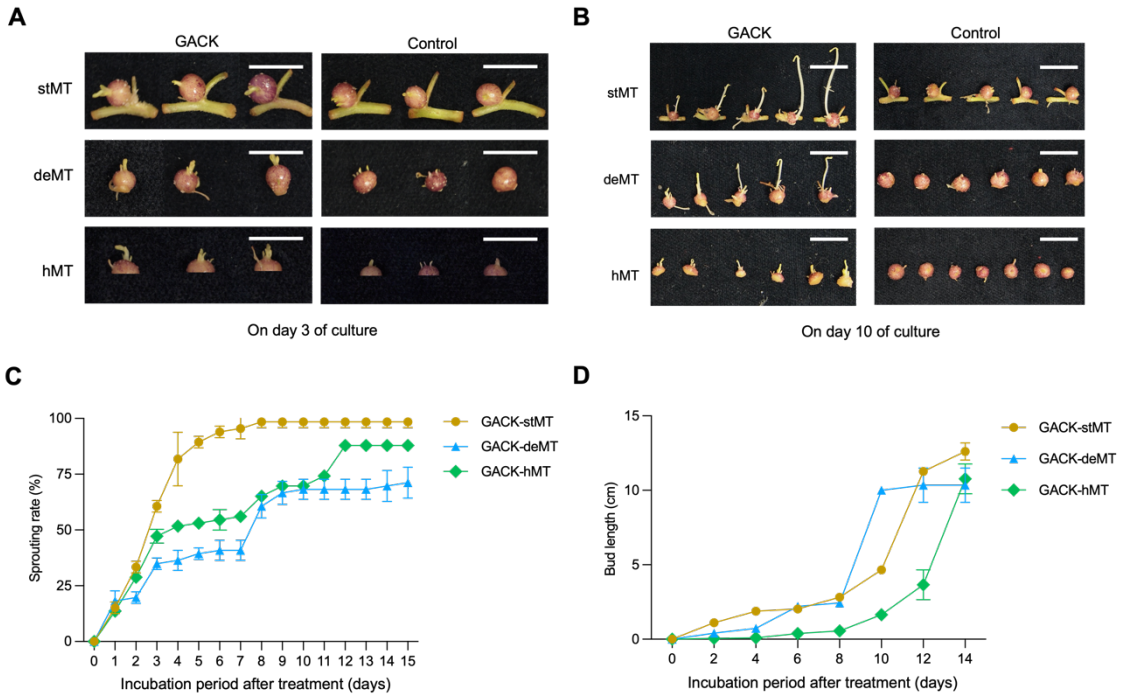


Figure 17. In vitro microtubers sprouting experiment using 2-week-old potato MTs after incubation with both gibberellin and cytokinin (GACK) treatment for 15 days.

Representative images of the visual appearance of sprouting on day 3 (**A**) and day 5 (**B**) of culture. The percentage of sprouted MTs (**C**) and the bud length (**D**) of stemmed microtubers (stMTs), destemmed microtubers (deMTs), and microtuber halves (hMTs), cultured with both GA and CK (GACK), or untreated (control), respectively. Each value represents the mean ± standard deviation of three replicates (n = 30). Bar = 10 mm.

The percentage of sprouting rate was determined as counts of sprouted microtubers compared with the whole counts of microtubers and were calculated every day for 15 days. The bud length of sprouting buds was determined as the average length among all sprouting buds of sprouted microtubers and was measured every two days for 2 weeks.

2.4 Discussion

It has been known for many years that secondary growth is caused by an imbalance of phytohormones in potato tubers, du e to the feeding of aboveground GA into the tuber. The exogenous GA promotes tuber sprout growth rather than dormancy release (Suttle, 2007). In this study, the fact that GA promoted the microtuber sprouting was found to be dependent on the presence of exogenous CK or the nodal stem. I used 10 μM GA to induce microtuber sprouting. GA application induced the sprouting of both stMTs and deMTs, but it reached 34% on day 4 of culture and stopped increasing thereafter in deMT, suggesting that the junction part (between the MT and the nodal stem) could support GA-induced sprouting like the nodal stem, but it was inadequate for subsequent sprouting. GA failed to terminate the dormancy of hMTs (**Figure 15**) and induced hMTs sprouting when the exogenous CK was co-applied (**Figure 17**). Although the shoot growth of hMTs was not as fast as that treated with GA in stMTs at the beginning, their elongation levels matched on day 15 of culture (**Figure 18**), agreeing with the report that GA has dormancy-terminating capacity but requires CK to induce sprouting growth in tubers (Sorce *et al.*, 2009). In other words, either CK or the nodal stem is essential for GA-induced microtuber sprouting. These results showed that the exogenous gibberellin was identified as a trigger in the process of microtuber sprouting, and cytokinin and the nodal stem were also found necessary to support GA-induced MT sprouting.

In addition, microtubers attached to the nodal with stem did not sprout until day 15 of culture (which was considered as the time of dormancy-breaking for MTs in the dark at 20 ◦C in this study) in the control, suggesting that the level of endogenous GA is not nearly sufficient to produce sprouts after microtuber formation. Coinciding with a sharp drop in GA levels at the stolon tip with the onset of tuber formation (Xu et al., 1998a).

CK has been known as the only chemical to release axillary buds from dormancy and is locally biosynthesized in the nodal stem and transported into axillary buds to promote bud outgrowth after decapitation (Francis and Sorrell, 2001), making the nodal stem necessary to help GA induce microtuber sprouting. This may be because I cultured MTs on a medium using a high-level sugar in the dark, leading to CK accumulation in the nodal stem. This assumption is supported by studies showing that sugars can promote CK

synthesis and accumulation to trigger the induction of bud outgrowth in potato stems (Salam et al., 2021).

Furthermore, previous studies reported that the effect of CK on tuber dormancy may be due to experimental systems, substances, or potato cultivars (Kolachevskaya *et al.*, 2019b; Siregar *et al.*, 2021). My study showed that CK application alone failed to cause any signs of visible sprouting duction for 15 days (**Figure 18**), regardless of the presence or absence of the nodal stem, except for some tissue surrounding the apical bud, unless exogenous GA was also applied, agreeing with the result of Hartmann et al., (Hartmann *et al.*, 2011). These results are shown to suggest that GA alone or CK alone is insufficient to initiate microtuber sprouting although both are essential for sprouting.

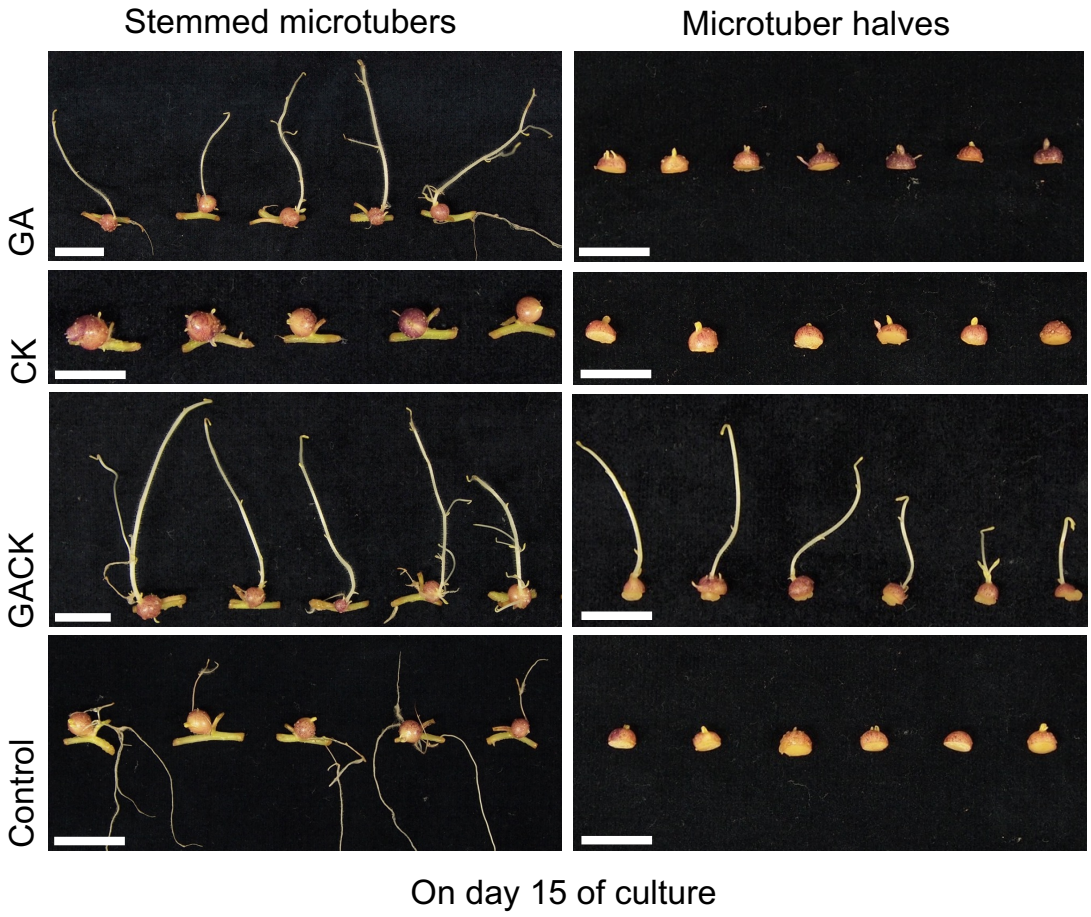


Figure 18. Representative images of the visual appearance of sprouting.

Representative images of the visual appearance of sprouting for stemmed microtubers and microtuber halves on day 15 of culture, respectively, cultured with 10 μM GA, CK, or GACK. Incubation without phytohormone was set as the control (untreated). Bar = 10 mm.

Chapter 3 Transcriptomic Analyses of Microtuber Sprouting Response to Phytohormone Treatments

3.1 Introduction

I have been studying the effects of some phytohormones co-regulating with GA on the tuber sprouting involved in secondary growth using microtuber halves (hMTs, with the nodal stem entirely removed), whereby I used exogenous auxin, jasmonic acid, ET, and CK to incubate hMTs on the GA-containing medium using microtubers made from potato tissue culture. Interestingly, in preliminary experiments in **Chapter 2**, I observed that in microtubers attached to the nodal stem, exogenous GA alone induced microtuber sprouting and promoted sprouting bud growth. However, the exogenous GA alone failed to induce hMT sprouting when the nodal stem was completely removed, and an exogenous CK co-application was found necessary for supporting GA to promote sprouting and bud growth. These results made me conclude that the nodal stem attached to microtubers might play a vital role in GA-induced sprouting.

Previous studies have significantly improved the understanding of the genetic pathways controlling potato tuber sprouting. RNA-seq analysis has been hugely helpful in determining the difference in gene expression, allowing the simultaneous comparison of transcript levels for thousands of genes (Stark et al., 2019). The complete sequencing of the potato genome provides an excellent opportunity to explore the genetic pathways for genes, enormously improving my understanding of genetic pathways that regulate potato tuber sprouting (Sharma et al., 2013; Xu et al., 2011b).

In the present study, I initiated a comprehensive transcriptome analysis based on the Illumina sequencing platform using potato microtubers treated with GA, CK, or both GA and CK (GACK). The aim was to figure out the regulation of tuber sprouting by GA and CK by screening out genes and profiles with differential expression during tuber meristem activation processes. Exogenous GA-only treatment accelerated tuber sprouting but did

not induce dormancy breakage of axillary buds (Woolley and Wareing, 1972), and exogenous CK treatment broke tuber dormancy rapidly and made buds sprout after 2-3 days (Hemberg, 1970). However, GA induced stMTs but not hMTs sprouting, while CK failed in my previous studies. Here, I used GA, CK, both GA and CK (GACK), or no treatment (control) to induce MT sprouting to understand the role of CK and the nodal stem in GA-induced sprouting at the molecular level by screening out genes and profiles with differential expression during tuber eye meristem activation processes (from the breakage of dormancy to the sprouting outgrowth.

3.2 Plant Materials and Methods

3.2.1 Plant Materials

Virus-free potato tubers of Solanum tuberosum. L ssp. *andigena* was kindly provided by the Agricultural Research Center.

3.2.2 Preparation of Secondary Growth Microtubers

The adjustment of microtubers was the same as described in **2.2.2 of Chapter 2**, except for deMTs. In this chapter, only stMTs and hMTs were used. These two treatments of microtubers were cultured on the MS medium supplemented with 10 μM GA, 10 μM CK, or GACK, or with no additional plant hormones (control), and then incubated for 3 days at 20 °C in the dark. Microtubers on day 3 of culture served as material for analysis of gene expression. For each condition, 30 microtubers were tested, and 3 biological replicates were collected simultaneously. The preparation methods for the microtubers are summarized in **Figure 19**.

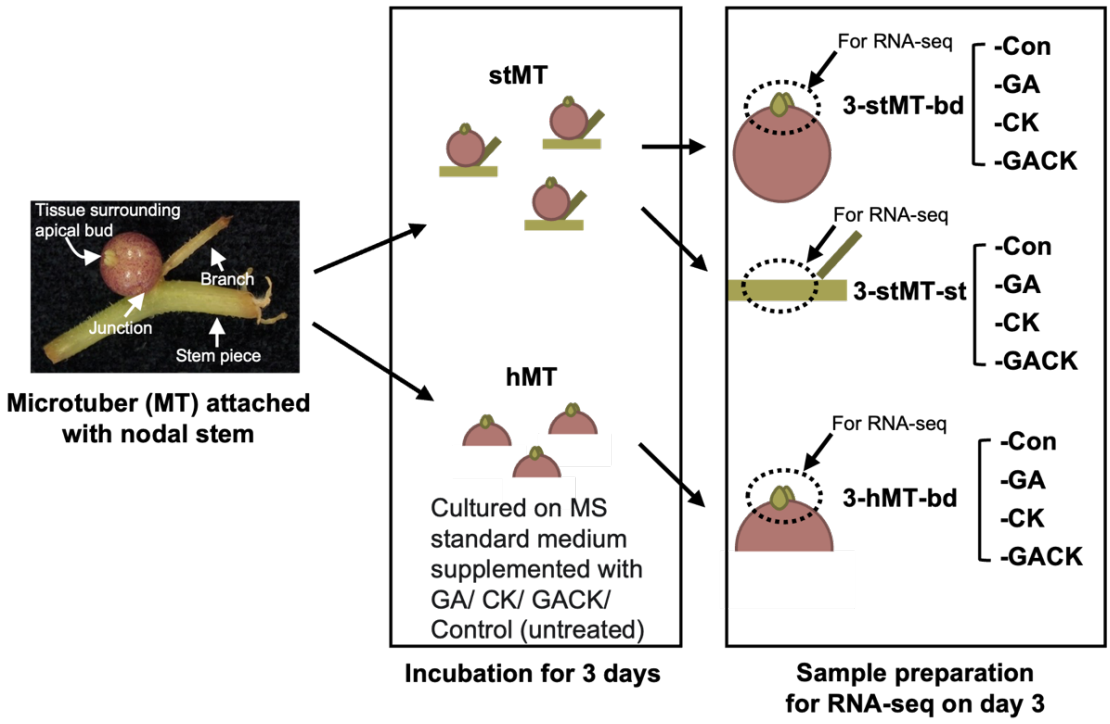


Figure 19. Schematic representation of microtuber (MT) treatment in this study.

Sample preparation for RNA-seq: the black dotted ellipses represent the sampled part for RNA extraction. For 3-stMT-bd-GA, -CK, -GACK, or -Con, the apical bud from stMT on day 3 of culture by GA, CK, GACK, or untreated Con; for 3-stMT-st-GA,-CK, -GACK, or -Con, the nodal stem with junction part from stMT on day 3 of culture by GA, CK, GACK, or culture by Con; for 3-hM-bd-GA, -CK, -GACK, or -Con, the apical bud from the MT half (hMT) on day 3 of culture by GA, CK, GACK, or untreated Con.

3.2.3 RNA Extraction and Sample Preparation

For extracting RNA from starch-rich seeds or plant tissues, protocols such as the TRIZOL kit (Invitrogen) and the Plant RNeasy mini kit (Qiagen) method often result in poor-quality RNA, making them inappropriate for downstream applications. In this study, a small part of microtubers was carried out when bud tissues were collected for RNA extraction due to the bud tissues were close to microtubers, and potato tubers were known to contain high amounts of polysaccharides such as starch. In my prepared experiments, I obtained the RNA with low yield and poor quality using TRIZOL kit (Invitrogen) or the Plant RNeasy mini kit (Qiagen) methods.

Therefore, Vennapusa A, et al. (2020) developed a method suitable for RNA extraction from seeds or plant tissues that contain a lot of polysaccharides such as starch by improving the SDS-LiCl method and modifying the extraction buffer and solution used for RNA precipitation compared to existing protocols to obtain high-yield and high-quality RNA from starch-rich plant tissues including seeds and roots (Vennapusa et al., 2020).

Microtubers attached to the nodal stem and microtuber halves prepared under each hormone culture condition were incubated at 20°C in the dark for 3 days. Samples from 12 conditions were pooled for total RNA extraction in triplicate on day 3 of culture using the SDS-LiCl method with some changes and treated with TURBO DNase (Invitrogen, Waltham, MA, USA), including apical bud tissues (about 100-120 mg) from stMTs or hMTs treated with GA, CK, GACK, or control (untreated), respectively; and nodal stem tissues (about 100-120 mg) from stMTs treated with GA, CK, GACK, or control. Sample (a total of 36) collection for RNA-seq analysis by detailed site on day 3 of culture is depicted in **Figure 19**. Taking tissue samples is the first critical step in isolating quality RNA. All samples taken in this experiment were flash-frozen in liquid nitrogen and stored in a freezer at -80 °C until RNA extraction.

In this experiment, RNA extraction was performed with slight modifications, referring to the SDS-LiCl method with some changes (**Figure 20**), followed by treatment with TURBO DNase (Invitrogen, Waltham, MA, USA) to eliminate trace genomic DNA. Samples were judged to be of good quality based on absorbance measurements and electrophoresis, then used for subsequent RNA-seq. The RNA extraction method is unable to completely remove DNA contamination from RNA preparations. To digest DNA concentrations below known levels of detection through PCR, and remove cations that degrade RNA, I perform an additional DNA removal treatment using a Turbo DNA-free kit.

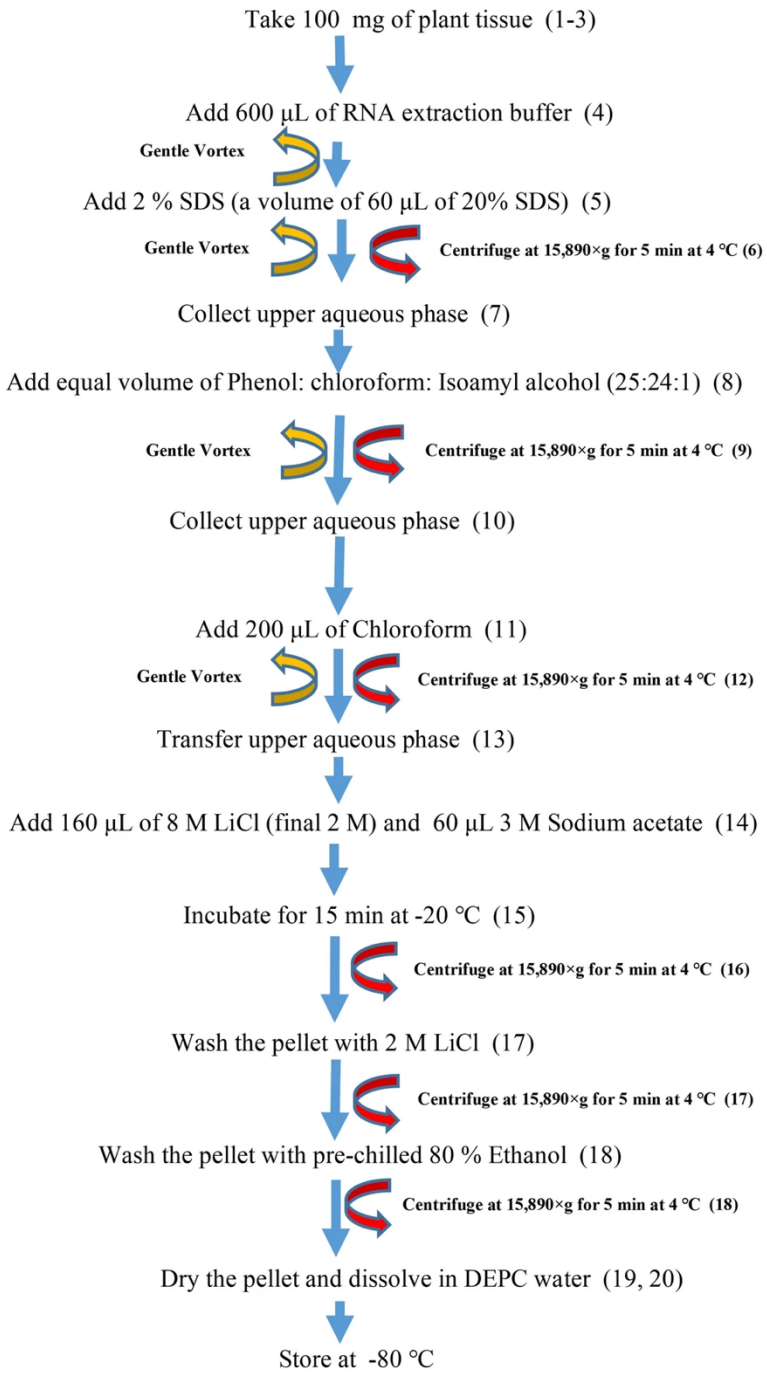


Figure 20. Flow chart describing the major steps involved in the total RNA extraction using the modified SDS-LiCl method (Vennapusa A, et al. 2020).

3.2.4 TPM Value Calculation and Differential Expression

Trimmomatic (version 2.13) (Bolger et al., 2014) and the Cutadapt program (Martin, 2011) were used to trim adapter sequences and low-quality reads from the above. The obtained clean reads were mapped to the potato genome sequence of doubled monoploid S. tuberosum (PGSC_DM_v4.03) downloaded from the Spud DB Potato Genomics Resource (Nuraini *et al.*, 2018), using the HISAT2 (version 2.0.1) (Kim et al., 2019). The default settings were used for mapping. In total, 84.96-89.14% of reads per sample aligned to the transcriptome. The mapped reads were assembled and counted using StringTie (version 2.2.1) (Shumate et al., 2022), and both the estimated raw count values and the normalized expression as transcript per million (TPM) for each gene were retrieved from the mapping. DESeq2 (Love et al., 2014), running through the R (version 4.2.2), was then used to analyze differentially expressed genes (DEGs) between the two samples based on the raw counts (DEGs were calculated by comparing the gene expression between the exact type of tissues in the same conditions) with an absolute value of log2 fold change (|log2 FC|) > 1 and a false discovery rate (FDR) < 0.05 selected as thresholds. Detected DEGs were then annotated against ENSEMBL release S. tuberosum SolTub_3.0 or a search tool for orthologous genes (g: Orth) in g: Profiler (Raudvere et al., 2019), Gene Ontology (GO), and KEGG. In this work, a p<0.05 cutoff was taken after enrichment analysis to indicate significantly enriched GO functions and KEGG pathways (Sherman et al., 2022) using DAVID Bioinformatics Resources. The gene expression profile was visualized using the ClusterProfiler 4.0 package through the R (Wu et al., 2021).

3.2.5 Module Construction using WGCNA Package

The weighted gene correlation network analysis (WGCNA) was conducted using the WGCNA package in R (Langfelder and Horvath, 2008). The parameters were as follows: the soft threshold power was 14; the min module size was 30; and the merge cut height was 0.25 for a total of 6515 DEGs involved in treatments on day 3 of culture, with a TPM value > 1 in at least one of the samples to be identified from the 36 samples used for performing the co-expression network analysis in my work. The eigengene values were computed for each module to identify associated links with potato MT sprouting, with a

visualization of the interaction network conducted via Cytoscape (version 3.10.0) (Bindea et al., 2013).

3.2.6 Quantitative Analysis of Candidate Genes Involved in Potato Microtuber Sprouting

Based on transcriptome results, eight genes involved in the regulation of MT sprouting were selected for quantitative real-time polymerase chain reaction (RT-qPCR) analysis to examine the transcriptomic profiles, with the primers listed in **Table 3**. Primer design was conducted based on the output results of Primer 3 (version 0.4.0): https://bioinfo.ut.ee/primer3-0.4.0/ (accessed on 28 August 2023). Oligonucleotides used for primers in RT-qPCR were synthesized by Fasmac Co., Ltd. (Atsugi, Japan). qPCR reactions were performed as follows: initial denaturation at 95 ◦C for 15 min, followed by 40 cycles, each with denaturation at 95 ◦C for 10 s and annealing at 60 ◦C for 30 s. Finally, melting curve analysis was conducted in a 65-95 ◦C temperature range. The samples from the three independent biological replicates were used for the analyses. The quantitative data of candidate genes were calculated using the $2^{-\Delta\Delta Ct}$ method (Livak and Schmittgen, 2001).

Table 3. Primer sequences were used to amplify target genes. α-tubulin for housekeeping as an internal control.

Gene ID PGSC0003DMG-	Primer	Primer Sequence (5' → 3')	Length of Oligonucleotides /bp
α-tubulin	α-Tub-rt-Fd1	CAACAAGTGTTGCTGAGGTCT	21
	α-Tub-rt-Rv1	CAGCCTACATCATTGCTCAGT	21
402022640	RR4-Fd2	CCAACTCTTTCACCTTCACCA	21
	RR4-Rv1	TGGCTGATCATTTTGAGTCG	20
400003084	RR9c-Fd2	TGTTTGGAAGAAGGAGCTGAA	21
	RR9c-Rv1	CAAATGTTCTGCAAAAAGATGC	22
400028331	CISZOG-Fd2	TTCGGGATGGAACTCTTTTCT	21
	CISZOG-Rv2	TCCATCAATGTTCTCACACCA	21
400012669	CYP735A-Fd1	ATGAAACCACTGCCCTTTTG	20
	CYP735A-Rv2	CCTCAAATGCCATTCTTGGT	20
400001655	SAUR71-Fd1	TTGGCTATACCTTGCGATGA	20
	SAUR71-Rv1	CCCAGTAACGCTCGAGATTC	20
400001614	SAUR50-Fd2	TCACAATCTCCTGTTTTGAAGC	22
	SAUR50-Rv1	GCCCATATCATGATCGAACC	20
400020139	*IAA15*-Fd1	ACCTGGAACAGAGCCATCAT	20
	IAA15-Rv1	TTAAATAAGCCGCACCATCC	20
400011033	PYL4-Fd1	GACGGTGACGTCGGTACTTT	20
	PYL4-Rv2	ATTCCACAACGATCGTCTCC	20
400021991	GID1-Fd2	AGGACATGGCTTCAAAGTGG	20
	GID1-Rv2	CCCGTCCAATCTCTTCTCAG	20
400006108	IAA22-Fd1	GGCTTTGCCTGAATCAACTC	20
	IAA22-Rv1	GGCACCATCCATGCTAACTT	20
400029339	IAA26-Fd1	TACAAGTGCCAGCAGTCAGG	20
	IAA26-Rv1	GATGCCCCTTTTCTTTCACA	20
400002945	RR9a-Fd1	CAGAATTTGCAGCAAGTGGA	20
	RR9a-Rv2	TGCCCCTTCTTCTAAGCATC	20
400029852	RR9d-Fd2	GGAATCTGCATCTCTGAGGAAC	22
	RR9d-Rv2	TGTTGTTTGGGGCTTTTACATT	22
400027597	RR17c-Fd1	GAARATGGTCTRAGGGCMTT	20
	RR17c-Rv1	ATMACAACTGGYACATCCTTCA	22
400008137	CISZOG-Fd1	TCTCCACCTCTCGAGGCTAA	20
	CISZOG-Rv2	ACGGAAATGGATTGTTGCAT	20
400000432	CISZOG-Fd2	AGCTAGCTATTGGGCTGGAAG	21
	CISZOG-Rv2	CTGTTGACGGGTGTCCTAAAA	21

3.2.7 Quantification and Statistical Analysis

In the case of the sprouting rate, data from three biological replicates were provided as means (±standard deviation); in the case of qPCR and TPM, data from three biological replicates were provided as means (±standard error). All data were subjected to analysis of variance (ANOVA) using GraphPad PRISM (version 10), and mean differences were tested for statistical significance using Tukey's multiple comparisons with a 95% confidence level outcome.

3.3 Results

3.3.1 Response of Microtuber Sprouting to Phytohormone Treatment

To understand the effect of the nodal stem on sprouting, I investigated microtuber (MT) sprouting using three kinds of MTs: stMTs, destemmed microtubers (deMTs), and hMTs, as described in **2.2.2** (**Figure 14**). For the stMTs, I observed that the sprouting behavior occurred after GA treatment alone and after both GA and CK treatment (GACK). GA and GACK treatment could induce sprouting on day 1, and there was barely a difference for shoots on day 15 of culture between GA and GACK treatments at the morphological level (**Figure 18**). I did not observe any sign of sprouting behavior with CK treatment alone after 15 days. There was no significant difference in sprouting rate between the GA and GACK treatments, as shown by the adjusted p value > 0.05 of Tukey's multiple comparisons test result (**Table 4**). The observation for deMT sprouting suggests that the junction part could support GA-induced sprouting and the CK co-application could make up for the insufficiency, which the deMT sprouting rate reached 34% on day 4 of culture and stopped increasing thereafter. There were significant differences in sprouting rate between the GA and GACK treatments with the adjusted p value = 0.003 (< 0.05) of Tukey's multiple comparisons test result (**Table 5**) due to the CK co-application.

I noticed that the sprouting behavior in hMTs only occurred after GACK treatment (**Figure 17, Figure 18**) when the nodal stem was excised, suggesting that both GA and CK are essential for MT sprouting, and that GA alone or CK alone was insufficient to induce the sprouting behavior. When treated with GACK, there were noticeable differences in shoot morphology between stMTs and hMTs on day 10 of the culture (**Figure 17**). However, this difference disappeared on day 15 of the culture (**Figure 18**).

In addition, I conducted a Tukey's multiple comparisons test in sprouting rate among three sprouting-induced conditions using one-way ANOVA with the adjusted p value > 0.05; there were no significant differences in the sprouting behavior among GA-treated and GACK-treated stMTs sprouting, and GACK-treated hMTs (**Table 7**). These results indicate that the nodal stem or exogenous CK co-application is essential for supporting GA to induce MT sprouting, and there was no significant difference in sprouting-induced

conditions between GA combined with the nodal stem and GA combined with CK co-application.

Table 4. Ordinary one-way ANOVA of sprouting rate in stemmed microtubers.

Tukey's-multiple comparisons test	Mean Diff.	95.00% CI of diff.	Below threshold	Summary	Adjusted P Value	
Control vs. GA	-68.37	-89.85 to -46.89	Yes	****	<0.0001	A-B
Control vs. CK	0.3788	-21.10 to 21.86	No	ns	>0.9999	A-C
Control vs. GACK	-78.22	-99.70 to -56.74	Yes	****	<0.0001	A-D
GA vs. CK	68.75	47.27 to 90.23	Yes	****	<0.0001	B-C
GA vs. GACK	-9.848	-31.33 to 11.63	No	ns	0.622	B-D
CK vs. GACK	-78.6	-100.1 to -57.12	Yes	****	<0.0001	C-D

Test details: Number of comparisons = 6; Alpha = 0.05; n1 = 16; n2 = 16;
SE of diff. = 8.128; DF = 60.

Table 5. Ordinary one-way ANOVA of sprouting rate in destemmed microtubers.

Tukey's-multiple comparisons test	Mean Diff.	95.00% CI of diff.	Below threshold	Summary	Adjusted P Value	
Control vs. GA	-28.41	-40.38 to -16.44	Yes	****	<0.0001	A-B
Control vs. CK	0	-11.97 to 11.97	No	ns	>0.9999	A-C
Control vs. GACK	-48.2	-60.17 to -36.23	Yes	****	<0.0001	A-D
GA vs. CK	28.41	16.44 to 40.38	Yes	****	<0.0001	B-C
GA vs. GACK	-19.79	-31.76 to -7.823	Yes	***	0.0003	B-D
CK vs. GACK	-48.2	-60.17 to -36.23	Yes	****	<0.0001	C-D

Test details: Number of comparisons = 6; Alpha = 0.05; n1 = 16; n2 = 16;
SE of diff. = 4.529; DF = 60.

Table 6. Ordinary one-way ANOVA of sprouting rate in microtuber halves.

Tukey's-multiple comparisons test	Mean Diff.	95.00% CI of diff.	Below threshold	Summary	Adjusted P Value	
Control vs. GA	0	-12.38 to 12.38	No	ns	>0.9999	A-B
Control vs. CK	0	-12.38 to 12.38	No	ns	>0.9999	A-C
Control vs. GACK	-58.45	-70.84 to -46.07	Yes	****	<0.0001	A-D
GA vs. CK	0	-12.38 to 12.38	No	ns	>0.9999	B-C
GA vs. GACK	-58.45	-70.84 to -46.07	Yes	****	<0.0001	B-D
CK vs. GACK	-58.45	-70.84 to -46.07	Yes	****	<0.0001	C-D

Test details: Number of comparisons = 6; Alpha = 0.05; n1 = 16; n2 = 16;
SE of diff. = 4.686; DF = 60.

Table 7. Ordinary one-way ANOVA of three sprouting-induced conditions.

Tukey's-multiple comparisons test	Mean Diff.	95.00% CI of diff.	Below threshold	Summ ary	Adjusted P Value	
stMT-GA vs. stMT-GACK	-9.848	-36.09 to 16.40	No	ns	0.6372	A-B
stMT-GA vs. hMT-GACK	10.3	-15.95 to 36.54	No	ns	0.6114	A-C
stMT-GACK vs. hMT-GACK	20.14	-6.102 to 46.39	No	ns	0.1621	B-C

Test details: Number of comparisons = 3; Alpha = 0.05; n1 = 16; n2 = 16;
SE of diff. = 10.83; DF = 45.

3.3.2 Transcriptome Sequencing and *de novo* Assembly

In this study, I used *Solanum tuberosum* L. ssp. *andigena* (2n = 4x = 48) for the research. For the transcriptome analysis, 36 samples generated 103.61Gb clean data through RNA sequencing. About 92.09-93.58% of clean data achieved a quality score of Q30 (sequencing error rate < 0.1%), and 84.96-89.14% of the clean reads were successfully mapped to the potato reference genome (S. tuberosum PGSC_DM_v4.03) (Nuraini *et al.*, 2018) (**Table 8**), indicating that all libraries were of high quality. Based on gene expression, principal component analysis (PCA) showed that the 36 samples were assigned to three groups, each associated with one tissue type from two kinds of MTs. As expected, no spurious sample clusters were identified. The first (PC1) and second (PC2) principal components accounted for 34.06% and 10.15% of the total variance, respectively. PC1 separated samples into two big groups corresponding to tissue differences between tissue types: apical bud tissues of stMTs and hMTs, and nodal stem tissues of stMTs. In comparison, PC2 separated samples into two big groups corresponding to the difference between MT types: stMTs including apical bud tissues and nodal stem tissues, and hMTs including apical bud tissues. The PC1 value was greater than PC2 value, demonstrating that gene expression patterns were more affected by different tissue types than MT types. Moreover, gene expression data from the same type of tissue clustered together but differed among the treatments with different phytohormones (**Figure 21**). The first and second principal components accounted for 34.06% and 10.15% of the total variance, respectively, showing a good correlation among the three biological replicates for the 36 samples of the RNA-seq results.

Table 8. Summary of RNA-seq data generated from 36 samples.

Sample name*	Clean reads	Mapped reads (%)	GC Content (%)	Q30 Bases Rate (%)
3-stMT-bd-Con_1	43,681,568	86.01	43.23	92.36
3-stMT-bd-Con_2	41,043,396	84.96	42.71	92.84
3-stMT-bd-Con_3	42,184,662	86.44	42.60	92.70
3-stMT-bd-GA_1	48,289,086	86.39	43.16	92.62
3-stMT-bd-GA_2	53,701,594	87.57	43.57	92.29
3-stMT-bd-GA_3	48,581,534	86.63	43.00	92.91
3-stMT-bd-CK_1	39,696,672	86.79	42.60	93.58
3-stMT-bd-CK_2	55,057,060	86.93	42.78	93.03
3-stMT-bd-CK_3	48,249,408	86.56	42.73	93.34
3-stMT-bd-GACK_1	54,286,264	86.61	43.15	92.98
3-stMT-bd-GACK_2	45,950,936	87.25	43.07	92.92
3-stMT-bd-GACK_3	45,743,028	87.76	43.44	93.39
3-stMT-st-Con_1	45,423,060	86.01	42.85	92.27
3-stMT-st-Con_2	53,654,956	84.96	42.91	93.00
3-stMT-st-Con_3	59,954,606	86.44	43.64	92.27
3-stMT-st-GA_1	53,629,136	86.39	43.25	92.78
3-stMT-st-GA_2	55,193,846	87.57	43.38	92.85
3-stMT-st-GA_3	49,795,808	86.63	43.49	92.97
3-stMT-st-CK_1	53,347,826	86.79	43.45	93.14
3-stMT-st-CK_2	54,308,396	86.93	43.13	93.25
3-stMT-st-CK_3	46,884,960	86.56	43.44	92.96
3-stMT-st-GACK_1	48,972,376	86.61	43.51	93.15
3-stMT-st-GACK_2	40,544,512	87.25	43.62	93.36
3-stMT-st-GACK_3	49,480,050	87.76	42.75	92.91
3-hMT-bd-Con_1	43,157,574	85.59	42.17	92.56
3-hMT-bd-Con_2	56,598,482	85.63	42.18	92.53
3-hMT-bd-Con_3	47,043,018	85.65	43.27	92.74
3-hMT-bd-GA_1	55,008,322	86.01	42.75	92.95
3-hMT-bd-GA_2	52,098,892	84.96	42.16	92.83
3-hMT-bd-GA_3	40,728,744	86.44	42.85	92.77
3-hMT-bd-CK_1	43,493,506	86.39	42.91	93.17
3-hMT-bd-CK_2	54,588,608	87.57	42.61	93.49
3-hMT-bd-CK_3	49,590,678	86.63	42.75	93.62
3-hMT-bd-GACK_1	44,376,982	86.79	42.82	93.23
3-hMT-bd-GACK_2	50,462,110	86.93	43.24	93.33
3-hMT-bd-GACK_3	46,772,868	86.56	43.83	93.27

* Sample name includes all tissues used to extract RNA, bd: apical bud tissue; st: nodal stem tissue; stMT: stemmed microtuber; hMT: microtuber half; Clean reads: Number of reads remaining after filtering; Q30 bases rate: Proportion of nucleotides with a quality value larger than 30 in the filtered reads.

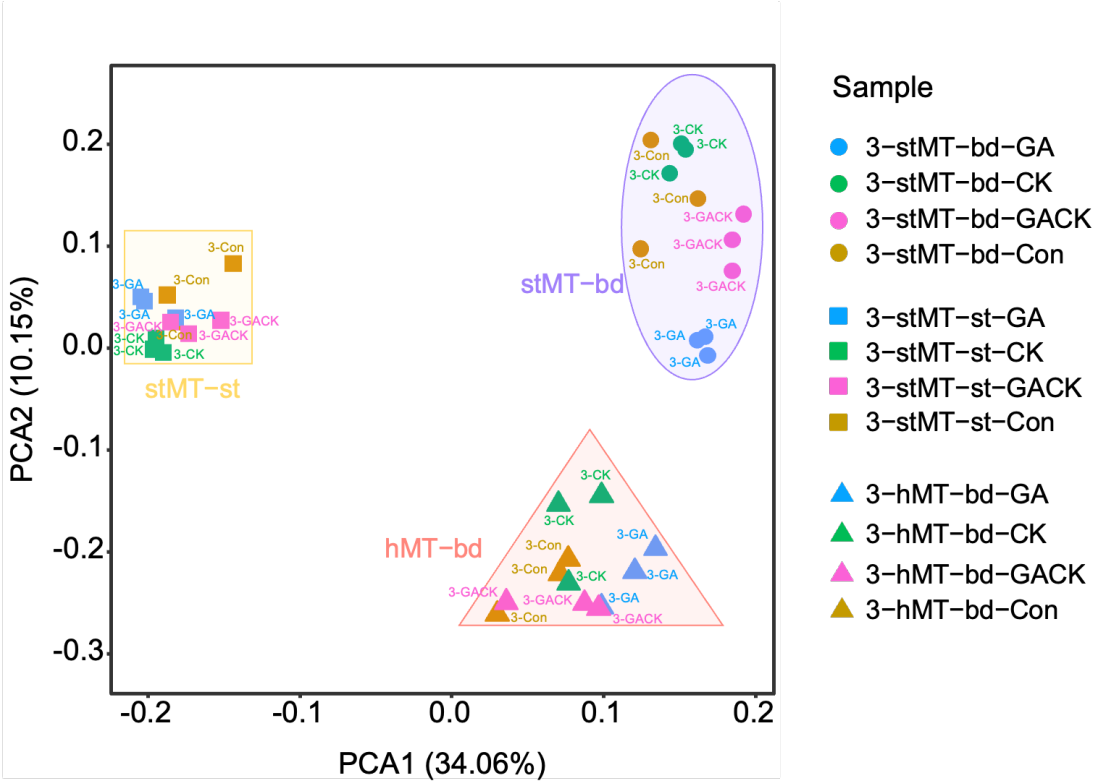


Figure 21. Principal component analysis (PCA) calculated TPM (Transcripts Per kilobase Million) values for RNA-seq data from 36 samples, visualized using the ggplot2 package in R.

Genes included had a TPM over one for all replicates within my study (39,028 genes included in the analysis). Principal components 1 and 2 (PC1 and PC2) could represent 34.06% and 10.15% of all differences among apical bud tissues (bd) and nodal stem tissues (st) of stemmed microtubers (stMTs), and apical bud tissues (bd) of microtubers halves (hMTs), respectively. PCA plots represent the transcript levels from three hormone-treated groups (GA, CK, and GACK) and one untreated group (Con) on day 3 (3-) of culture. Each treatment has three biological replicates.

3.3.3 Differential Transcriptome Response to Exogenous Hormone Treatments

I first calculated the differentially expressed genes (DEGs) using DESeq2 for nine pairwise comparisons between the phytohormone treatment (GA, CK, or GACK) and the untreated control (Con) in the apical buds of stMTs or hMTs or the nodal stems of stMTs cultured on day 3 (3-), respectively (**Figure 22**). For the apical buds of stMTs (3-stMT-bd), 2789 DEGs were detected after treatment with GA when compared to Con (3-stMT-bd-GA/Con), 698 DEGs were detected after treatment with CK when compared to Con (3-stMT-bd-CK/Con), and 1811 DEGs were detected after treatment with GACK when compared to Con (3-stMT-bd-GACK/Con). For the apical buds of hMTs (3-hMT-bd), 2095, 1667, and 4058 DEGs were detected in the comparisons of 3-hMT-bd-GA/Con, 3-hMT-bd- CK/Con, and 3-hMT-bd-GACK/Con, respectively. For the nodal stems of stMT (3-stMT-st), 239, 516, and 850 DEGs were detected in the comparison of 3-stMT-st-GA/Con, 3-stMT-st-CK/Con, and 3-stMT-st-GACK/Con, respectively. Excluding duplicates, a total of 6515 DEGs were detected. The amount of DEGs was much larger in both 3-stMT-bd-GA/Con and 3-hMT-bd-GACK/Con, indicating that the combination of GA and the nodal stem, and the combination of GA and CK treatments play a vital role in this sprouting behavior.

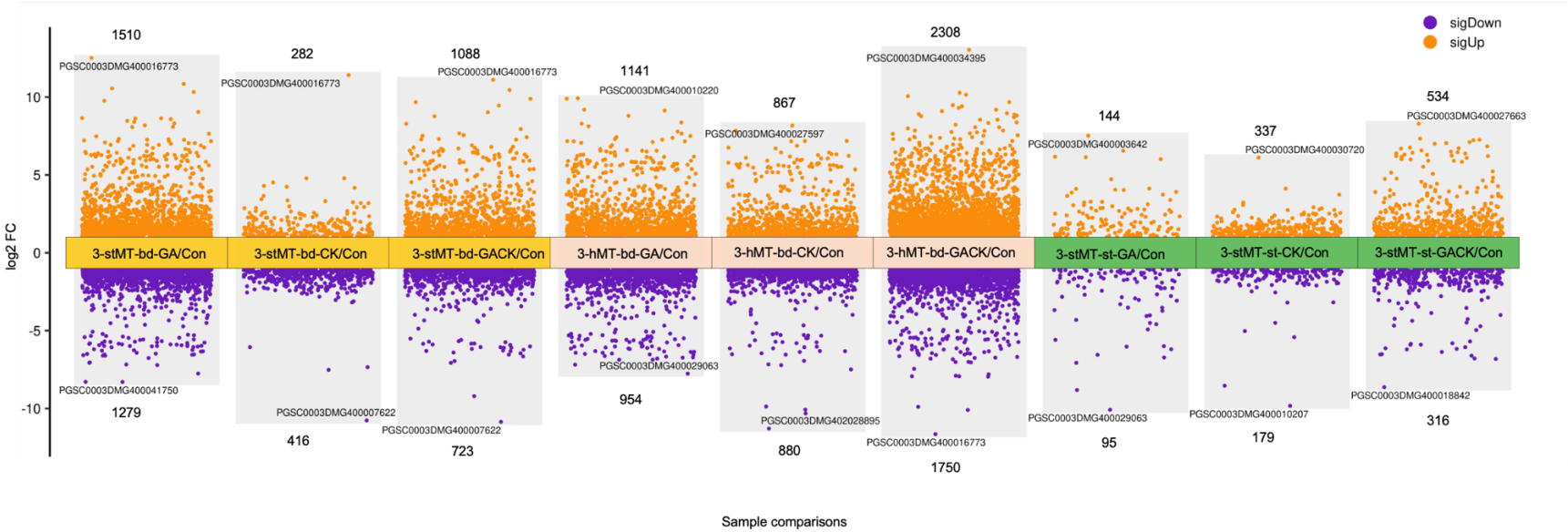


Figure 22. Identification of differentially expressed gene (DEG) between hormone treatment with untreated control.

Volcano plot and numbers (next to the dots) of the differentially upregulated (orange) and downregulated (purple) DEGs in the pairwise comparisons of phytohormone treatment (GA, CK, or GACK) with control (Con, untreated) in apical bud tissues (bd) of stemmed microtubers (stMTs) (A) and microtuber halves (hMTs) (B), and in the nodal stem tissue (st) of stMTs (C) on day 3 (3-) of culture. DEGs were calculated using the DEseq2 package in R. The up- or down-regulated counts of DEGs and genes with the highest or lowest log2FC value were shown next to the volcano plot.

To better understand the difference in the transcriptional response of sprouting to exogenous hormone treatment, I performed DEG annotation and functional categorization using Gene Ontology (GO) (**Table 9**) and KEGG pathway enrichment (**Table 10**) analysis for 6515 DEGs. GO enrichment analysis has three major categories: biological processes, cellular components, and molecular functions. This study mainly focused on biological processes to identify the vital processes in sprouting behavior. Interestingly, I detected that several hormone-related terms associated with auxin, including "response to auxin", "auxin polar transport", "auxin efflux", and "auxin-activated signaling pathway", were significantly enriched in biological processes. This result indicates that endogenous auxin responded to hormone treatment. Next, KEGG pathway enrichment analysis showed that genes were enriched into sixteen pathway terms (p<0.05). Of the sixteen terms, "Plant hormone signal transduction" (sot04075) was the central pathway with the lowest p value. Notably, a CK-related pathway, "Zeatin biosynthesis" (sot00904), was also significantly enriched. These results suggest that terms like "response to auxin", "Plant hormone signal transduction", and "Zeatin biosynthesis" should be the main focus of this transcriptome analysis.

Table 9. Gene Ontology (GO) enrichment analysis for 6515 DEGs

(Top 10 of GO terms in each category).

Term ID	Term Description	Gene Count	Gene (%)	*p* Value
Category of Biological Processes				
GO:0042546	cell wall biogenesis	17	0.46	1.49E-08
GO:0010411	xyloglucan metabolic process	18	0.49	9.59E-08
GO:0009416	response to light stimulus	26	0.71	3.98E-07
GO:0045893	positive regulation of transcription, DNA-templated	30	0.82	1.28E-05
GO:0046274	lignin catabolic process	13	0.35	1.75E-05
GO:0002238	response to molecule of fungal origin	36	0.98	2.73E-05
GO:0009805	coumarin biosynthetic process	36	0.98	2.73E-05
GO:0006355	regulation of transcription, DNA-templated	114	3.10	6.20E-05
GO:0010597	green leaf volatile biosynthetic process	57	1.55	7.42E-05
Category of Cellular Component				
GO:0005886	plasma membrane	256	6.96	4.93E-28
GO:0005576	extracellular region	108	2.94	2.91E-13
GO:0048046	apoplast	43	1.17	2.50E-08
GO:0005634	nucleus	466	12.68	4.40E-07
GO:0000786	nucleosome	25	0.68	4.14E-06
GO:0031225	anchored component of membrane	18	0.49	9.07E-06
GO:0005615	extracellular space	25	0.68	2.05E-04
GO:0046658	anchored component of plasma membrane	29	0.79	7.02E-04
GO:0009523	photosystem II	18	0.49	7.26E-04
GO:0009506	plasmodesma	15	0.41	0.00113
Category of Molecular Function				
GO:0003700	transcription factor activity, sequence-specific DNA binding	179	4.87	3.17E-11
GO:0000976	transcription regulatory region sequence-specific DNA binding	82	2.23	9.90E-09
GO:0043565	sequence-specific DNA binding	75	2.04	4.81E-07
GO:0052716	hydroquinone:oxygen oxidoreductase activity	13	0.35	1.07E-05
GO:0016762	xyloglucan:xyloglucosyl transferase activity	17	0.46	1.20E-05
GO:0016717	oxidoreductase activity, acting on paired donors	11	0.30	1.75E-05
GO:0005507	copper ion binding	26	0.71	2.48E-05
GO:0016491	oxidoreductase activity	86	2.34	3.29E-05
GO:0019901	protein kinase binding	13	0.35	1.11E-04
GO:0015250	water channel activity	11	0.30	4.52E-04

Table 10. KEGG pathway enrichment analysis for 6515 DEGs.

Term ID	Term Description	Gene Count	Gene (%)	*p* Value
Category of KEGG pathways				
sot04075	Plant hormone signal transduction	74	2.01	5.54E-10
sot01100	Metabolic pathways	375	10.20	1.66E-06
sot01110	Biosynthesis of secondary metabolites	232	6.31	1.77E-06
sot00940	Phenylpropanoid biosynthesis	46	1.25	6.18E-05
sot00904	Diterpenoid biosynthesis	14	0.38	1.56E-04
sot00196	Photosynthesis - antenna proteins	12	0.33	0.001436
sot00053	Ascorbate and aldarate metabolism	19	0.52	0.001925
sot00040	Pentose and glucuronate interconversions	26	0.71	0.009549
sot02010	ABC transporters	17	0.46	0.011213
sot00480	Glutathione metabolism	24	0.65	0.011783
sot04814	Motor proteins	21	0.57	0.01533
sot01250	Biosynthesis of nucleotide sugars	21	0.57	0.020771
sot00908	Zeatin biosynthesis	14	0.38	0.023116
sot00062	Fatty acid elongation	10	0.27	0.02734
sot00052	Galactose metabolism	13	0.35	0.039452
sot04712	Circadian rhythm - plant	11	0.30	0.048449

3.3.4 Weighted Gene Co-expressed Gene Network Analysis (WGCNA)

To further investigate the gene regulatory network of phytohormone signaling involved in this sprouting behavior, I employed a weighted gene co-expression network analysis (WGCNA) using a total of 6515 DEGs. The analysis resulted in 12 co-expression modules labeled and highlighted using different colors (**Figure 23**, **Supplementary Table S6** of Zhang et al,. (Zhang et al., 2023)). The results revealed that the magenta module ($r = 0.63$, p value $= 4 \times 10^{-5}$) was highly and positively correlated with GACK-triggered gene expression. In this gene set (117 genes), genes involved in the nodal stem of stMTs treated with GA and GACK (**Figure 24**) were highly upregulated in this module, according to the kME value (eigengene-based connectivity) value. KEGG enrichment analysis showed that four genes related to only CK and auxin were enriched in the "Plant hormone signal transduction" pathway (**Table 11**), including *RR4* and *SAUR 71*. These results suggest that endogenous CK was involved in the nodal stem, given that the upregulation of DEGs relevant to sprouting were detected in the nodal stem with GA-only treatment.

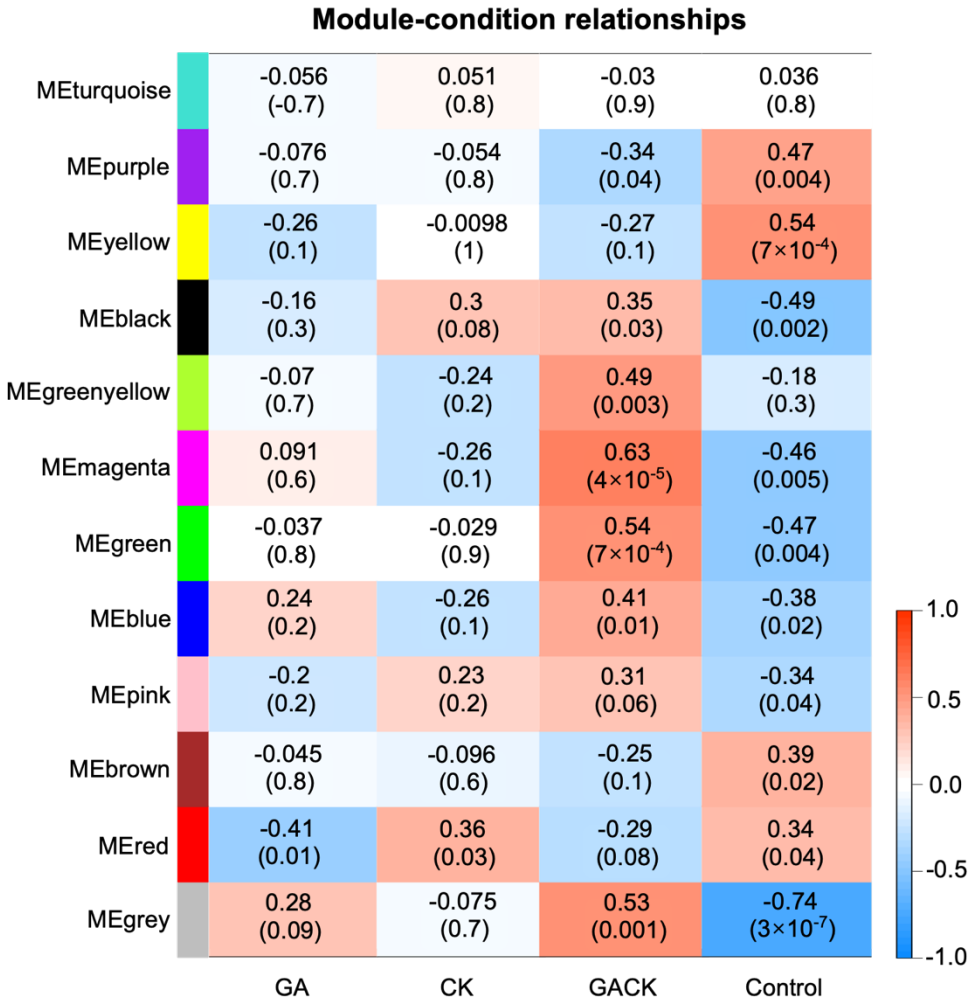


Figure 23. A weighted-gene co-expression network for a total of 6515 DEGs detected in this work.

Module-condition relationships were established, and module-trait associations were based on Pearson correlations.

Each row represents one module, and the gene numbers in each module are shown in **Supplementary Table S6** of Zhang et al., (Zhang *et al.*, 2023).

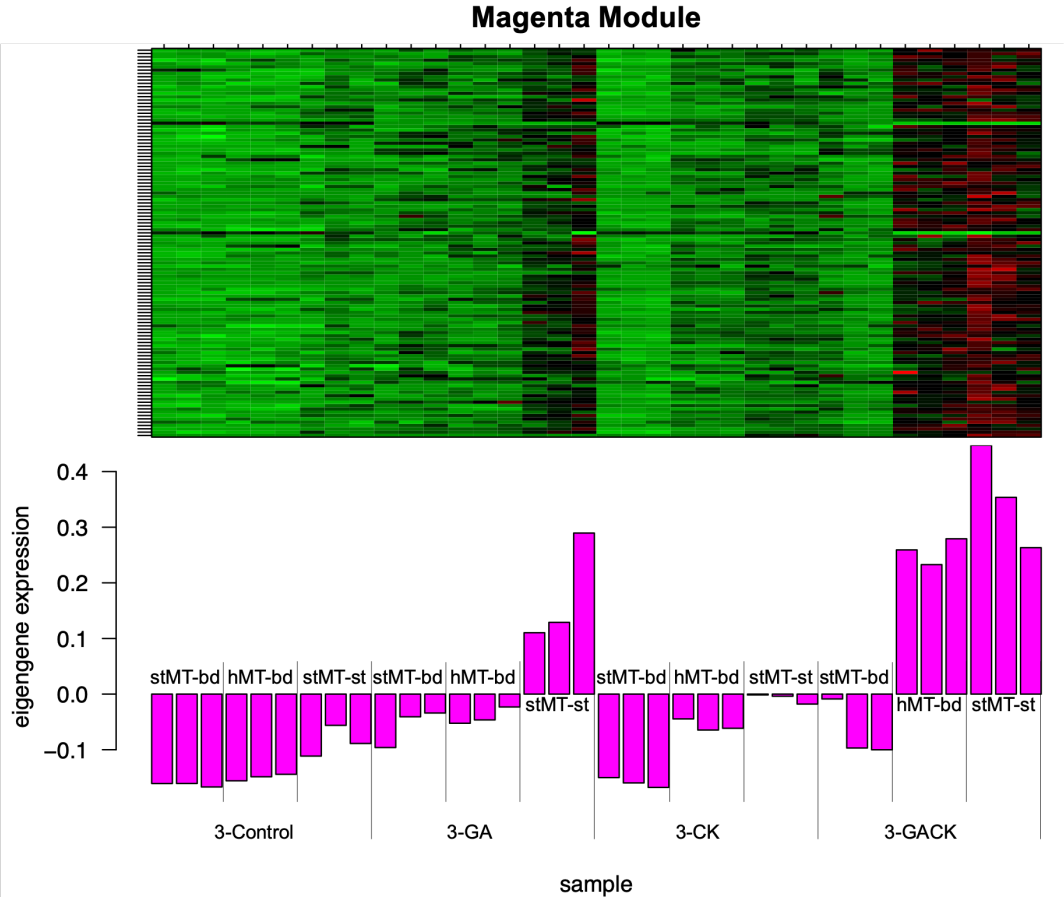


Figure 24. A weighted-gene co-expression network for a total of 6515 DEGs detected in this work.

Expression pattern of genes in the magenta module.

Genes in this magenta module are shown in **Supplementary Table S7** of Zhang et al., (Zhang *et al.*, 2023).

Table 11. The hub genes enriched in "Plant hormone signal transduction" pathway for 117 DEGs.

Gene ID PGSC0003DMG	Gene Description	Function	kME (eigengene-based connectivities) value
402022640	RR4	Type-A response regulator	0.78
400029852	RR9d	Type-A response regulator	0.78
400029190	SAUR	Auxin responsive SAUR family	0.83
400001655	SAUR	Auxin responsive SAUR family	0.89

In contrast, the red module (r = -0.41, *p* value = 0.01) had the highest negative correlation with GA-triggered gene expression. In this gene set (275 genes), genes involved in the nodal stem and apical buds of stMTs and in the apical buds of hMTs treated with GA and GACK (**Figure 25**) were highly downregulated in this module according to the kME value (**Supplementary Table S7** of Zhang et al., (Zhang *et al.*, 2023)). GO enrichment analysis revealed that genes involved in the "cytokinin biosynthetic process" connecting with the "cytokinin-activated signaling pathway" were downregulated (**Figure 26**, **Supplementary Table S8** of Zhang et al., (Zhang *et al.*, 2023)), reflecting that GA could result in the inactivation of genes related to CK biosynthesis because DEGs in this term were downregulated even in sprouting-failed buds of hMTs with GA-treatment. These results further suggest that treatment with GA alone could cause a reduction in gene expression relevant to CK in apical buds, and the nodal stem might be a source of endogenous CK for GA-induced sprouting.

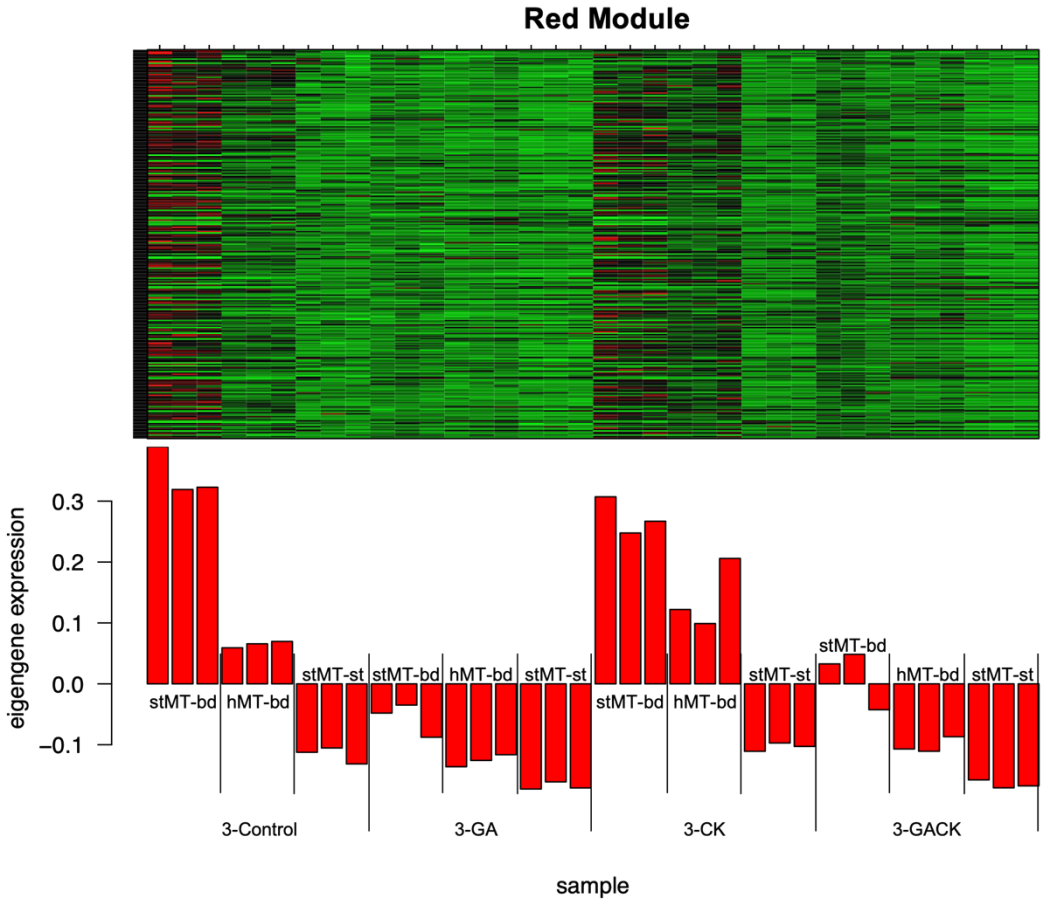


Figure 25. A weighted-gene co-expression network for a total of 6515 DEGs detected in this work.

Expression pattern of genes in the red module.

Genes in this red module are shown in Table **Supplementary Table S7** of Zhang et al., (Zhang *et al.*, 2023).

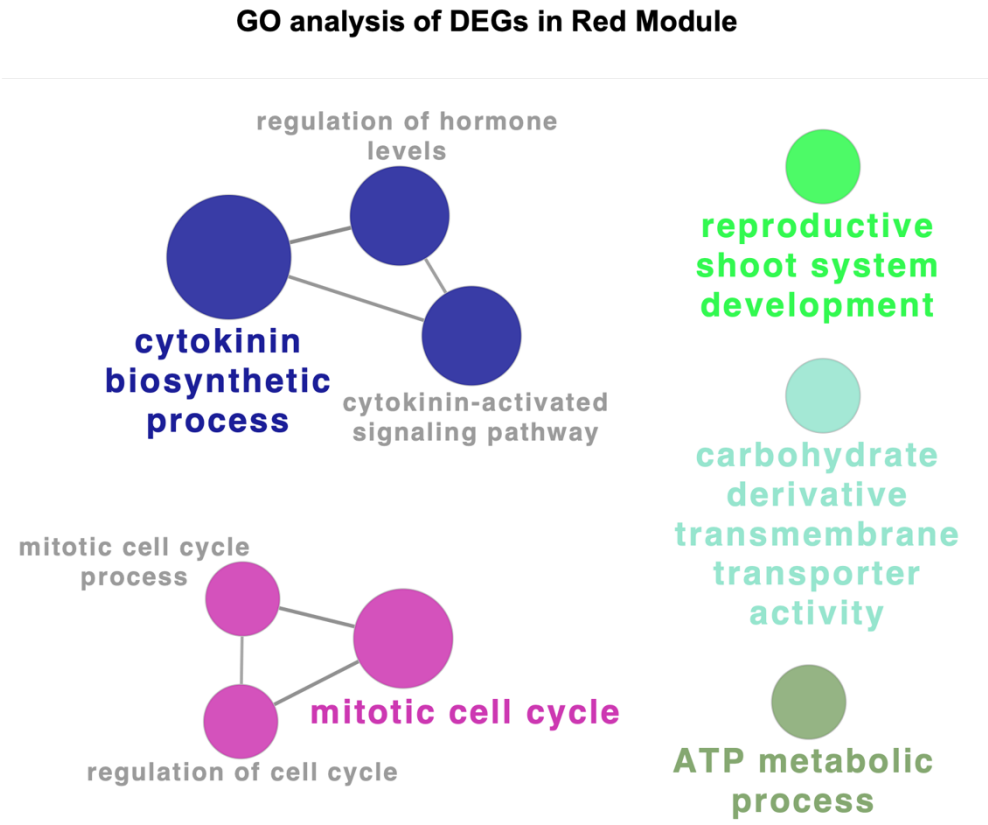


Figure 26. A weighted-gene co-expression network for a total of 6515 DEGs detected in this work.

Network analysis of enriched GO terms (*p* value < 0.05) for 275 DEGs in the red module was visualized by the ClueGO plugin in Cytoscape (v 3.10.0).

Genes in this each term are shown in **Supplementary Table S8** of Zhang et al., (Zhang *et al.*, 2023).

3.3.5 Cytokinin- and Auxin-activated Signaling are Involved in Microtuber Sprouting

To figure out the detailed gene response to sprouting growth, I compared the differences in DEGs in apical bud tissue among the three sprouting-inducible conditions (stMTs treated with GA or GACK, or hMTs treated with GACK) with the untreated Con: 2789, 1811, and 4058 DEGs in comparison to 3-stMT-bd-GA/Con, 3-stMT-bd-GACK/Con, and 3-hMT-bd-GACK/Con, respectively (**Figure 22**, **Figure 27A**). They shared 1064 DEGs and harbored 910, 172, and 2396 unique DEGs, respectively. The largest number (4058) of DEGs were detected in the GACK-treated apical bud tissues of hMTs, followed by 2789 DEGs detected in the GA-treated apical bud tissues of stMTs, suggesting that this sprouting behavior was mainly in response to GA combined with CK and GA combined with the nodal stem.

To reveal the molecular similarities in this sprouting behavior, I analyzed the 1064 shared DEGs. KEGG pathway enrichment analysis revealed that six pathway terms were significantly enriched (p<0.05) (**Figure 27B**). In the "Plant hormone signal transduction" pathway (**Figure 28**), fifteen genes were grouped: one was type A response regulator *RR9a* involved in the negative regulation of cytokinin signaling; two were ABA-related genes, *PYL4* (ABA core regulator) and *ABF* (annotated as ABA-responsive bZIP transcriptional factor); two were GA receptors, *GID1*; and ten were auxin-related genes, *AUX1* (auxin influx carrier), Aux/IAA, and *SAUR* (small auxins upregulated by RNA, auxin early-responsive genes). Out of the fifteen genes, only three were downregulated: *GID1s* and *ABF*. In contrast, genes related to CK, auxin, and *PYL4* were upregulated. These results suggest that genes related to CK, and auxin are critical in sprouting growth. Five genes were detected in the "Zeatin biosynthesis" pathway: two were cis-zeatin (cis-CK) O-glucosyltransferase (*CISZOG*) involved in the synthesis of cis-zeatin riboside; two were UDP-glycosyltransferase, *UGT85A1*, associated with the process of CK homeostasis; and one was *CYP735A*, annotated as cytokinin trans-hydroxylase, zeatin synthesis. This suggests that the expression of genes related to CK homeostasis and signaling are enhanced in sprouting growth.

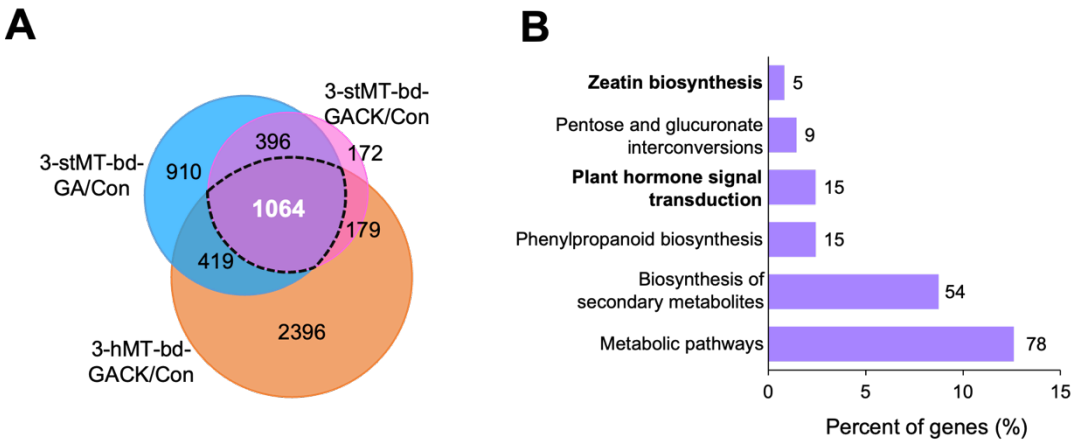


Figure 27. DEGs identified in apical buds of microtuber in sprouting-inducible condition.

(**A**) A Venn diagram to visualize the similarities and differences of DEGs among three comparisons: 3-stMT-bd-GA vs Con (3-stMT-bd-GA/Con), 3-stMT-bd-GACK/Con, and 3-hMT-bd-GACK/Con. The 1064 DEGs of overlap in the diagram represent genes that were coregulated with each respective group of genes.

(**B**) Enriched KEGG pathways for the 1064 shared DEGs analyzed by DAVID (*p* value < 0.05). Counts of DEGs included in each KEGG pathway are shown next to the bar in the graph.

KEGG pathway	Gene ID PGSC0003DMG	Gene Description	Function	Sprouting(-induced) 3-stMT-bd GA/Con	3-stMT-bd GACK/Con	3-hMT-bd GACK/Con	(-failed) 3-hMT-bd GA/Con
Zeatin biosynthesis	400028278	UGT85A1	UDP-glycosyltransferase	1.52	1.27	1.35	
	400003901	UGT85A1	UDP-glycosyltransferase	1.99	1.61	1.60	not enriched pathways
	400012669	CYP735A	Cytokinin hydroxylase-like	2.06	1.73	3.97	
	400029489	CISZOG	*cis*-Zeatin O-glucosyltransferase	2.30	2.08	2.49	
	400008137	CISZOG	*cis*-Zeatin O-glucosyltransferase	1.45	1.50	1.60	
Plant hormone signal transduction	400002945	RR9a	Type-A response regulator	2.89	3.28	4.54	2.04
	400003849	GID1	Gibberellin receptor	-2.30	-1.40	-2.23	-1.76
	400021991	GID1	Gibberellin receptor	-1.47	-1.16	-1.27	not DEG
	400011033	PLY4	Abscisic acid receptor	1.55	2.15	1.40	not DEG
	400023897	ABF	ABA-responsive element Binding Factor	-1.52	-1.75	-1.24	-1.11
	400008504	AUX1	Auxin influx carrier	1.16	1.29	1.51	1.32
	400006550	AUX1	Auxin influx carrier	2.05	1.51	1.97	1.40
	400005327	IAA10	AUX/IAA gene family	2.88	2.37	2.37	1.74
	400005338	IAA11	AUX/IAA gene family	4.89	4.64	3.81	3.74
	400020139	IAA15	AUX/IAA gene family	2.04	2.24	4.13	not DEG
	400006108	IAA22	AUX/IAA gene family	1.19	1.13	1.39	not DEG
	400006093	IAA23	AUX/IAA gene family	1.80	1.42	2.16	1.51
	400029339	IAA26	AUX/IAA gene family	1.51	1.12	4.56	2.21
	400003673	SAUR	Auxin-responsive SAUR family	1.45	1.55	2.74	2.63
	400001614	SAUR	Auxin-responsive SAUR family	2.36	2.27	3.28	not DEG

-2.30 4.89

Figure 28. DEGs identified in apical buds of microtuber in sprouting-inducible condition.

The table shows genes included in the two pathways ("Zeatin biosynthesis" and "Plant hormone signal transduction") among four comparisons: 3-stMT-bd-GA/Con, 3-stMT-bd-GACK/Con, 3-hMT-bd-GACK/Con, and 3-hMT-bd-GA/Con, with a heatmap showing gene expression levels as log2 Fold Change.

Orange represents upregulation, and purple represents downregulation compared to Control (untreated).

Of the 1064 shared DEGs, 335 genes were downregulated and 725 were upregulated (**Figure 29**), suggesting that the activation of genes played a more critical role in responding to this sprouting behavior. I next performed GO analysis for both groups independently to reveal the molecular difference between the up- and down-regulated common DEGs in sprouting buds (**Figure 30 and Figure 31**). ClueGO network analysis showed that seven significantly enriched GO terms classified into five groups were detected for 335 DEGs using GO term fusion with the criteria of p value < 0.05. The most significantly enriched terms (with the lowest p value) were summarized as the cytokinin biosynthesis process, including cytokinin-activated signaling pathway, shoot system development, purine ribonucleotide biosynthesis, cyclin partner regulatory, and chemical reactions and pathways (**Figure 30**). During cell development's proliferation and expansion stages, CK is known to promote cell division and increase cell expansion. The downregulation of genes related to cytokinin biosynthesis may result in the cells ceasing to develop and grow. Therefore, the co-application of exogenous CK is necessary to ensure the sprouting of apical buds.

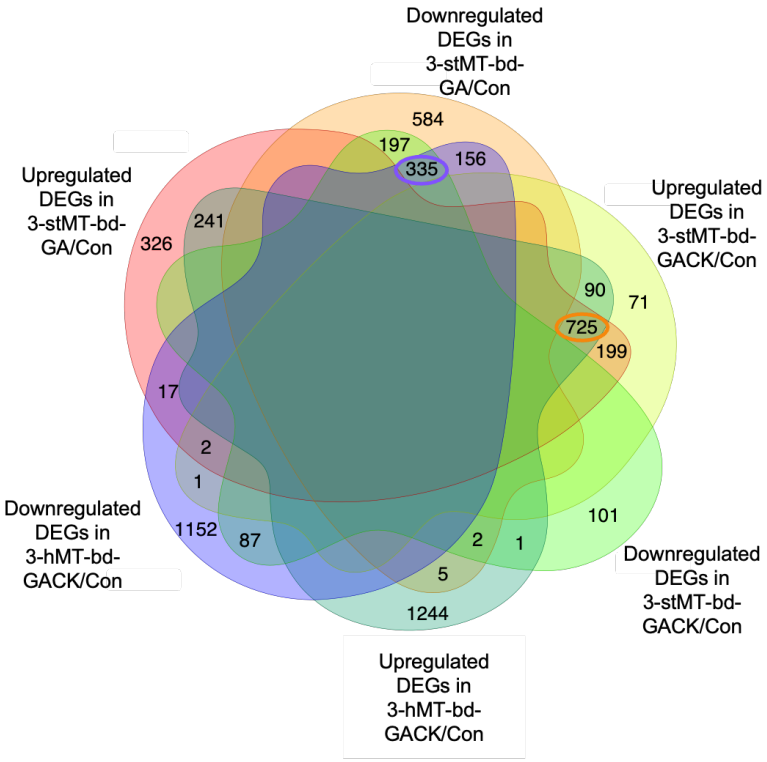


Figure 29. DEGs identified in bud tissues of microtuber in sprouting-inducible condition.

A detailed Venn diagram to visualize the similarities and differences of DEGs among three sprouting-induced comparisons: 3-stMT-bd-GA vs Con (3-stMT-bd-GA/Con), 3-stMT-bd-GACK/Con, and 3-hMT-bd-GACK/Con. 335 and 725 DEGs of overlap in the diagram represent genes that were co-downregulated and co-upregulated, respectively.

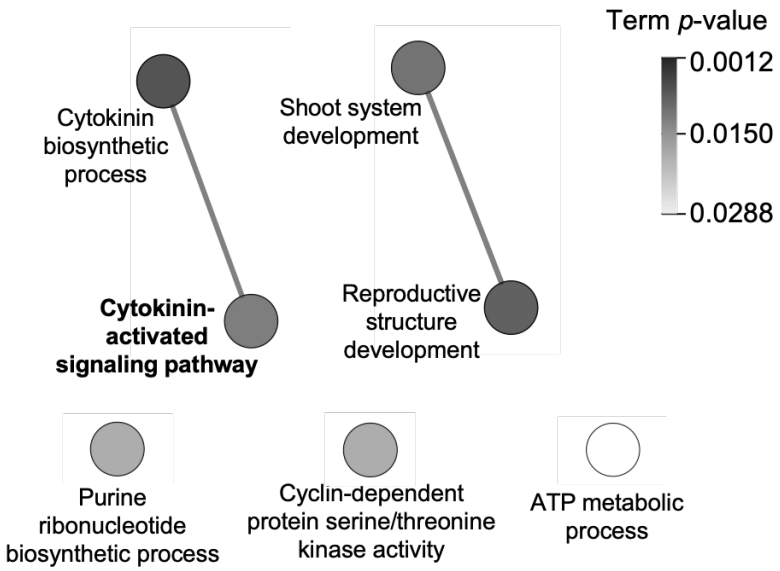


Figure 30. GO analysis of DEGs downregulated in bud tissues of microtuber in sprouting-inducible condition.

Network analysis of enriched GO terms for 335 co-downregulated DEGs and significantly enriched GO terms (p value < 0.05) were used to visualize the network by ClueGO plugin in Cytoscape.

The size of each circle represents gene numbers in each process.

On the other hand, thirty-five significantly enriched GO terms clustered into five groups were detected for 725 DEGs using GO term fusion with the criteria of p value < 0.05 (**Figure 31**). The highest overrepresented GO term (with the lowest p value) was "response to hormone" including auxin-activated signaling pathway, followed by DNA-binding transcription factor activity, organic substance catabolic process, hydrogen peroxide catabolic process, and phenylpropanoid metabolic process, suggesting that the regulation of transcription activity and chemical reactions resulting in the breakdown of organic substances and hydrogen peroxide are essential for regulating the state or activity of organisms during the development of sprouting, including hormone-induced signaling. These results gave a preliminary recognition of gene expression changes in this sprouting behavior, showing that genes related to shoot formation associated with CK-activated signaling were downregulated, while genes related to regulating the organism's state associated with auxin-activated signaling were upregulated during sprouting growth. The detailed genes involved in each term were filed in **Supplementary Table S3** of Zhang et al., (Zhang *et al.*, 2023).

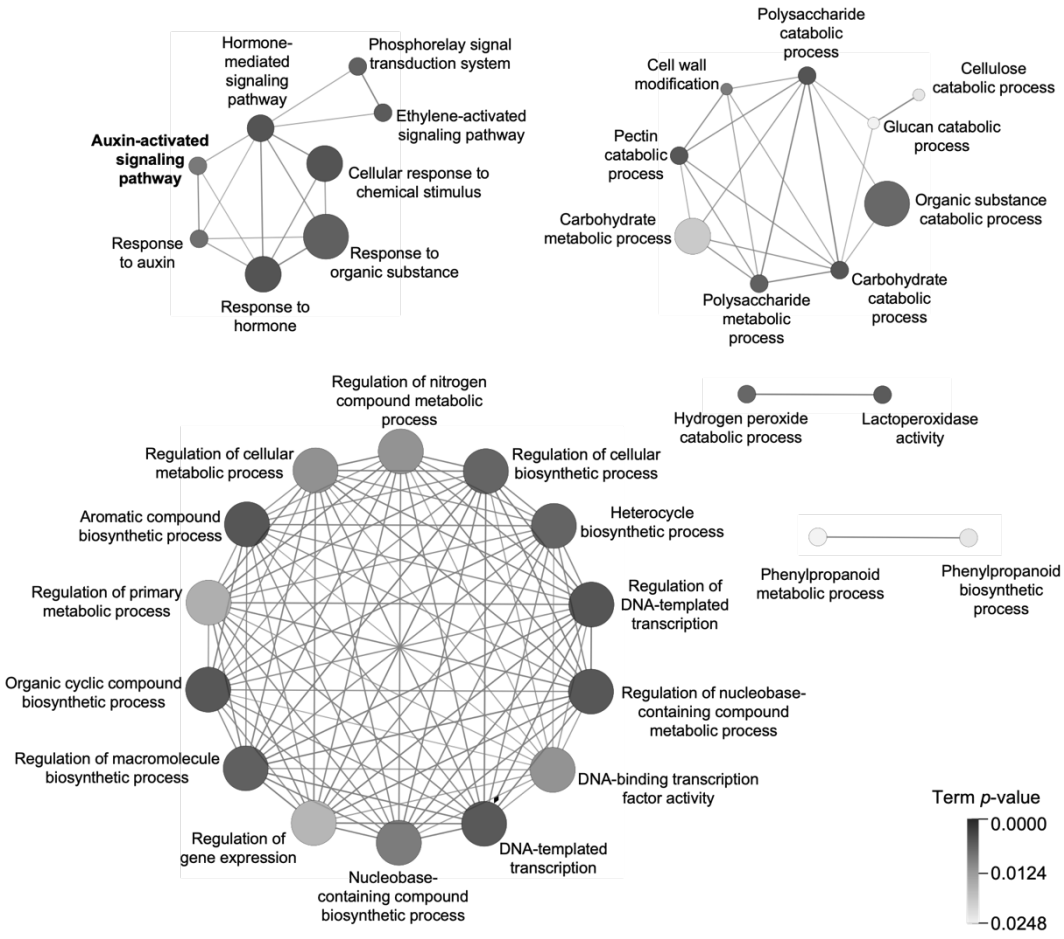


Figure 31. GO analysis of DEGs upregulated in bud tissues of microtuber in sprouting-inducible condition.

Network analysis of enriched GO terms for 725 co-upregulated DEGs and significantly enriched GO terms (p value < 0.05) were used to visualize the network by ClueGO plugin in Cytoscape.

The size of each circle represents gene numbers in each process.

3.3.6 The Effect of GA on Microtuber Sprouting in the Absence of Nodal Stem

Interestingly, when I performed KEGG and GO enrichment analysis for 3-hMT-bd-GA/Con (**Supplementary Table S4** of Zhang et al., (Zhang *et al.*, 2023)), I found that the "Zeatin biosynthesis" pathway was not enriched in GA-treated hMT (the right-most column, "Sprouting-failed", in **Figure 47**), but the "Plant hormone signaling transduction" pathway was enriched; in this pathway, twenty-two genes were enriched (**Figure 51**), and seven of them were auxin-related genes, which also were detected in sprouting-induced conditions. They had the exact expression change (up- or down-regulated) as that in sprouting-induced conditions. Only four genes, *PYL4*, *IAA15*, *IAA22*, and *SAUR50*, were detected explicitly in sprouting buds, reflecting the significance of the upregulation of *PYL4*, *IAA15*, *IAA22*, and *SAUR50* in response to sprouting. Notably, GO terms showed that "response to auxin" connected with the "auxin-activated signaling pathway" was also enriched, and genes related to this term were all downregulated (**Supplementary Table S4** of Zhang et al., (Zhang *et al.*, 2023)). According to the results, GA can activate auxin signaling even in failed sprouting conditions. However, GA treatment failed to change the expression of genes related to the "Zeatin biosynthesis" pathway, *PYL4* (one ABA core regulator), and some auxin-related genes (such as *IAA15*, *IAA22*, and *SAUR50*) under conditions without the nodal stem. These results suggest that the lack of regulation for genes related to the pathway and *PYL4*, *IAA15*, *IAA22*, and *SAUR50* could explain why GA fails to induce sprouting without the support of the nodal stem. This indicates that the auxin-related *IAA15*, *IAA22*, and *SAUR50*, the ABA-related *PYL4*, and the "Zeatin biosynthesis" pathway-related *CYP735A*, *CISZOG*, and *UGT85A1* play a vital role during sprouting growth.

Plant hormone signal transduction pathway

Gene ID PGSC0003DMG	Gene Description	Function	sprouting-failed 3-hMT-bd GA/Con
400023897	**ABF**	ABA-responsive element Binding Factor	-1.11
400002945	RR9a	Type-A response regulator	2.04
400003084	RR9c	Type-A response regulator	1.24
400016643	RR17a	Type-A response regulator	-1.29
400018579	PHP4	Phosphotransfer protein 4-like	7.50
400003849	GID1	Gibberellin receptor	-1.76
400006550	AUX1	Auxin influx carrier	1.40
400008504	AUX1	Auxin influx carrier	1.32
400005327	IAA10	AUX/IAA gene family	1.74
400005338	IAA11	AUX/IAA gene family	3.74
400006093	IAA23	AUX/IAA gene family	1.51
400029339	IAA26	Aux/IAA gene family	2.21
400003771	ARF5	Auxin response factor	-1.15
400012261	ARF9	Auxin response factor	1.40
400003673	SAUR	Auxin-responsive SAUR family	2.63
400003773	SAUR	Auxin-responsive SAUR family	-1.73
400001668	SAUR	Auxin responsive SAUR family	1.69
400029190	SAUR	Auxin responsive SAUR family	1.66
400008070	SAUR	Auxin-responsive SAUR family	5.92
400015667	JAZ	Jasmonate-zim-domain protein	-1.19
400023678	TGA	bZIP transcription factor	-1.02
400005116	PR-1	Pathogenesis-related protein	-1.70

-1.76 7.50

Figure 32. DEGs identified in apical buds of microtuber in sprouting-failed condition with GA alone treatment.

The table shows genes included in the pathway of Plant hormone signal transduction in a comparison of 3-hMT-bd-GA/Con, with a heatmap showing gene expression levels as $\log_2$ Fold Change.

Orange represents upregulation, and purple represents downregulation compared to Control (untreated).

3.3.7 The Effect of Nodal Stem on GA-induced Microtuber Sprouting

Given that the nodal stem (-st) attached to MTs might play a vital role in this sprouting behavior, I first compared gene expression changes in the nodal stem involved in sprouting on day 3 of culture between GA and GACK treatment. KEGG enrichment analysis (**Figure 33**) showed that they shared three pathways. Genes related to the GA receptor (*GID1*) and ABA-responsive bZIP transcriptional factor (*ABF*) were downregulated in both comparisons. Three genes involved in CK negative response regulators (*RR4*, *RR9a*, and *RR17a*) were upregulated in 3-stMT-st-GACK/Con. However, *RR17c* was downregulated in 3-stMT-st-GA/Con, indicating that the activation of CK is involved in the nodal stem due to the negative regulation of *RR17c*; one *PR-1* (400005117) and *GH3.6* (400021803) (an auxin inactivation gene) were uniquely upregulated (**Figure 34**) in 3-stMT-st-GA/Con, reflecting that the reduction in auxin biosynthesis signaling may be involved in GA-treated nodal stems, given that the enhanced expression of *StPR1* could downregulate the expression of *StYUC1* (an auxin synthesis gene) and upregulate *StGH3.6* in potatoes (Natarajan et al., 2018).

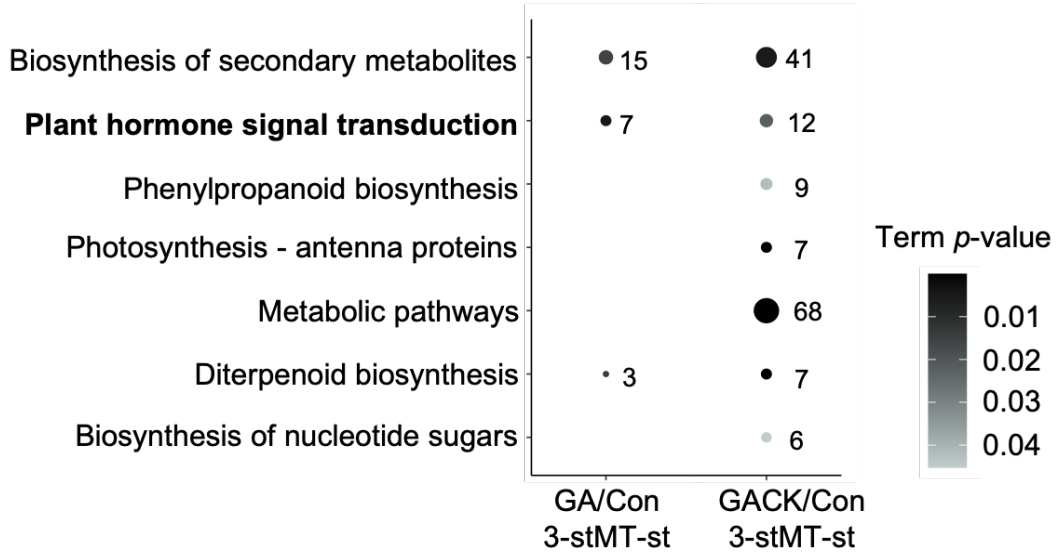


Figure 33. KEGG pathway enrichment analysis of DEGs in the nodal stem with exogenous GA and GACK treatment, respectively.

A comparison of enriched KEGG pathways between two comparisons of phytohormone treatment (GA or GACK) with Control (Con, untreated) in the nodal stem of stMT using DAVID (p value < 0.05).

Counts of DEGs included in each KEGG pathway are shown next to the plot.

Plant hormone signal transduction

Gene ID PGSC0003DMG	Gene Description	Function	Sprouting-induced 3-stMT-st GA/Con	Sprouting-induced 3-stMT-st GACK/Con
400003849	GID1	GID1-like gibberellin receptor	-1.87	-1.65
400021991	GID1	GID1-like gibberellin receptor	-1.01	-1.07
400023897	ABF	ABA-responsive element Binding Factor	-2.26	-3.46
400024978	GH3.6	Auxin responsive CH3 gene family	-1.65	-1.87
400021803	GH3.6	Auxin responsive CH3 gene family	1.83	not DEG
400025856	GH3	Auxin responsive CH3 gene family	not DEG	-1.89
400019182	AUX1	Auxin influx carrier	not DEG	1.06
400016643	RR17a	Type-A response regulator	-1.76	not DEG
402022640	RR4	Type-A response regulator	not DEG	1.49
400002945	RR9a	Type-A response regulator	not DEG	6.69
400027597	RR17c	Type-A response regulator	not DEG	3.19
401015433	CYCD3	Cyclin-D3-like	not DEG	1.33
400015442	BKI1	Negative regulator of brassinosteroid signalling	not DEG	-1.30
400005117	PR-1	Pathogenesis-related protein	6.14	not DEG
400005115	PR-1	Pathogenesis-related protein	not DEG	-5.90



Figure 34. Functional annotations of DEGs in the nodal stem on day 3 of culture with exogenous GA and GACK, respectively.

The table shows genes included in the pathways "Plant hormone signal transduction" for each comparison, with a heatmap showing gene expression levels as $\log_2$ Fold Change.

Orange represents upregulation, and purple represents downregulation compared to Control (untreated).

In contrast, another *PR-1* (400005115) and *GH3.6* (400024978) were downregulated in 3-stMT-st-GACK/Con, probably because the exogenous CK co-application led to a negative feedback regulatory loop via endogenous CK biosynthesis, which finally influenced the expression of genes related to auxin and CK. GO enrichment analysis showed that they shared three GO terms in the biological process (**Figure 35**), and the "positive regulation of gibberellic acid induced signaling pathway" term was only enriched in 3-stMT-st-GA/Con. These results indicate that treatment with GA alone induced the changes in CK-related gene expression, and CK signaling was inhibited when CK was co-applied in the presence of the nodal stem.

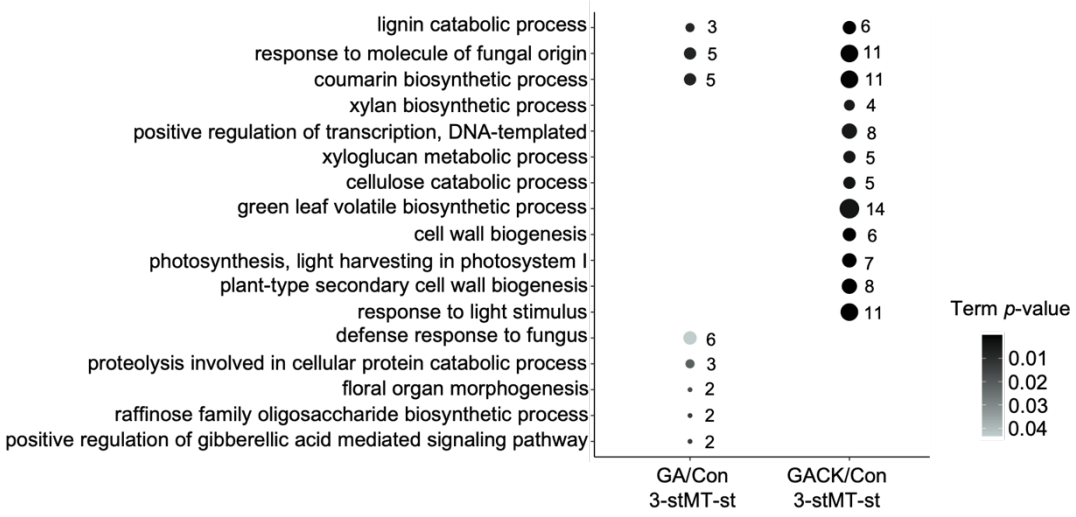


Figure 35. GO enrichment analysis of DEGs in the nodal stem on day 3 of culture with exogenous GA and GACK, respectively.

A comparison of enriched GO terms in biological processes between two comparisons of phytohormone treatment (GA or GACK) with Control (Con, untreated) in the nodal stem of stMT using DAVID (p value < 0.05).

Counts of DEGs included in each KEGG pathway are shown next to the plot.

To examine the effect of stem excision on the expression of genes, I next focused on the differences in DEGs detected in 1512 and 818 unique DEGs harbored by 3-stMT-bd-GA/Con and 3-hMT-bd-GA/Con, respectively (**Figure 36A**). They shared three KEGG pathway terms (**Figure 36B**), including the "Plant hormone signal transduction" pathway. Eighteen genes were grouped tor the 1512 unique DEGs. Nine genes were related to auxin, four genes were associated with ABA, three were *PYL4*, and one was *PP2C* (the regulator for ABA signaling) (**Figure 37**).

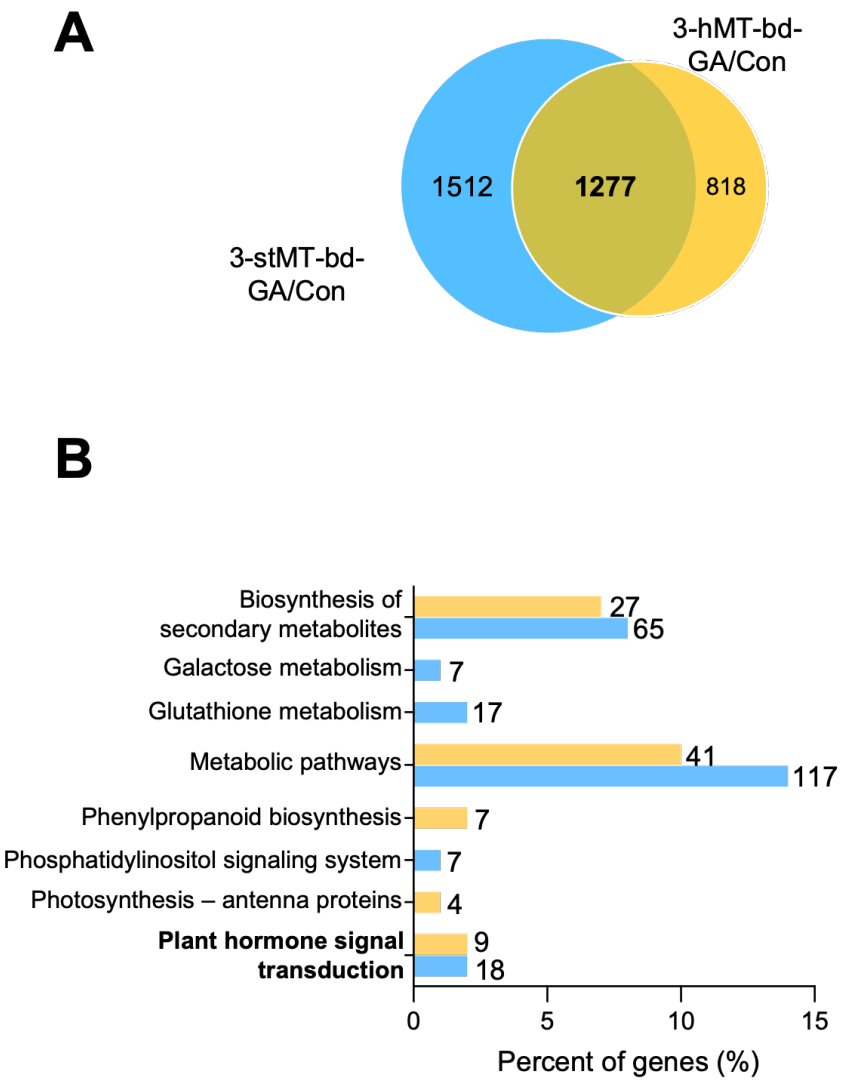


Figure 36. DEGs identified in apical bud tissues (bd) between stemmed microtubers (stMTs) and microtuber halves (hMTs) on day 3 (3-) of culture treated with GA.

(**A**) A Venn diagram to visualize the similarities and differences of DEGs between 3-stMT-bd-GA/Con and 3-hMT-bd-GA/Con, and they harbored 1515 and 818 unique DGEs, respectively.

(**B**) The comparison of enriched KEGG pathways for each harbored unique DEGs using DAVID ($p < 0.05$), visualized using GraphPad PRISM.

Counts of DEGs included in each KEGG pathway are shown next to the bar in the graph.

On the other hand, nine genes were detected for the 818 unique DEGs. Four genes were related to auxin, such as *ARF5* and *ARF9*, no Aux/IAA genes were detected, and two genes were related to CK, *RR9* and *PHP4b* (known to suppress CK signaling) (**Figure 37**). This comparison suggests that the expression level of CK-, auxin-, and ABA-related genes changes in response to GA-involved MT sprouting in the presence of the nodal stem.

Plant hormone signal transduction

Gene ID PGSC0003DMG	Gene Description	Function	Unique 1512 3-stMT-bd GA/Con	Unique 818 3-hMT-bd GA/Con
400016317	IAA12	AUX/IAA gene family	1.57	not DEG
400020139	IAA15	AUX/IAA gene family	2.04	not DEG
400006108	IAA22	AUX/IAA gene family	1.19	not DEG
400021803	CH3.6	Auxin responsive CH3 gene family	2.09	not DEG
400024995	CH3.6	Auxin responsive CH3 gene family	-1.72	not DEG
400001601	SAUR	Auxin responsive SAUR family	3.42	not DEG
400001604	SAUR	Auxin responsive SAUR family	1.30	not DEG
400001614	SAUR	Auxin responsive SAUR family	2.36	not DEG
400001654	SAUR	Auxin responsive SAUR family	6.23	not DEG
400021991	GID1	Gibberellin receptor	-1.47	not DEG
400011033	PYL4	Abscisic acid receptor	1.55	not DEG
400015897	PYL4	Abscisic acid receptor	2.45	not DEG
400017514	PYL4	Abscisic acid receptor	1.14	not DEG
400002573	PP2C	Protein phosphatase 2C ABI2	-1.10	not DEG
400015853	EBF1/2	EIN3-binding F-box protein 1-like	-1.51	not DEG
400028694	EIN4	Ethylene receptor	-1.12	not DEG
400029834	NPR5	Regulatory protein	-1.08	not DEG
400005109	PR-1	Pathogenesis-related protein	2.45	not DEG
400003084	RR9c	Type-A response regulator	not DEG	1.24
400018579	PHP4	Phosphotransfer protein 4-like	not DEG	7.50
400003771	ARF5	Auxin response factor	not DEG	-1.15
400012261	ARF9	Auxin response factor	not DEG	1.40
400001668	SAUR	Auxin responsive SAUR family	not DEG	1.69
400029190	SAUR	Auxin responsive SAUR family	not DEG	1.66
400015667	JAZ	Jasmonate-zim-domain protein	not DEG	-1.19
400023678	TGA	bZIP transcription factor	not DEG	-1.02
400005116	PR-1	Pathogenesis-related protein	not DEG	-1.70

-1.72 7.50

Figure 37. DEGs identified in apical bud tissues (bd) between stemmed microtubers (stMTs) and microtuber halves (hMTs) on day 3 (3-) of culture treated with GA.

The table shows genes in the "Plant hormone signal transduction" pathway for each harbored unique DEGs group, with a heatmap showing gene expression levels as log_2Fold Change.

Orange represents upregulation, and purple represents downregulation compared to control (untreated).

3.3.8 The Effect of CK on Microtuber Sprouting

Notably, GA can induce hMTs sprouting when exogenous CK was co-applied (**Figure 17, Figure 18**). To examine the effect of the existence of CK on the expression of plant hormone-related genes, I next compared DEGs between 2428 and 465 unique DEGs harbored by 3-hMT-bd-GACK/Con and 3-hMT-bd-GA/Con, respectively (**Figure 38A**). No KEGG pathways were significantly enriched for the 465 unique DEGs, and nine KEGG pathways were enriched for the 2428 unique DEGs (**Figure 38B**). Twenty-four genes were included in the "Plant hormone signal transduction" pathway (**Figure 39**); fifteen were related to auxin, five genes were associated with CK, and there was one ABA core regulator *PYL4*. This comparison shows that the expression level changes in CK- and auxin-related genes are vital in sprouting.

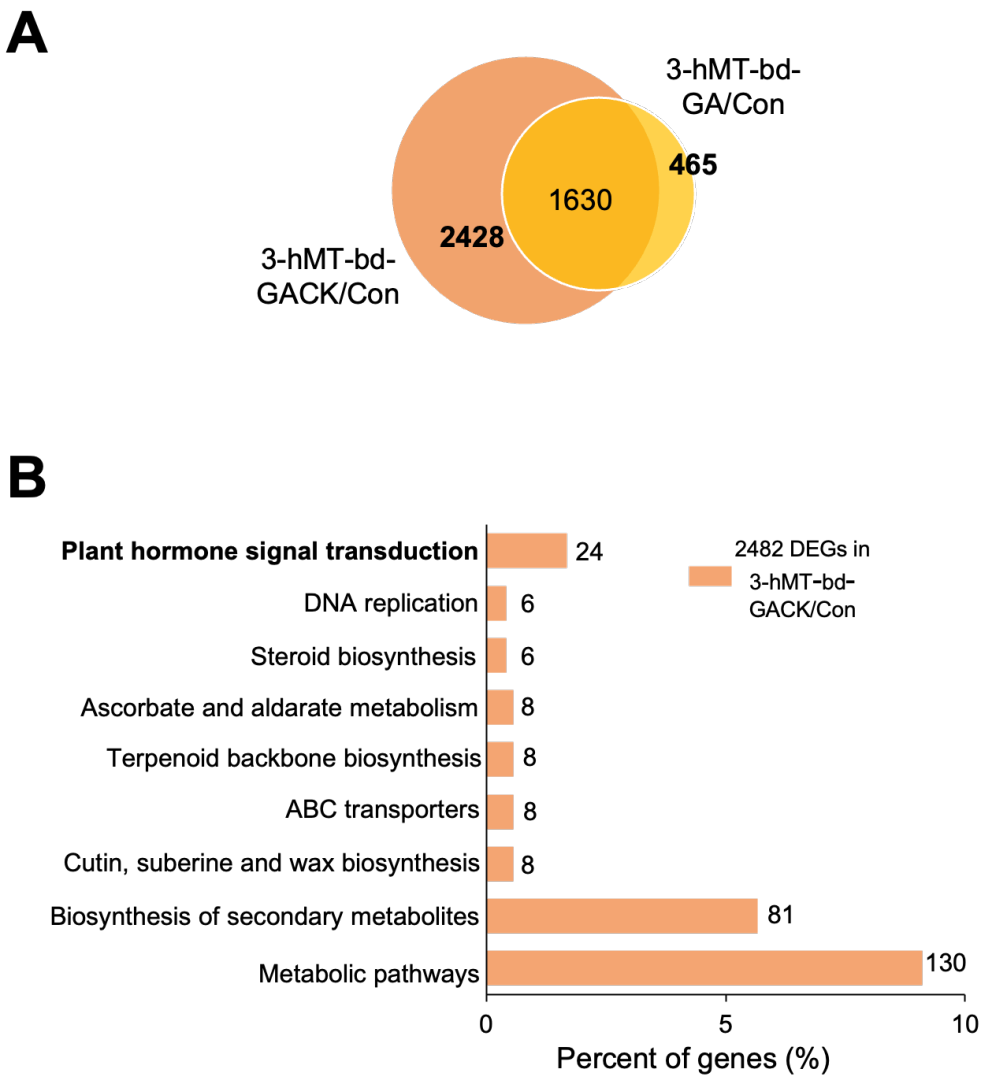


Figure 38. DEGs identified in apical buds (bd) between GACK- and GA-treated microtuber halves (hMTs) on day 3 of culture.

(**A**) A Venn diagram to visualize the similarities and differences of DEGs between 3-hMT-bd-GACK/Con and 3-hMT-bd-GA/Con, and they harbored 2428 and 465 unique DGEs, respectively.

(**B**) Comparison of enriched KEGG pathways for each harbored unique DEGs using DAVID (p<0.05). Counts of DEGs included in each KEGG pathway are shown next to the bar in the graph.

Plant hormone signal transduction

Gene ID PGSC0003DMG	Gene Description	Function	Unique 2482 3-hMT-bd GACK/Con	Unique 465 3-hMT-bd GA/Con
400001589	AUX1	Auxin influx carrier	1.76	
400019182	AUX1	Auxin influx carrier	2.51	
400023205	AUX1	Auxin influx carrier	2.65	
400020139	IAA15	Aux/IAA gene family	4.13	
400006108	IAA22	Aux/IAA gene family	1.39	
400024997	GH3.6	Auxin responsive GH3 gene family	1.60	
400026186	GH3.6	Auxin responsive GH3 gene family	-1.38	
400001601	SAUR	Auxin-responsive SAUR family	2.91	
400001613	SAUR	Auxin-responsive SAUR family	5.45	
400001614	SAUR	Auxin-responsive SAUR family	3.28	
400001653	SAUR	Auxin-responsive SAUR family	-6.17	
400001654	SAUR	Auxin-responsive SAUR family	4.95	not enriched pathways
400001655	SAUR	Auxin-responsive SAUR family	2.93	
400022233	SAUR	Auxin-responsive SAUR family	-2.05	
400028254	SAUR	Auxin-responsive SAUR family	-2.64	
400029463	HK4	Cytokinin receptor histidine kinase	1.36	
402022640	RR4	Type-A response regulator	2.17	
400029839	RR9b	Type-A response regulator	1.96	
400029852	RR9d	Type-A response regulator	3.96	
400027597	RR17b	Type-A response regulator	9.67	
400021991	GID1	Gibberellin receptor	-1.27	
400011033	PYL4	Abscisic acid receptor	1.40	
400015442	BKI1	Negative regulator of brassinosteroid signaling	-1.54	
400013975	TCH4	Xyloglucan endotransglycosylase	-1.62	

-6.17 9.67

Figure 39. DEGs identified in apical buds (bd) between GACK- and GA-treated microtuber halves (hMTs) on day 3 of culture.

The table shows genes in the "Plant hormone signal transduction" pathway for each harbored unique DEGs group, with a heatmap showing gene expression levels as $\log_2$ Fold Change.

Orange represents upregulation, and purple represents downregulation compared to Control (untreated).

KEGG enrichment analysis was used to determine the detailed genes associated with CK treatment, which failed to induce MT spouting. The result showed that the "Plant hormone signal transduction" pathway was shared by 3-stMT-st-CK/Con and 3-hMT- bd-CK/Con (**Figure 40**). The genes related to the GA receptor, such as *GID1*, were not enriched, suggesting that CK treatment could not change the expression of genes related to GA. This may explain why CK failed to cause signs of sprouting, given that GA is a negative regulator of potato tuberization and that bioactive GA levels are rapidly reduced in stolons with the onset of tuberization. Genes related to the CK negative receptor were upregulated. Four auxin-related genes (*AUX1* and *IAA26*) were upregulated (**Figure 41**) which were also detected in sprouting-induced conditions (**Figure 28**).

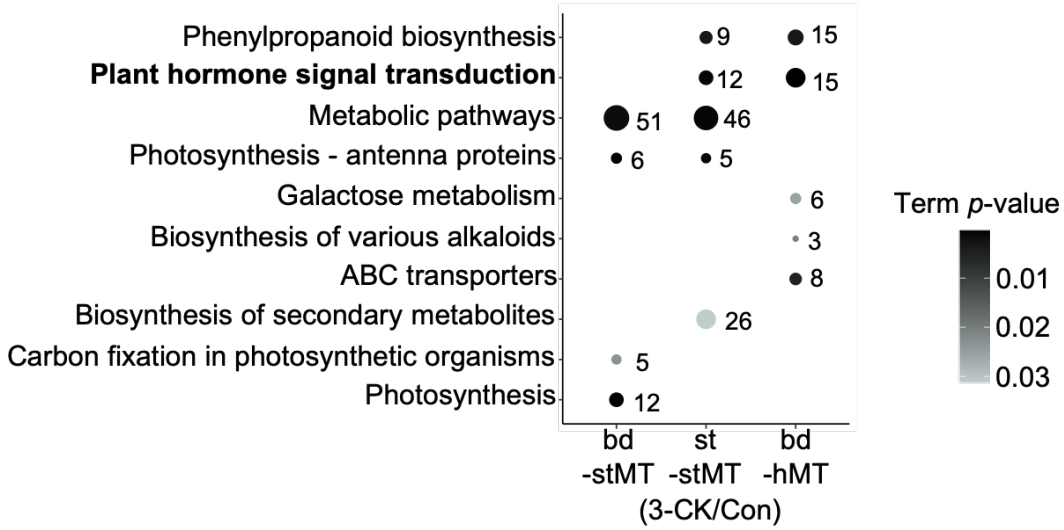


Figure 40. KEGG enrichment analysis of DEGs in apical bud tissues (bd) and the nodal stem tissues (st) of stemmed microtubers (stMTs) and bd of microtuber halves (hMTs), respectively, on day 3 of culture with CK treatment compared with control (untreated).

A comparison of enriched KEGG pathways among three comparisons using DAVID (p<0.05), visualized using the ggplot2 package in R.

Counts of DEGs included in each KEGG pathway are shown next to the plot.

Plant hormone signal transduction

Gene ID PGSC0003DMG	Gene Description	Function	Sprouting-failed 3-stMT-bd CK/Con	3-stMT-st CK/Con	3-hMT-bd CK/Con
400003084	RR9c	Type-A response regulator	not	1.29	2.21
400002945	RR9a	Type-A response regulator	enriched	not DEG	1.89
400029839	RR9b	Type-A response regulator	pathways	not DEG	1.22
400029852	RR9d	Type-A response regulator		not DEG	2.18
402022640	RR4	Type-A response regulator		not DEG	1.21
400027597	RR17b	Type-A response regulator		not DEG	8.17
400029463	HK4	Cytokinin receptor histidine kinase		not DEG	1.17
400018579	PHP4b	Phosphotransfer protein 4-like		-1.87	6.87
400001589	AUX1	Auxin influx carrier		1.03	not DEG
400023205	AUX1	Auxin influx carrier		not DEG	1.83
400001589	AUX1	Auxin influx carrier		not DEG	1.48
400006093	IAA23	AUX/IAA gene family		-1.28	not DEG
400029339	IAA26	Aux/IAA gene family		not DEG	2.86
400019274	GH3.6	Auxin responsive CH3 gene family		1.06	not DEG
400024978	GH3.6	Auxin responsive CH3 gene family		1.31	not DEG
400026186	GH3.6	Auxin responsive GH3 gene family		not DEG	-1.63
400021803	GH3.6	Auxin responsive GH3 gene family		not DEG	-1.86
400030234	SAUR	Auxin-responsive SAUR family		-1.07	-1.26
400004786	SAUR	Auxin-responsive SAUR family		-1.23	not DEG
400022233	SAUR	Auxin-responsive SAUR family		-1.86	-2.08
400001655	SAUR	Auxin-responsive SAUR family		-1.25	not DEG
400035783	SAUR	Auxin-responsive SAUR family		not DEG	1.36
400028254	SAUR	Auxin-responsive SAUR family		not DEG	-3.17
400003673	SAUR	Auxin-responsive SAUR family		not DEG	2.01
400001653	SAUR	Auxin-responsive SAUR family		not DEG	-3.78
400026010	SAUR	Auxin-responsive SAUR family		not DEG	-1.08
400001643	SAUR	Auxin-responsive SAUR family		not DEG	-5.49
400017186	ETR	Ethylene receptor 2-like		1.09	not DEG
400017231	ERF1	Ethylene-responsive transcription factor 1B-		1.14	not DEG
400015667	JAZ	Jasmonate-zim-domain protein		not DEG	-2.51
401018740	TCH4	Xyloglucan endotransglycosylase		not DEG	-1.01
400013975	TCH4	Xyloglucan endotransglycosylase		not DEG	-1.24
400007110	TGA	bZIP transcription factor		not DEG	-1.72
400005116	PR-1	Pathogenesis-related protein		not DEG	-2.02

-5.49 8.17

Figure 41. KEGG enrichment analysis of DEGs in apical bud tissues (bd) and the nodal stem tissues (st) of stemmed microtubers (stMTs) and bd of microtuber halves (hMTs), respectively, on day 3 of culture with CK treatment compared with control (untreated).

The table shows genes included in “Plant hormone signal transduction” for each comparison, with a heatmap showing gene expression levels as log2 Fold Change.

Orange represents upregulation, and purple represents downregulation compared to control (untreated).

Strikingly, the regulation of *IAA23* was in reverse to that detected in sprouting-induced conditions. GO enrichment analysis showed that three comparisons shared no terms in the biological process (**Figure 42**, **Supplementary Table S5** of Zhang et al., (Zhang *et al.*, 2023)), and the term "response to auxin" was significantly enriched in 3-stMT-st-CK/Con and 3-hMT-bd-CK/Con. Genes involved in this GO term are mostly downregulated *SAURs*, compared with the genes detected in response to sprouting. However, *SAUR50* was not detected as DEGs. Moreover, no DEGs related to GA were detected in CK-treated conditions, indicating that although CK treatment may be involved in inhibiting genes related to auxin, the lack of regulating *SAUR50* and genes related to GA made CK fail to induce sprouting.

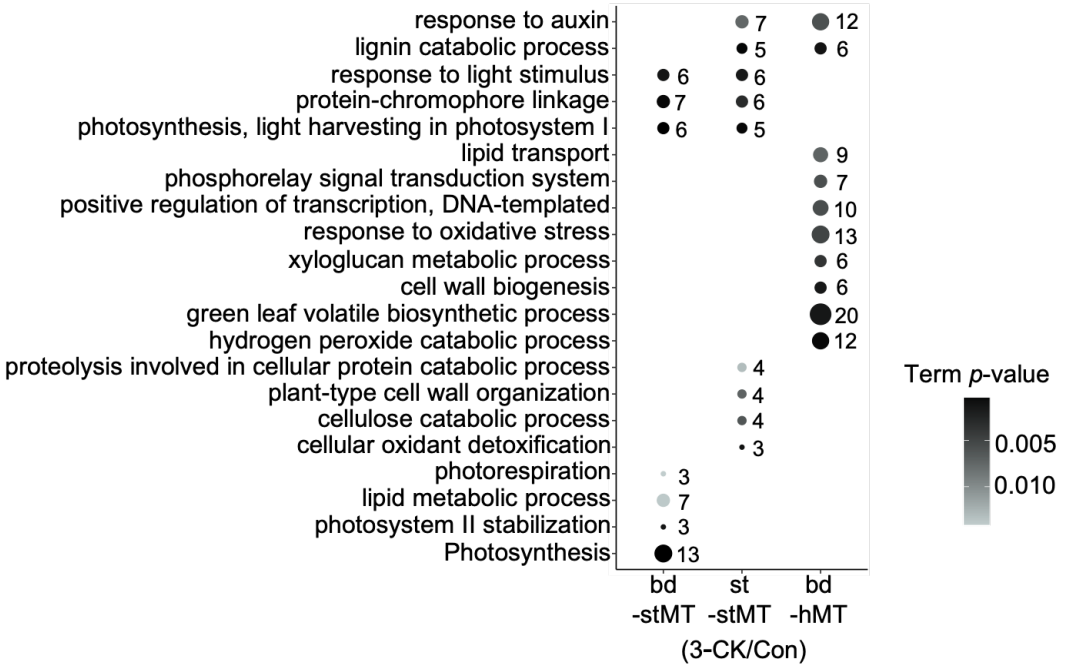


Figure 42. GO enrichment analysis of DEGs involved in CK alone treatment.

A comparison of enriched GO terms (top ten) in biological processes for DEGs among apical bud tissues (bd) and the nodal stem tissues (st) of stemmed microtubers (stMTs) and bd of microtuber halves (hMTs), respectively, on day 3 of culture with CK treatment compared with control (untreated) using DAVID (p<0.05), visualized using the ggplot2 package in R.

Counts of DEGs included in each GO term are shown next to the plot.

3.3.9 Genetic Analysis of Microtuber Sprouting Response to GA and Both GA and CK

RNA-seq analyses showed that the lack of regulation for auxin-related *IAA15*, *IAA22*, and *SAUR50*; CK-related *CYP735A*, *UGT85A1*, and *CISZOG*; and ABA-related PYL4 may be responsible for GA failure to induce sprouting in the absence of the nodal stem. Additionally, I also selected other auxin-related IAA26 for comparison with *IAA15*, *IAA22*, CK-related genes, *RR4* and *RR9*, and auxin-related *SAUR 71*, given that these three genes were the hub genes enriched in the "plant hormone signaling transduction" of 117 genes set in the magenta module of WGCNA (**Supplementary Table S7** of Zhang et al., (Zhang *et al.*, 2023)). To see the difference in MT sprouting among the three kinds of MTs, qPCR was tested on the apical bud tissue's gene expression in GA-treated stMTs, deMTs, hMTs, and GACK-treated hMTs, with each untreated control comparison on day 3 of culture.

For genes *IAA26*, *IAA22* (**Figure 43**), *GID1*, *PYL4* (**Figure 44**), 37_*CISZOG*, *CYP735A*, and *RR17* (**Figure 45**), there was no significance among the three spouted MTs (GA-treated stMTs, deMTs, and GACK-treated hMTs). For gene *IAA15* (**Figure 43**), *RR4*, and *RR9a* (**Figure 45**), there was no significance between GA-treated stMTs and GACK-treated hMTs; GA-treated stMTs and GA-treated deMTs, while there was significance between GA-treated deMTs and GACK-treated hMTs. For gene *SAUR50* (**Figure 43**), there was no significance between GA-treated stMTs and GACK-treated hMTs; GA-treated deMTs and GACK-treated hMTs, while there was significance between GA-treated deMTs and GACK-treated hMTs. For gene *SAUR 71* (**Figure 43**), 31_*CISZOG*, *CYP735A*, *RR9b*, *RR9d* (**Figure 45**), there was no significance between GA-treated deMTs and GA-treated deMTs, while there was significance between GA-treated stMTs and GACK-treated hMTs; GA-treated deMTs and GACK-treated hMTs.

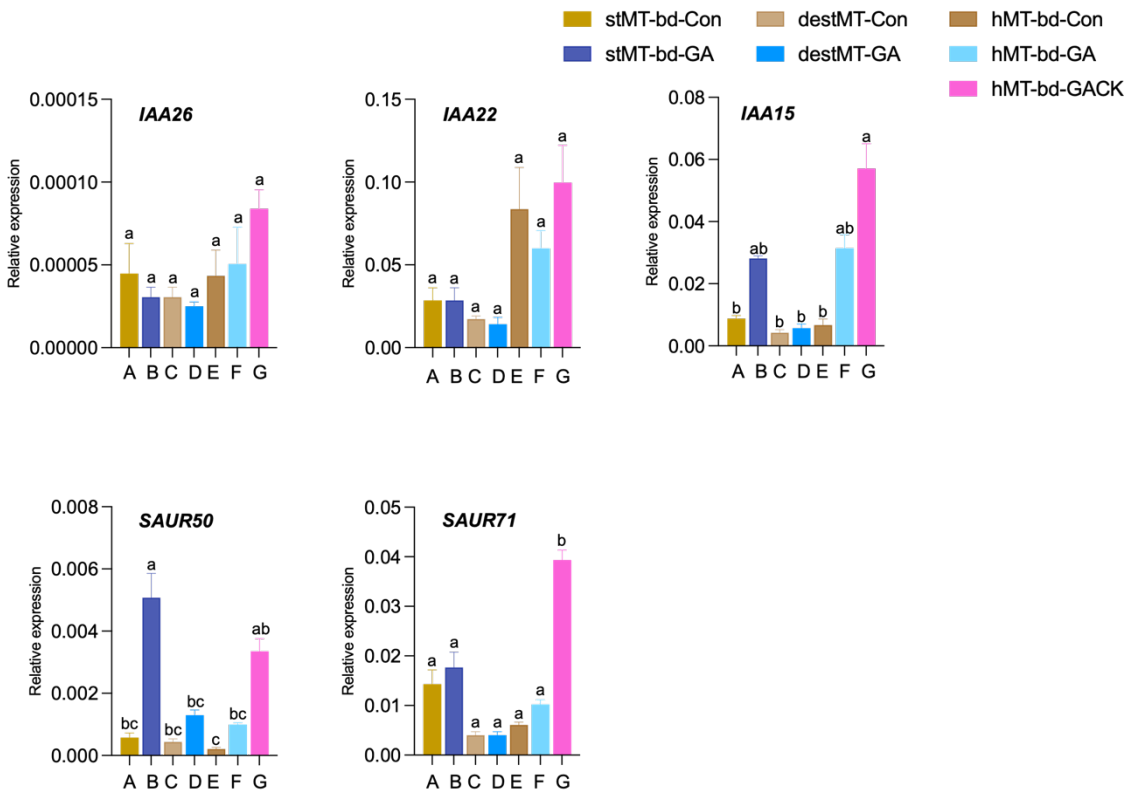


Figure 43. Genetic Analysis of genes related to auxin using RT-qPCR (real-time qPCR).

Five auxin-related genes involved in sprouting were selected for qPCR analysis using the stMTs, deMTs, and hMTs on day 3 of culture.

TPM values were obtained after RNA-seq reads had been mapped to reference genes. TPM values and qPCR data of three replicates are shown as mean (±SE).

IAA26: PGSC0003DMG400029339.

IAA22: PGSC0003DMG400006108.

IAA15: PGSC0003DMG400020139.

SAUR50: PGSC0003DMG400001614.

SAUR71: PGSC0003DMG400001655.

A, B, C, D, E, F, and G represent 3-stMT-bd-Con, 3-stMT-bd-GA, 3-deMT-bd-Con, 3-deMT-bd-GA, 3-hMT-bd-Con, 3-hMT-bd-GA, and 3-hMT-bd-GACK, respectively.

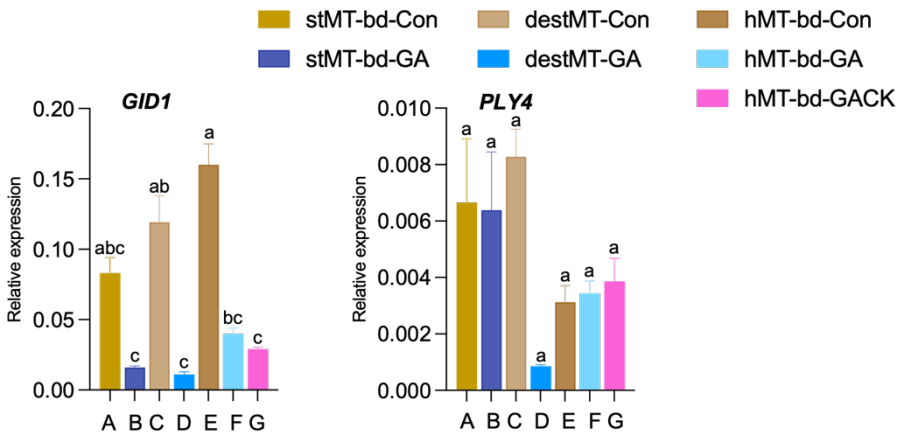


Figure 44. Genetic Analysis of genes related to GA and ABA using RT-qPCR (real-time qPCR).

GA-related gene and ABA related gene involved in sprouting were selected for qPCR analysis using the stMTs, deMTs, and hMTs on day 3 of culture.

TPM values were obtained after RNA-seq reads had been mapped to reference genes. TPM values and qPCR data of three replicates are shown as mean (±SE).

GID1: PGSC0003DMG400021991.

PYL4: PGSC0003DMG400011033.

A, B, C, D, E, F, and G represent 3-stMT-bd-Con, 3-stMT-bd-GA, 3-deMT-bd-Con, 3-deMT-bd-GA, 3-hMT-bd-Con, 3-hMT-bd-GA, and 3-hMT-bd-GACK, respectively.

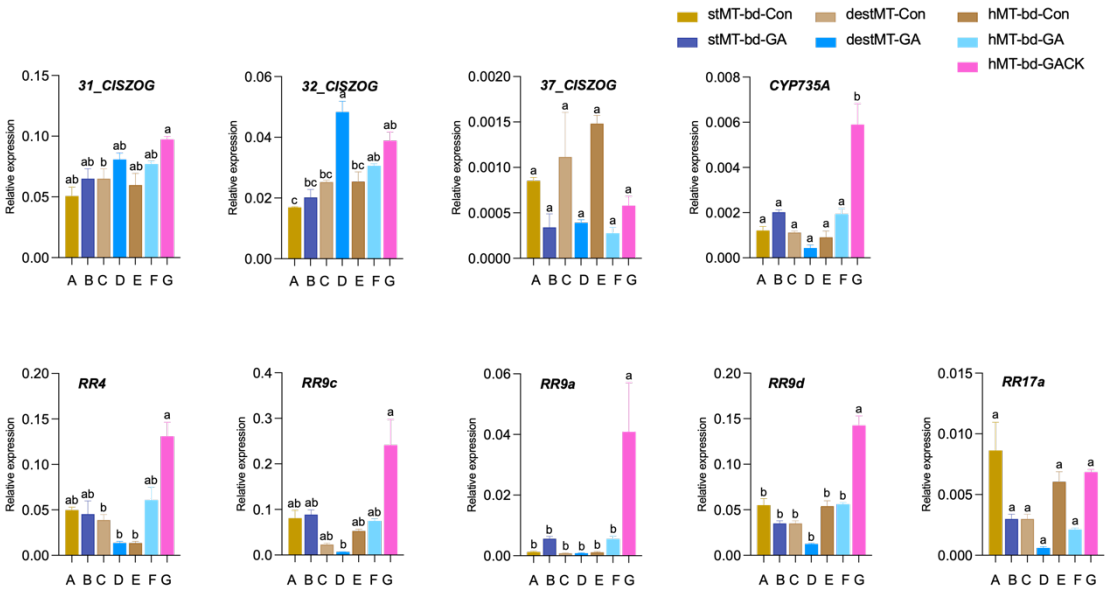


Figure 45. Genetic Analysis of genes related to CK using RT-qPCR (real-time qPCR).

Nine CK-related genes response to GA treatment were selected for qPCR analysis using the stMTs, deMTs, and hMTs on day 3 of culture.

TPM values were obtained after RNA-seq reads had been mapped to reference genes.

TPM values and qPCR data of three replicates are shown as mean (±SE).

31_CISZOG: PGSC0003DMG400028331.

32_CISZOG: PGSC0003DMG400000432.

37_CISZOG: PGSC0003DMG400008137.

CYP735A: PGSC0003DMG400012669.

RR4: PGSC0003DMG402022640.

RR9c: PGSC0003DMG400003084.

RR9a: PGSC0003DMG400002945.

RR9a: PGSC0003DMG400029852.

RR17a: PGSC0003DMG400027597.

A, B, C, D, E, F, and G represent 3-stMT-bd-Con, 3-stMT-bd-GA, 3-deMT-bd-Con, 3-deMT-bd-GA, 3-hMT-bd-Con, 3-hMT-bd-GA, and 3-hMT-bd-GACK, respectively.

3.3.10 Correlations of RT-PCR and RNA-seq Datasets

I next selected eight relevant genes to verify the RNA-seq expression profile associated with GA treatment (**Figure 46**), including *IAA15*, *SAUR50*, *SAUR 71*, *CYP735A*, *CISZOG*, *RR4*, *RR9*, and *PYL4*, with the criterion of the higher TPM value in RNA-seq results. qPCR was tested on the apical bud tissue's gene expression in GA-treated stMTs and hMTs, and GACK-treated hMTs. The results showed that despite variations between RNA-seq data and qPCR results regarding the relative expression of the selected genes, the linear regression analysis indicated a high correlation ($R^2 = 0.8864$), demonstrating that the expression profiles of the selected genes were broadly consistent with data derived from the RNA-Seq analysis. This suggests that the transcriptome results were highly reliable and repeatable.

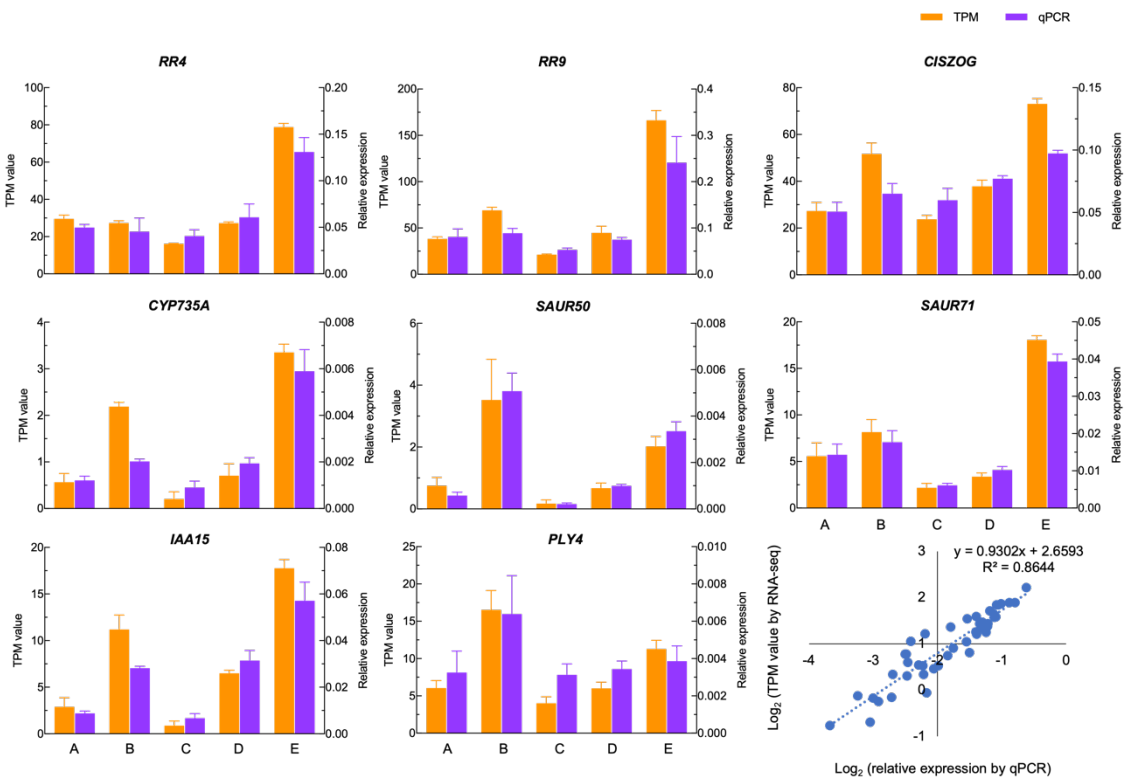


Figure 46. Correlation of expression patterns of selected genes from RNA-Seq and RT-qPCR.

Eight genes involved in sprouting were selected for transcriptomic and qPCR analysis using the stMTs and hMTs on day 3 of culture.

TPM values were obtained after RNA-seq reads had been mapped to reference genes. TPM values and qPCR data of three replicates are shown as mean (±SE).

RR4: PGSC0003DMG402022640.

RR9: PGSC0003DMG400003084.

CISZOG: PGSC0003DMG400028331.

CYP735A: PGSC0003DMG400012669.

SAUR50: PGSC0003DMG400001614.

SAUR71: PGSC0003DMG400001655.

IAA15: PGSC0003DMG400020139.

PYL4: PGSC0003DMG400011033.

A, B, C, D, and E represent 3-stMT-bd-Con, 3-stMT-bd-GA, 3-hMT-bd-Con, 3-hMT-bd-GA, and 3-hMT-bd-GACK, respectively.

3.4 Discussion

3.4.1 Response of Microtuber Sprouting to Phytohormone Treatment

It has been known for many years that the exogenous GA promotes tuber sprout growth rather than dormancy release (Suttle, 2004b). However, the ability of GA to induce sprouting remains controversial. In this study, I used 10 μM GA_3 (GA) to induce MT sprouting. The GA-only application induced the sprouting of both stMTs and deMTs, but it failed to terminate the dormancy of hMTs (**Figure 15**). Interestingly, the hMTs recovered and sprouted after the exogenous CK was co-applied (**Figure 17**). Although the shoot growth of hMTs was not as fast as that treated with GA in stMTs at the beginning, their elongation levels matched on day 15 of culture (**Figure 18**), agreeing with the report that GA has a dormancy-terminating capacity but requires CK to induce sprouting growth in tubers (Hartmann *et al.*, 2011). CK has been known as the only chemical to release axillary buds from dormancy and is locally biosynthesized in the nodal stem and transported into axillary buds to promote bud outgrowth after decapitation (Tanaka et al., 2006). In the magenta module of the WGCNA results, genes related to CK in the "plant hormone signaling pathway" were positively regulated in the nodal stem of stMTs with GA alone treatment (**Figure 24**, **Supplementary Table S7** of Zhang et al., (Zhang *et al.*, 2023)), suggesting that endogenous CK was involved in the nodal stem (**Figure 24**) in response to sprouting because the GA treatment resulted in the downregulation of genes involved in the "cytokinin-activated signaling pathway" (**Figures 28**, **Figure 26,** and **Supplementary Table S7** of Zhang et al., (Zhang *et al.*, 2023)). This makes the nodal stem necessary to help GA induce MT sprouting. This may be because I cultured MTs on a medium using a high level of sugar in the dark, leading to CK accumulation in the nodal stem. This assumption is supported by studies showing that sugars can promote CK synthesis and accumulation to trigger the induction of bud outgrowth in rose, potato stems, and Arabidopsis shoots (Barbier et al., 2015; Salam *et al.*, 2021).

Furthermore, previous studies reported that the effect of CK on tuber dormancy may be due to experimental systems, substances, or potato cultivars (Suttle, 2008; Xu et al., 1998b). My study showed that the CK-only application failed to cause any signs of

sprouting for 15 days, except for some tissue surrounding the apical bud, unless exogenous GA was also applied, agreeing with the result of Hartmann et al., (Hartmann *et al.*, 2011). These results further led me to infer that GA alone or CK alone is inadequate to initiate MT sprouting. Both are essential for sprouting.

3.4.2 Regulation of the Phytohormone Signaling Response to Microtuber Sprouting

WGCNA results demonstrated that the GA-only application significantly downregulated genes involved in the "cytokinin-activated signaling pathway" (**Figure 25**), including genes in the apical bud of hMTs treated with GA, which failed to induce sprouting. Zhuang et al. reported that the application of GA failed to induce bud outgrowth through an antagonistic interaction with CK because the GA decreased the endogenous CK content (Zhuang et al., 2019). However, my network analysis showed that gene expression in the "cytokinin-activated signaling pathway" and "auxin-activated signaling pathway" was induced and enhanced, respectively, during sprouting growth (**Figure 30, Figure 31**). These results indicate that the GA-only application can cause a reduction in "cytokinin-activated signaling", but CK and GA have been known to act synergistically to accelerate potato sprouting (Kolachevskaya *et al.*, 2019b), which may explain why GA requires CK to initiate sprouting. However, this reduction in CK-activated signaling may be caused by auxin involvement, which was induced by GA application.

The elevated auxin level would reduce the active CK content in potatoes (Kolachevskaya et al., 2017). My RNA-seq analysis showed that GA alone elevated the auxin level by upregulating the expression of genes involved in the "auxin-activated signaling pathway", connecting with the "response to auxin" of enriched GO terms for 3-hMT-bd-GA/Con (**Supplementary Table S4** of Zhang et al., (Zhang *et al.*, 2023)). CK can biosynthesize de novo locally in the nodal stem to promote axillary bud outgrowth, but auxin suppresses the local biosynthesis of CK (Tanaka *et al.*, 2006) by negatively regulating the expression of the adenosine phosphate-isopentenyltransferase (IPT) gene, which encodes a key enzyme in CK biosynthesis (Takei et al., 2001). Agreeing with that, *StIAA15* and *StIAA22* were reported to be highly expressed in potato tuber sprouts (Gao

et al., 2016), and my results showed that the gene expression of *IAA15* and *IAA22* were only increased in sprouting conditions (**Figure 28**, **Figure 39,** and **Figure 41**). Buskila et al. found that NAA (a synthetic auxin) treatment suppressed the promotive effects of GA and CK on the bud elongation of tubers (Buskila et al., 2016). These results indicate that the GA application might activate auxin-activated signaling, resulting in a repression of CK-activated signaling, which makes it even more necessary for CK to help GA induce MT sprouting in this study. These results allowed me to conclude that GA application elevated auxin levels, reducing CK content. The levels of endogenous auxin and CK content during sprouting require further investigation with a time course design to understand the interaction among GA, CK, and auxin in this sprouting behavior.

RNA-seq analysis also revealed that an ABA core regulator, *PYL4*, was upregulated in sprouting conditions but not detected as DEGs in sprouting-failed conditions (**Figure 32**). *PYLs* function at the first step of the ABA signal pathway, activating the downstream ABA signaling cascade (Zhao et al., 2020) and playing a primary role in seed dormancy and germination (Tuan et al., 2018). Notably, the downregulation of *PP2C* was only detected in 1512 unique DEGs in 3-stMT-bd-GA/Con (**Figure 36**, **Figure 37**). In the absence of ABA, *PYLs* cannot bind to *PP2C*, and therefore *PP2C* activity is high, which prevents the phosphorylation and activation of SnRK2s and downstream substrates, such as ABA-responsive element-binding factors (ABFs) (Née et al., 2017; Soma et al., 2020). Upon binding with ABA, *PYLs* interact with *PP2C* and inhibit *PP2C* by repressing phosphatase activity; in turn, the inhibition of *PP2C* results in the inactivation of ABA (Park et al., 2009), which are core components of the ABA signaling pathway (Biemelt et al., 2000; Park *et al.*, 2009), allowing accumulation of phosphorylated downstream substrates and ABA transcriptional responses. Given that *PYL4* (upregulated) and PP2C (downregulated) were only detected as DEGs in sprouting-induced conditions (**Figure 32**, **Figure 36**, and **Figure 37**) in this RNA-seq analysis, PYL4 *likely* interacted with *PP2C* in response to ABA, reducing the ABA level. As the balance of ABA/GA levels constitutes a vital regulatory mechanism to maintain and release seed dormancy in cereal crops (Finch-Savage and Leubner-Metzger, 2006), although there is no clear correlation between the ABA content and the tuber sprouting in different potato varieties (Nishimura et al., 2007), I speculate that it is possible that the change in ABA level was involved in sprouting growth, providing a reference on potential mechanisms initiating and inhibiting

tuber sprouting growth for further study.

3.4.3 Regulation of the Cytokinin Homeostasis Response to Sprouting Growth

Cytochrome P450 monooxygenases *CYP735A* catalyzed the hydroxylation of iPRDP and iPRTP nucleotides to produce trans-CK (Skalický et al., 2018; Takei et al., 2004) in the "Zeatin biosynthesis" pathway (**Figure 28**), and the upregulated *CYP735A* indicates that CK biosynthesis signaling was activated in sprouting, agreeing with *CYP735A* being actively expressed in tuber sprouts (Lomin et al., 2020). Cis- to trans-isomerization was initially considered as a potential route to trans-CK, and cis-CK most likely plays a role in housekeeping to maintain a minimal CK activity (Gajdosová et al., 2011; Wang et al., 2020). *CISZOG* genes encode a stereo-specific O-glucosylation of cis-zeatin, and *UGT85A1* codes the CK O-glucosylation through O-glucosyltransferases, representing zeatin O-glucosyltransferease with a preference for trans-zeatin and substantially contributing to CK homeostasis (Šmehilová et al., 2016; Wang et al., 2011). *CISZOG* raises the possibility that cis-CK derivatives play a vital role in cytokinin homeostasis (Martin et al., 2001). Cis-CK was also considered as a potato tuber dormancy regulator (Suttle and Banowetz, 2000), and the upregulation of *CISZOG* and *UGT85A1* (**Figure 28**) suggests that CK homeostasis plays a significant role in the developmental process of sprouting. Moreover, almost all cis-CKs are believed to be resistant to cytokinin dehydrogenase/oxidase (CKX), which is essential for mediating CK degradation (Werner et al., 2006). However, this study detected no genes related to CKX as DEGs. These results suggest that CK homeostasis played a crucial role in GA-induced sprouting.

Chapter 4 Transcriptomic Analyses of Microtuber Sprouting Response to Incubation Periods with Gibberellin Treatment

4.1 Introduction

Corps, such as potatoes are often subjected to environmental stresses such as high temperatures, leading to plant hormone chaos or crosstalk, which adversely affect tuber temporary dormancy during the growth and development of potatoes. In my previous studies (in **Chapter 3**), I investigated the profiling of gene expression change at the transcriptome level using MTs (stMTs and hMTs) with the treatment of GA, CK, GACK, or the untreated control to understand the role of CK and the nodal stem in GA-induced sprouting. RNA-seq analyses showed that the pathway of "Plant hormone biosynthesis and signal transduction" was concluded as the hub pathway in GA-induced sprouting.

In this present study, I initiated a comprehensive transcriptome analysis based on the Illumina sequencing platform using stemmed microtubers (stMTs) treated with GA for 36 hours or 72 hours, stMTs before incubation with GA (i.e., on hour 0 of culture) were set as control samples. I compared the differences in genes involved in the "Plant hormone biosynthesis and signal transduction" pathway and the “Zeatin biosynthesis” pathway of apical bud tissues and nodal stem tissues on hour 36 and 72 of culture.

The aim was to figure out the difference in differentially expressed genes (DEGs) between 36-hour-GA treatment with 72-hour-GA treatment, which responds to the regulation of microtuber sprouting by screening out genes and profiles with differential expression during tuber meristem activation processes.

4. 2 Plant Materials and Methods

4.2.1 Plant Materials

Virus-free potato tubers of Solanum tuberosum. L ssp. *andigena* was kindly provided by the Agricultural Research Center.

4.2.2 Preparation of Secondary Growth Microtubers

The adjustment of microtubers was the same as described in **2.2.2 of Chapter 2**, except for deMTs and hMTs. In this chapter, only stMTs were used. These microtubers were cultured on the MS medium supplemented with 10 μM GA, and then incubated for 36 hours or 72 hours at 20 °C in the dark. The microtubers before incubation were set as control (0-hour). Microtubers on hour 0, 36, and 72 of culture served as material for analysis of gene expression. For each condition, 30 microtubers were tested, and 3 biological replicates were collected simultaneously. The preparation methods for the microtubers are summarized in **Figure 47**.

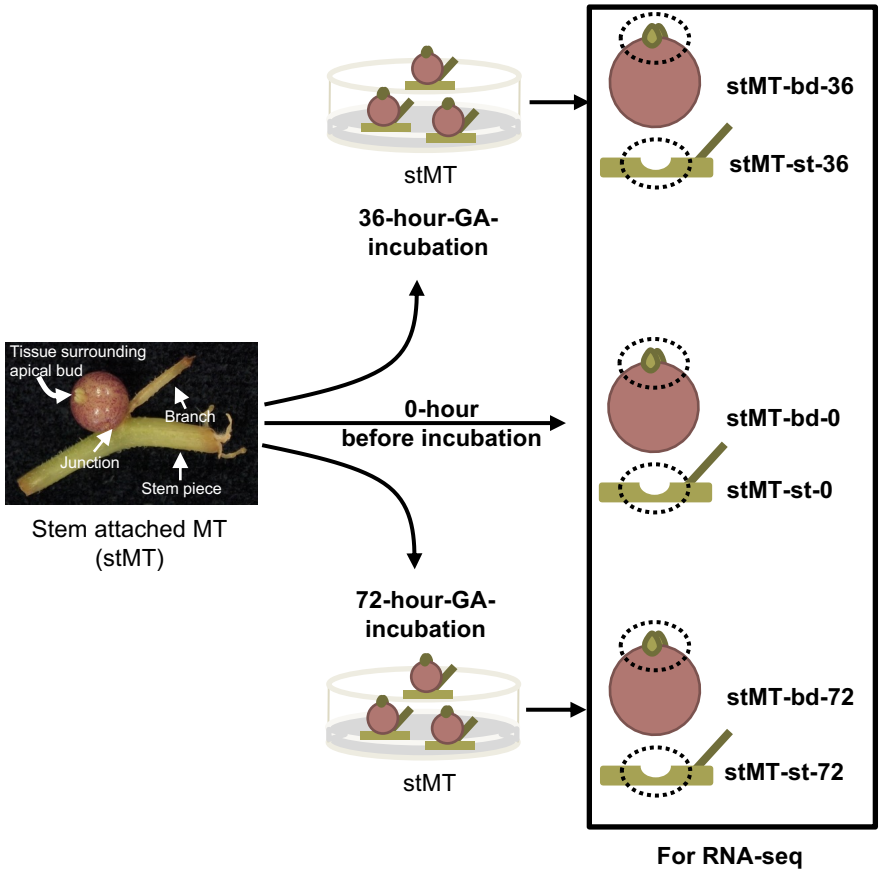


Figure 47. Schematic representation of microtuber (MT) treatment in this study.

Sample preparation for RNA-seq: the black dotted ellipses represent the sampled part for RNA extraction. For stMT-bd-0, -36, -72 the apical bud tissues (bd) and the nodal stem tissues (st) from stMT on hour 0, 36, and 72 of culture by GA treatment, respectively.

4.2.3 RNA Extraction and Sample Preparation

The RNA extraction and sample preparation of microtubers was the same as described in **3.2.3 of Chapter 3**.

4.2.4 TPM Value Calculation and Differential Expression

The R TPM Value Calculation and Differential Expression were the same as described in **3.2.4 of Chapter 3**.

4.3 Results

4.3.1 Transcriptome Sequencing and de novo assembly

In this study, I used *Solanum tuberosum* L. subsp. *andigena* (2n = 4x = 48) for gene analysis. For the transcriptome analysis, 18 samples generated 46.77Gb clean data through RNA sequencing. About 92.09-95.62% of clean data achieved a quality score of Q30 (sequencing error rate < 0.1%), and 85.26-91.06% of the clean reads were successfully mapped to the potato reference genome (S. tuberosum PGSC_DM_v4.03) (Nuraini *et al.*, 2018) (**Table 12**), indicating that all libraries were of high quality. Based on gene expression, principal component analysis (PCA) showed that the 18 samples were assigned to two groups, each associated with one tissue type. The first (PC1) and second (PC2) principal components accounted for 36.34% and 20.02% of the total variance, respectively, showing a good correlation among the three biological replicates for the 18 samples of the RNA-seq results. PC1 separated samples into two big groups corresponding to tissue differences between tissue types: apical bud tissues (bd) and nodal stem tissues (st). The PC1 value was greater than the PC2 value, demonstrating that gene expression patterns were more affected by different tissue types. Moreover, gene expression data from the same type of tissue clustered together but differed among the treated time (**Figure 48**).

Table 12. Summary of RNA-seq data generated from 18 sample.

Sample name*	Clean reads	Mapped reads (%)	GC Content (%)	Q30 Bases Rate(%)
0-stMT-bd-Con_1	53,304,128	85.59	42.71	92.25
0-stMT-bd-Con_2	41,714,966	85.26	42.57	92.97
0-stMT-bd-Con_3	39,696,466	85.65	42.75	92.88
0-stMT-st-Con_1	49,329,484	88.90	43.34	92.75
0-stMT-st-Con_2	47,942,268	88.79	43.24	92.09
0-stMT-st-Con_3	49,656,416	88.94	43.31	92.31
36-stMT-bd-GA_1	21,119,957	89.07	43.21	94.91
36-stMT-bd-GA_2	21,491,017	90.92	44.92	95.43
36-stMT-bd-GA_3	25,863,236	91.06	45.32	95.41
36-stMT-st-GA_1	23,379,770	89.33	43.41	95.62
36-stMT-st-GA_2	24,551,920	88.52	43.94	95.31
36-stMT-st-GA_3	23,794,255	88.69	43.32	95.53
72-stMT-bd-GA_1	48,289,086	86.39	43.16	92.62
72-stMT-bd-GA_2	53,701,594	87.57	43.57	92.29
72-stMT-bd-GA_3	48,581,534	86.63	43.00	92.91
72-stMT-st-GA_1	48,289,086	86.39	43.16	92.62
72-stMT-st-GA_2	53,701,594	87.57	43.57	92.29
72-stMT-st-GA_3	48,581,534	86.63	43.00	92.91

* Sample name includes all tissues used to extract RNA, bd: apical bud tissue; st: nodal stem tissue; stMT: stemmed microtuber; Clean reads: Number of reads remaining after filtering; Q30 bases rate: Proportion of nucleotides with a quality value larger than 30 in the filtered reads.

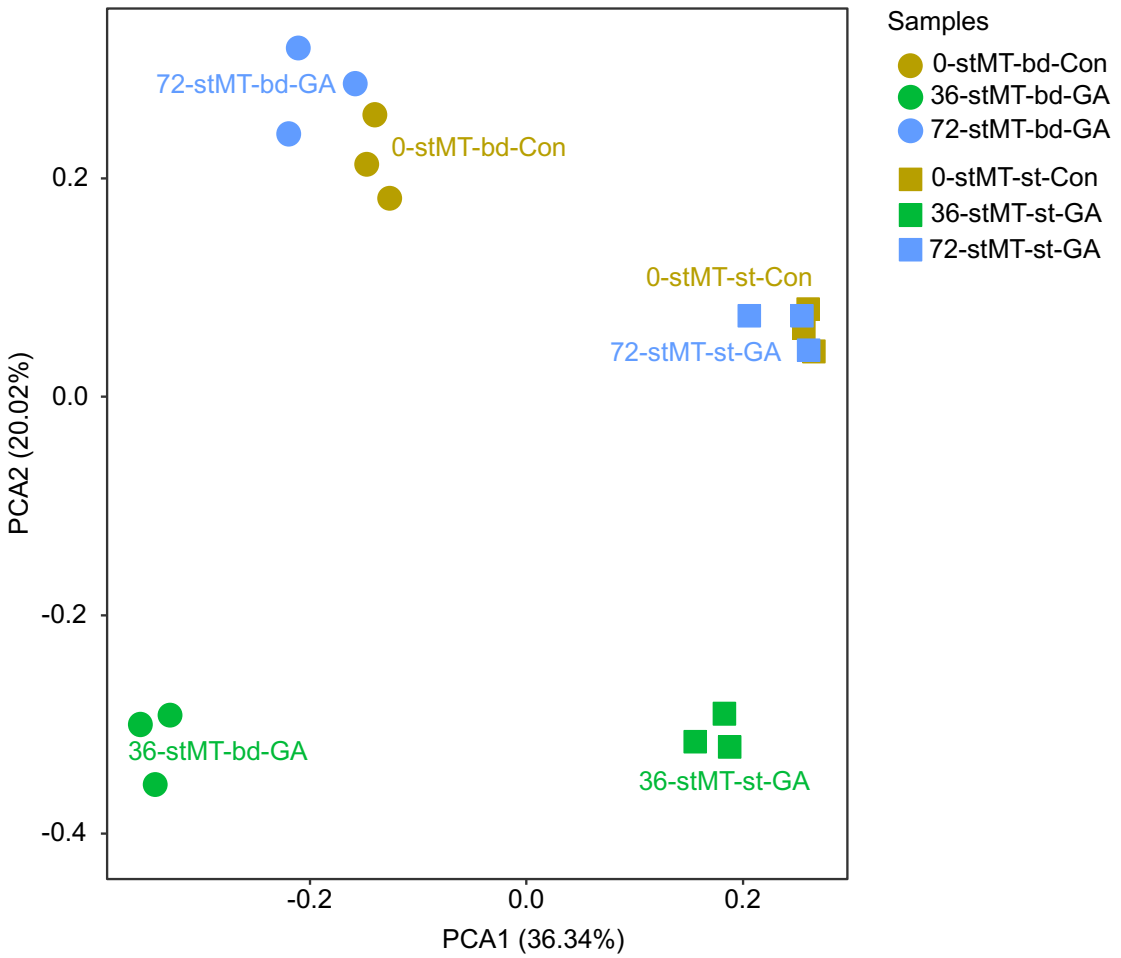


Figure 48. Principal component analysis (PCA) calculated TPM (Transcripts Per kilobase Million) values for RNA-seq data from 18 samples, visualized using the ggplot2 package in R.

Genes included had a TPM over one for all replicates within my study (39,028 genes included in the analysis). Principal components 1 and 2 (PC1 and PC2) could represent 36.34% and 20.20% of all differences among apical bud tissues (bd) and nodal stem tissues (st) of stemmed microtubers (stMTs). PCA plots represent the transcript levels on hour 0, 36, and 72 of culture. Each treatment has three biological replicates.

4.3.2 Differential Transcriptome Response to GA-incubated Periods

I first calculated the differentially expressed genes (DEGs) using DESeq2 for four pairwise comparisons between the GA treatment on hour 36 of culture and the untreated control (0, before incubation) in the apical buds (bd) or the nodal stems (st) of stemmed microtubers (stMTs), respectively (**Figure 49**). For the apical buds of stMTs (stMT-bd), 8266 DEGs (including 4601 upregulated and 3665 downregulated genes) and 2239 DEGs (including 1372 upregulated and 867 downregulated genes) were detected after treatment with GA for 36 and 72 hours, respectively, when compared to control (stMT-bd-36vs0 and stMT-bd-72vs0); for the nodal stems of stMTs (stMT-st), 4938 DEGs (including 3051 upregulated and 1887 downregulated genes) and 930 DEGs (including 444 upregulated and 486 downregulated genes) were detected after treatment with GA for 36 hours and 72 hours, respectively, when compared to control (stMT-st-36vs0 and stMT-st-72vs0). The largest number of differentially expressed genes was found in the comparison of stMT-bd-36vs0, indicating GA treatment induced more changes in gene expression on hour 36 of culture in the apical buds of microtubers than on hour 72 of culture.

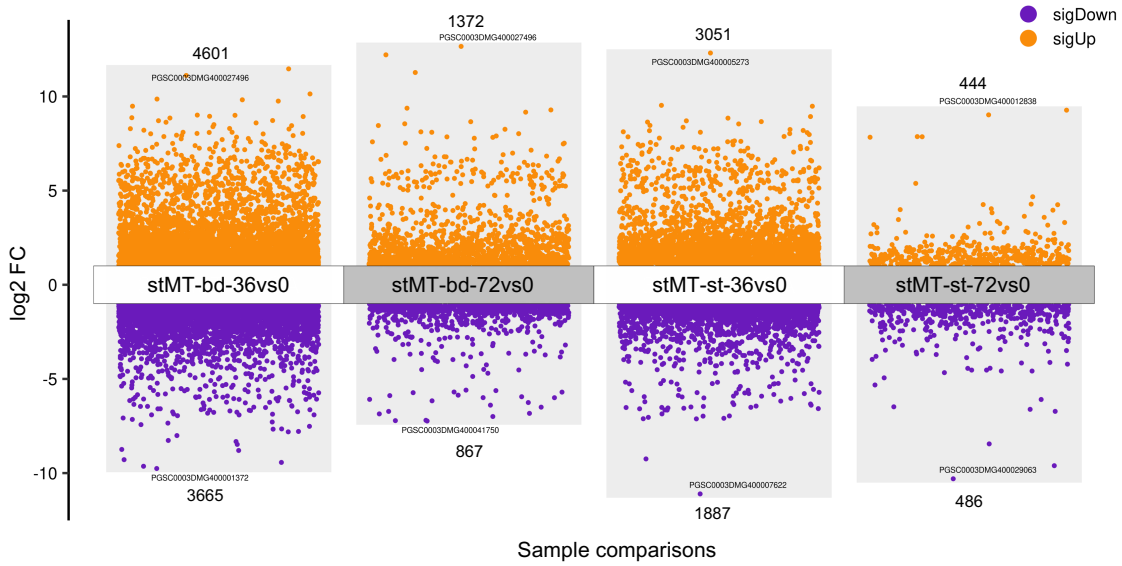


Figure 49. Identification of the differentially expressed gene (DEG) between GA-incubated hours with 0 hour.

Volcano plot and numbers of the differentially upregulated (orange) and downregulated (purple) DEGs in the pairwise comparisons of GA-incubated hours with 0 hour (before incubation) in apical bud tissues (bd) and the nodal stem tissue (st) of stemmed microtubers (stMTs) on hour 36 and 72 of culture, respectively. DEGs were calculated using the DEseq2 package in R. The up- or down-regulated counts of DEGs and genes with the highest or lowest log2FC value were shown next to the volcano plot.

4.3.3 Plant Hormone Signal Transduction Pathway Response to Apical Bud Tissues

To better understand the difference in microtuber sprouting response to GA-treated periods at the molecular level. I first compared the differences in DEGs in apical bud tissues between stMT-bd-36vs0 and stMT-bd-72vs0 (**Figure 50**). They shared 1321 DEGs, of which 834 genes were upregulated, 327 were downregulated in both comparisons, 120 genes were downregulated in stMT-bd-36vs0 but upregulated in stMT-bd-72vs0, another 40 genes were upregulated in stMT-bd-36vs0 but downregulated in stMT-bd-72vs0 (**Figure 50A**). To reveal the molecular differences in sprouting response to the GA-treated period, I focused on all DEGs detected in stMT-bd-36vs0 and stMT-bd-72vs0. When stMTs were exposed to exogenous GA for 36 hours and 72 hours, the 8 and 5 most significant Kyoto Encyclopedia of Genes and Genomes (KEGG) pathways ($p < 0.05$) were significantly enriched, respectively (**Figure 50**). Four co-annotated metabolic pathways were found in both comparisons (**Figure 50B**), which were "Plant hormone signal transduction pathway", "Photosynthesis pathway", "Glutathione metabolism pathway", and "Photosynthesis-antenna proteins pathway".

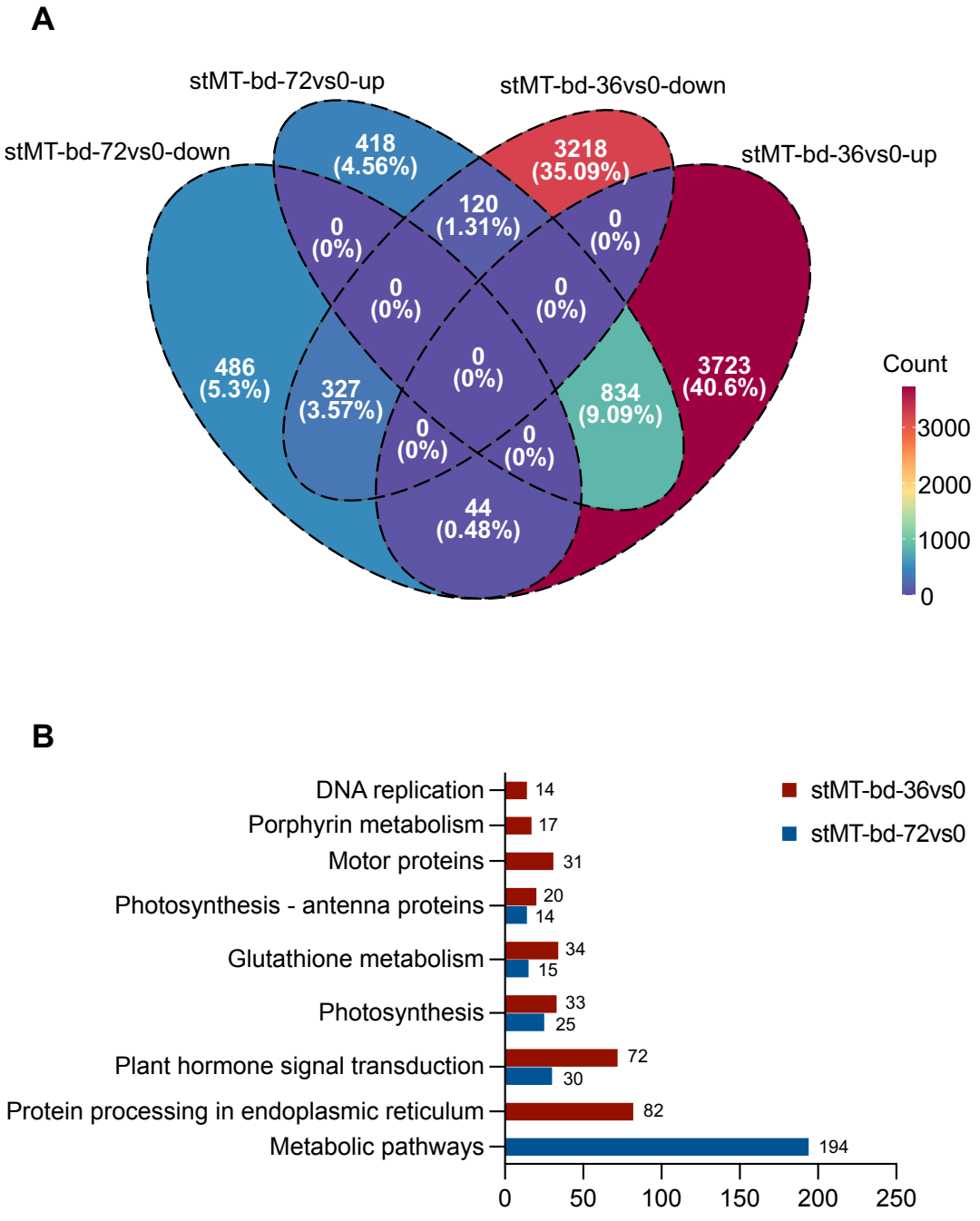


Figure 50. DEGs identified in apical bud tissues (bd) of stemmed microtubers.

(**A**) A Venn diagram to visualize the similarities and differences of DEGs among four comparisons: stMT-bd-36vs0-up, stMT-bd-36vs0-down, stMT-bd-72vs0-up, and stMT-bd-72vs0-down.

(**B**) The comparison of enriched KEGG pathways for DEGs of stMT-bd-36vs0 and stMT-bd-72vs0 using DAVID ($p < 0.05$), visualized using GraphPad PRISM.

I found the Plant hormone signal transduction pathway hub pathway, which plays an important role in response to microtuber sprouting in **Chapter 4;** this study mainly focuses on the Plant hormone signal transduction pathway. According to the analysis of the Plant hormone signal transduction pathway (**Figure 51, Figure 52**), the results showed that 72 DEGs were annotated in the comparison group of stMT-bd-36vs0. Among them, 19 DEGs were upregulated and 53 DEGs were downregulated. In the comparison group of stMT-bd-72vs0, 30 DEGs were annotated. Among them, 14 DEGs were upregulated and 16 DEGs were downregulated. Especially, there were 18 DEGs co-annotated to stMT-bd-36vs0 and stMT-bd-72vs0 comparison groups (**Figure 53**). Among these 84 genes, the expression levels of genes involved in *SAUR* were downregulated when exogenous GA was applied for 36 hours, but the expression levels of the comparison group were upregulated when exogenous GA was applied for 72 hours. In contrast, the expression levels of the auxin response factor, *ARF*, were the opposite (**Figure 51, Figure 52**). Suggesting that PGSC0003DMG400003673 (*SAUR*), PGSC0003DMG400003771 (*ARF5*), PGSC0003DMG400002392 (*ARF7*), and PGSC0003DMG400012261 (*ARF9*) were auxin-related important genes involved in the changes from dormancy breaking to sprouting of microtuber.

Remarkably, the expression levels of PGSC0003DMG400006550 (*AUX1*), PGSC0003DMG400016317 (*IAA4*), PGSC0003DMG400005327 (*IAA16*), PGSC0003DMG400024997 (*GH3*), PGSC0003DMG400021803 (*GH3*), PGSC0003DMG400001601 (*SAUR*), PGSC0003DMG400001654 (*SAUR*) were all upregulated, while PGSC0003DMG400003773 (*SAUR*), PGSC0003DMG400016643 (*ARR17*), PGSC0003DMG400003849 (*GID1*), PGSC0003DMG400021991 (*GID1*), PGSC0003DMG400023897 (*ABF*), PGSC0003DMG400030928 (*EBF1/2*), PGSC0003DMG400015853 (*EBF1/2*), PGSC0003DMG400013255 (*ERF1/2*), PGSC0003DMG400014204 (*ERF1/2*), and PGSC0003DMG400015853 (*NPR5*) were all downregulated on hour 36 and 72 of culture (**Figure 53**).

Therefore, these 21 DEGs (**Figure 53**) are affected by exogenous GA addition, actively participate in dormancy breaking, and play an important role in the plant hormone signal transduction pathway.

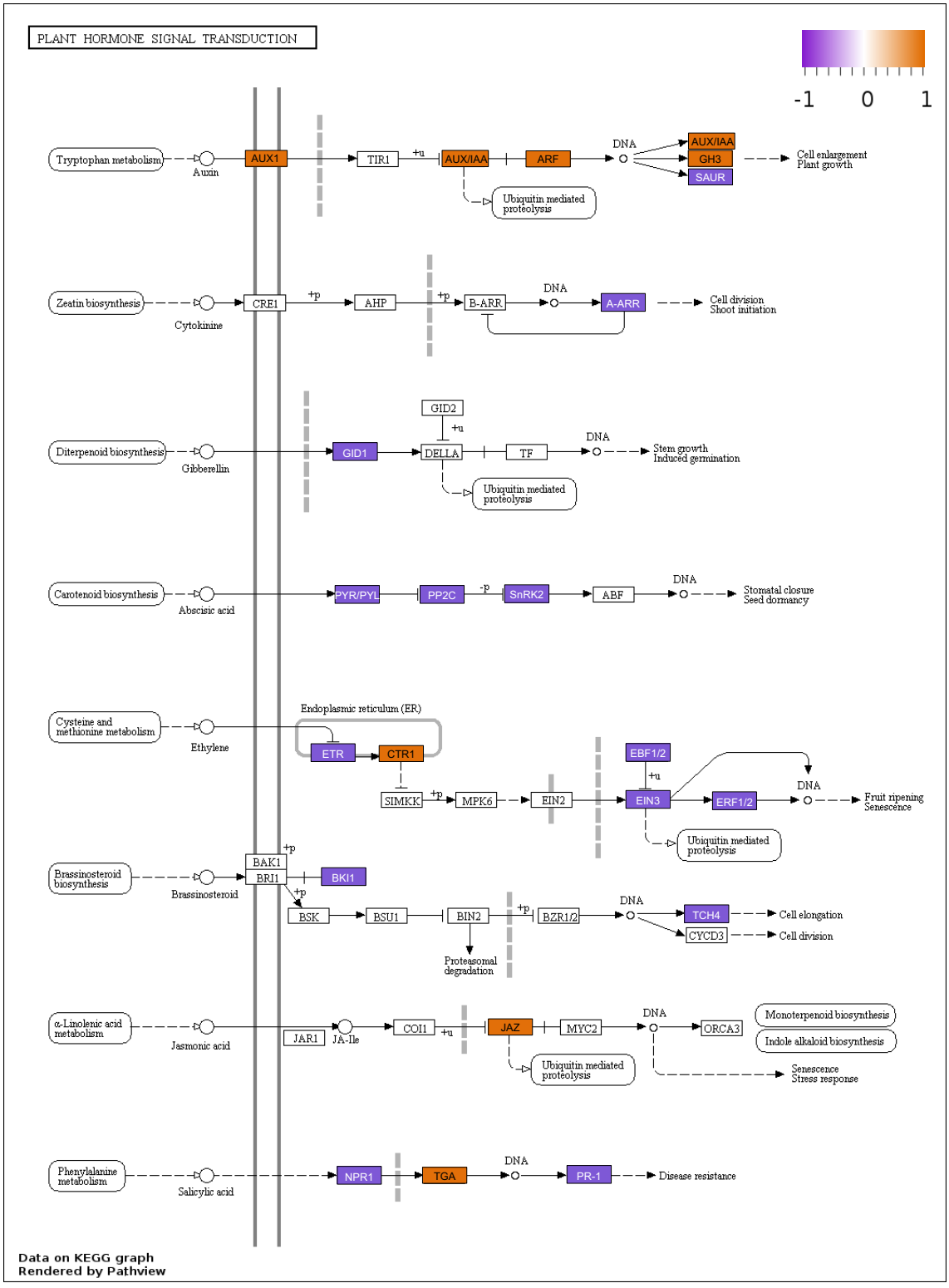


Figure 51. The differentially upregulated (orange) and downregulated (purple) DEGs involved in the pathway of "Plant hormone signal transduction" in the apical bud tissues (bd) on hour 36 of culture.

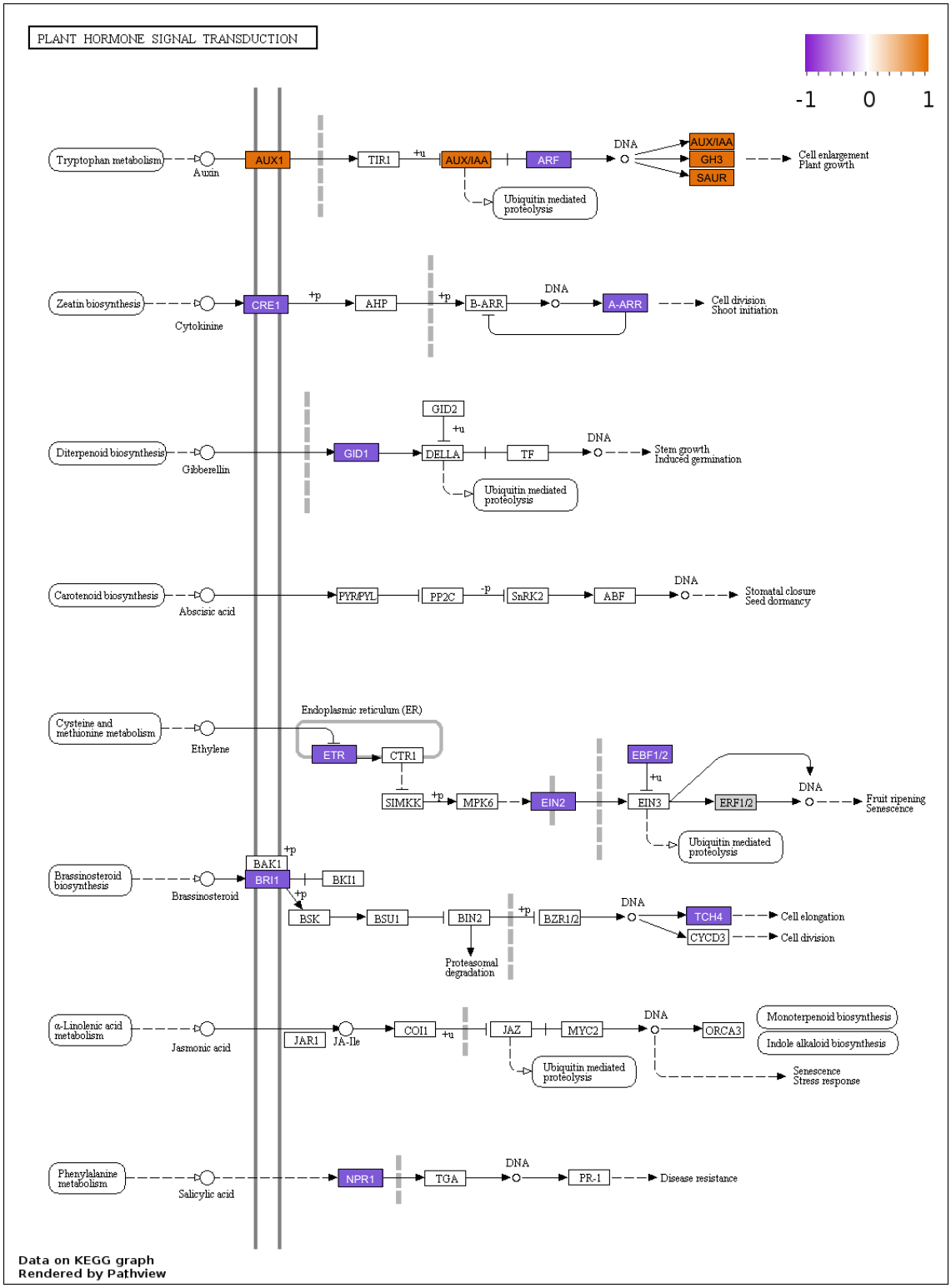


Figure 52. The differentially upregulated (orange) and downregulated (purple) DEGs involved in the pathway of "Plant hormone signal transduction" in apical bud tissues (bd) on hour 72 of culture.

Plant hormone signal transduction

Gene ID PGSC0003DMG	Gene Description	Function	stMT-bd-36vs0	stMT-bd-72vs0
400006550	AUX1	Auxin influx transport protein	2.57	1.40
400008504	AUX1	Auxin influx transport protein	1.25	not DEG
400023205	AUX1	Auxin influx transport protein	2.52	not DEG
400001589	AUX1	Auxin influx transport protein	2.24	not DEG
402002635	IAA1	AUX/IAA gene family	-3.11	not DEG
400005338	IAA3	AUX/IAA gene family	not DEG	3.06
400016317	IAA4	AUX/IAA gene family	1.76	1.86
400006108	IAA4	AUX/IAA gene family	not DEG	1.14
400002636	IAA6	AUX/IAA gene family	6.41	not DEG
400006093	IAA14	AUX/IAA gene family	not DEG	1.46
400005327	IAA16	AUX/IAA gene family	2.27	2.90
400020139	IAA22	AUX/IAA gene family	not DEG	1.31
400019302	IAA22	AUX/IAA gene family	-1.67	not DEG
400003771	ARF5	Auxin response factor 5	not DEG	-1.39
400012261	ARF7	Auxin response factor 7	2.56	not DEG
400002392	ARF9	Auxin response factor 9	1.06	not DEG
400024997	GH3	Indole-3-acetic acid-amido synthetase GH3.6-like	2.27	1.36
400021803	GH3	Indole-3-acetic acid-amido synthetase GH3.6	2.47	1.65
400024978	GH3	Indole-3-acetic acid-amido synthetase GH3.6-like	2.19	not DEG
400021676	GH3	Indole-3-acetic acid-amido synthetase GH3.5	3.03	not DEG
400019274	GH3	Indole-3-acetic acid-amido synthetase GH3.1	1.15	not DEG
400026186	GH3	Indole-3-acetic acid-amido synthetase GH3.6-like	-2.16	not DEG
400001601	SAUR	Auxin-induced protein 15A-like	5.66	6.69
400003673	SAUR	Auxin-induced protein 15A-like	-2.45	1.43
400008070	SAUR	Indole-3-acetic acid-induced protein ARG7	not DEG	2.23
400022233	SAUR	Indole-3-acetic acid-induced protein ARG7	-1.98	not DEG
400001654	SAUR	Auxin-induced protein 15A	4.99	5.85
400001614	SAUR	Auxin-induced protein 15A	not DEG	2.00
400003773	SAUR	Auxin-induced protein 15A	-5.03	-1.77
400008950	SAUR	Auxin-induced protein 15A	-5.48	not DEG
400028254	SAUR	Auxin-induced protein 15A	-4.30	not DEG
400001647	SAUR	Auxin-induced protein 15A	-1.23	not DEG
400030234	SAUR	Auxin-responsive protein SAUR32	-1.07	not DEG
400026010	SAUR	Auxin-responsive protein SAUR36	-2.36	not DEG
400004786	SAUR	Auxin-responsive protein SAUR36	-1.26	not DEG
400004785	SAUR	Auxin-responsive protein SAUR36	-1.98	not DEG
400035783	SAUR	Auxin-responsive protein SAUR71	-3.50	not DEG
400020701	SAUR	Auxin-responsive protein SAUR71	-2.70	not DEG
400029463	CRE1	Cytokinin receptor 1, histidine kinase 4	not DEG	-1.01
402022640	ARR5	Type-A response regulator	-1.41	not DEG
400003084	ARR8	Type-A response regulator	-2.15	not DEG
400002945	ARR9	Type-A response regulator	3.22	not DEG
400016643	ARR17	Type-A response regulator	-3.04	-1.27

Figure 53. *Cont.*

Plant hormone signal transduction. Cont.

Gene ID PGSC0003DMG	Gene Description	Function	stMT-bd-36vs0	stMT-bd-72vs0
400021991	GID1	GID1-like gibberellin receptor	-2.62	-1.60
400003849	GID1	GID1-like gibberellin receptor	-3.22	-2.67
400029194	PYL4	Abscisic acid receptor	-2.98	not DEG
400027118	PYL4	Abscisic acid receptor	-7.67	not DEG
400000215	PYL7	Abscisic acid receptor	-1.81	not DEG
400009108	PYL8	Abscisic acid receptor	-1.07	not DEG
400012155	PYL9	Abscisic acid receptor	-1.46	not DEG
400030332	PP2C	Protein phosphatase 2C	-1.89	not DEG
400016742	PP2C	Protein phosphatase 2C	-1.38	not DEG
400023803	SnRK2	Serine/threonine-protein kinase SRK2B-like	-1.06	not DEG
400023897	ABF	BZIP transcription factor 27-like	-2.05	-1.80
400028694	ETR	Ethylene receptor homolog, protein EIN4	not DEG	-1.10
400017186	ETR	Ethylene receptor 2-like	-1.05	not DEG
400008384	CTR1	Serine/threonine-protein kinase CTR1	1.09	not DEG
400021547	EIN2	Ethylene signaling proteine 2	not DEG	-1.24
400008712	EIN3	ETHYLENE INSENSITIVE 3-like, EIL2	-1.57	not DEG
400030928	EBF1/2	EIN3-binding F-box protein 1	-1.39	-1.04
400015853	EBF1/2	EIN3-binding F-box protein 1	-1.25	-2.44
400013255	ERF1/2	ERF transcription factor 5	-2.71	-1.40
400014204	ERF1/2	Ethylene-responsive transcription factor TSRF1	-3.41	-1.62
400017231	ERF1/2	Ethylene-responsive transcription factor TSRF1	-1.92	not DEG
400023619	ERF1/2	Ethylene-responsive transcription factor 1B-like	-2.78	not DEG
400014594	ERF1/2	Ethylene-responsive transcription factor 1B-like	-1.68	not DEG
400013257	ERF1/2	Ethylene-responsive transcription factor 1B-like	-1.45	not DEG
400019698	BRI1	BRI1 protein	not DEG	-1.08
400015442	BKI1	BRI1 kinase inhibitor 1	-2.10	not DEG
400013975	TCH4	Xyloglucan endotransglycosylase/hydrolase XTH-6	-1.52	not DEG
400004367	JAZ	TIFY/JAZ family	-1.33	not DEG
400015667	JAZ	TIFY/JAZ family	2.63	not DEG
400010635	NPR5	Regulatory protein NPR5	not DEG	-1.05
400029834	NPR5	Regulatory protein NPR5	-2.08	-1.53
400012962	TGA	Transcription factor HBP-1b(C1)	1.11	not DEG
400005116	PR-1	PR1 protein	-4.92	not DEG
400005112	PR-1	PR1 protein	-4.16	not DEG
400005111	PR-1	PR1 protein	-3.98	not DEG
400005110	PR-1	PR1 protein	-5.34	not DEG
400005109	PR-1	PR1 protein	-4.94	not DEG
400005108	PR-1	PR1 protein	-7.08	not DEG
400002027	PR-1	PR1 protein	-4.09	not DEG
400002028	PR-1	PR1 protein	-4.38	not DEG
400002029	PR-1	PR1 protein	-6.91	not DEG

-7.67 6.69

Figure 53. Functional annotations of DEGs in the apical bud tissues (bd) on hour 36 and 72 of culture with exogenous GA, respectively.

The table shows genes included in the pathways "Plant hormone signal transduction" for each comparison, with a heatmap showing gene expression levels as $\log_2$ FC.

Orange represents upregulation, and purple represents downregulation compared to Control (untreated).

4.3.4 Gene Ontology (GO) Terms Response to Apical Bud Tissues

When stMTs were exposed to exogenous GA for 36 hours and 72 hours, the 62 and 33 most significant biological processes (BP) terms (**Table 13, Table 14**), 28 and 12 cellular components (CC) terms (**Table 15, Table 16**), 48 and 25 molecular functions (MF) terms (**Table 17, Table 18**) were significantly enriched ($p < 0.05$), respectively. Six co-annotated GO terms in the top 10 BP terms were found in both comparisons (**Figure 54**), which were "xyloglucan metabolic process", "cell wall biogenesis", "photosynthesis", "light harvesting in photosystem I", "photosynthesis", "response to light stimulus", and "protein oligomerization". For stMT exposed to exogenous GA for 36 hours, "positive regulation of transcription, DNA-templated", "response to salt stress", "response to hydrogen peroxide", and "response to heat" played the essential role in response to the dormancy breaking. For stMT exposed to exogenous GA for 72 hours, "regulation of transcription, DNA-templated", "glutathione metabolic process", "nucleosome assembly", and "protein-chromophore linkage" played the essential role in response to microtuber sprouting.

Table 13. Biological Processes of Gene Ontology (GO) enrichment analysis for 8266 DEGs in stMT-bd-36vs0

Term ID	Term Description	Gene Count	Gene (%)	*p* Value
Category of Biological Processes				
GO:0009408	response to heat	33	0.67	2.79E-10
GO:0051259	protein oligomerization	21	0.43	4.20E-10
GO:0009416	response to light stimulus	37	0.75	8.56E-10
GO:0015979	photosynthesis	39	0.79	1.13E-08
GO:0009768	photosynthesis, light harvesting in photosystem I	20	0.41	6.45E-08
GO:0042546	cell wall biogenesis	18	0.37	8.62E-07
GO:0042542	response to hydrogen peroxide	21	0.43	1.23E-06
GO:0010411	xyloglucan metabolic process	20	0.41	1.58E-06
GO:0009651	response to salt stress	28	0.57	3.62E-06
GO:0045893	positive regulation of transcription, DNA-templated	38	0.77	1.89E-05
GO:0015995	chlorophyll biosynthetic process	14	0.28	2.6E-05
GO:0007018	microtubule-based movement	21	0.43	6.82E-05
GO:0000727	double-strand break repair via break-induced replication	8	0.16	0.000126
GO:0034620	cellular response to unfolded protein	11	0.22	0.000132
GO:0006270	DNA replication initiation	9	0.18	0.000306
GO:0016584	nucleosome positioning	9	0.18	0.000306
GO:0042026	protein refolding	15	0.30	0.000372
GO:0000209	protein polyubiquitination	27	0.55	0.001153
GO:0045165	cell fate commitment	6	0.12	0.001169
GO:0006457	protein folding	48	0.97	0.001216
GO:0009299	mRNA transcription	8	0.16	0.002085
GO:0006414	translational elongation	10	0.20	0.002767
GO:0010158	abaxial cell fate specification	8	0.16	0.00341
GO:0018298	protein-chromophore linkage	26	0.53	0.003462
GO:0006334	nucleosome assembly	19	0.39	0.003804
GO:0006995	cellular response to nitrogen starvation	8	0.16	0.005292
GO:0009414	response to water deprivation	16	0.32	0.007161
GO:0030261	chromosome condensation	7	0.14	0.007187
GO:0045910	negative regulation of DNA recombination	8	0.16	0.007855
GO:0034605	cellular response to heat	11	0.22	0.009026
GO:0009944	polarity specification of adaxial/abaxial axis	4	0.08	0.011671

Table 13. *Cont.*

GO:1990592	protein K69-linked ufmylation	4	0.08	0.011671
GO:1902975	mitotic DNA replication initiation	4	0.08	0.011671
GO:0034389	lipid particle organization	5	0.10	0.011708
GO:1905786	positive regulation of anaphase-promoting complex-dependent catabolic process	5	0.10	0.011708
GO:0051085	chaperone mediated protein folding requiring cofactor	14	0.28	0.011716
GO:0006412	translation	82	1.66	0.011939
GO:0010597	green leaf volatile biosynthetic process	63	1.28	0.013137
GO:0051301	cell division	29	0.59	0.014084
GO:0006749	glutathione metabolic process	25	0.51	0.015104
GO:0009805	coumarin biosynthetic process	35	0.71	0.021865
GO:0002238	response to molecule of fungal origin	35	0.71	0.021865
GO:0009738	abscisic acid-activated signaling pathway	16	0.32	0.023294
GO:0016567	protein ubiquitination	63	1.28	0.024274
GO:0035067	negative regulation of histone acetylation	4	0.08	0.025954
GO:2000024	regulation of leaf development	4	0.08	0.025954
GO:0006271	DNA strand elongation involved in DNA replication	4	0.08	0.025954
GO:0098869	cellular oxidant detoxification	4	0.08	0.025954
GO:0006261	DNA-dependent DNA replication	8	0.16	0.027426
GO:0071555	cell wall organization	30	0.61	0.029077
GO:0009926	auxin polar transport	7	0.14	0.030576
GO:0006616	SRP-dependent cotranslational protein targeting to membrane, translocation	5	0.10	0.032908
GO:0031222	arabinan catabolic process	5	0.10	0.032908
GO:0044772	mitotic cell cycle phase transition	12	0.24	0.033375
GO:0008360	regulation of cell shape	8	0.16	0.035204
GO:0080163	regulation of protein serine/threonine phosphatase activity	11	0.22	0.039564
GO:0006511	ubiquitin-dependent protein catabolic process	41	0.83	0.043864
GO:0009638	phototropism	4	0.08	0.046224
GO:0042549	photosystem II stabilization	4	0.08	0.046224
GO:0009908	flower development	10	0.20	0.046988
GO:0009788	negative regulation of abscisic acid-activated signaling pathway	5	0.10	0.048523
GO:0000079	regulation of cyclin-dependent protein serine/threonine kinase activity	14	0.28	0.049754

Table 14. Biological Processes of Gene Ontology (GO) enrichment analysis for 2339 DEGs in stMT-bd-72vs0

Term ID	Term Description	Gene Count	Gene (%)	*p* Value
Category of Biological Processes				
GO:0015979	photosynthesis	27	1.87	2.79E-13
GO:0009768	photosynthesis, light harvesting in photosystem I	14	0.97	2.03E-09
GO:0009416	response to light stimulus	20	1.38	7.03E-09
GO:0018298	protein-chromophore linkage	17	1.18	7.81E-06
GO:0010411	xyloglucan metabolic process	11	0.76	1.17E-05
GO:0042546	cell wall biogenesis	10	0.69	1.2E-05
GO:0051259	protein oligomerization	8	0.55	0.00041
GO:0006334	nucleosome assembly	11	0.76	0.000537
GO:0006749	glutathione metabolic process	14	0.97	0.000832
GO:0006355	regulation of transcription, DNA-templated	55	3.80	0.000834
GO:0009408	response to heat	11	0.76	0.000995
GO:0002238	response to molecule of fungal origin	18	1.24	0.001227
GO:0009805	coumarin biosynthetic process	18	1.24	0.001227
GO:0044772	mitotic cell cycle phase transition	8	0.55	0.002355
GO:0045490	pectin catabolic process	14	0.97	0.003352
GO:0042542	response to hydrogen peroxide	8	0.55	0.003566
GO:0050832	defense response to fungus	33	2.28	0.00366
GO:0045893	positive regulation of transcription, DNA-templated	14	0.97	0.004761
GO:0009873	ethylene-activated signaling pathway	11	0.76	0.0063
GO:0010167	response to nitrate	4	0.28	0.008988
GO:0099402	plant organ development	6	0.41	0.009419
GO:0010597	green leaf volatile biosynthetic process	25	1.73	0.011058
GO:0000079	regulation of cyclin-dependent protein serine/threonine kinase activity	8	0.55	0.011127
GO:0006021	inositol biosynthetic process	3	0.21	0.019057
GO:0009651	response to salt stress	9	0.62	0.019502
GO:0071555	cell wall organization	13	0.90	0.023327
GO:0042549	photosystem II stabilization	3	0.21	0.027727
GO:0010584	pollen exine formation	3	0.21	0.037655
GO:1905786	positive regulation of anaphase-promoting complex-dependent catabolic process	3	0.21	0.037655
GO:0008643	carbohydrate transport	7	0.48	0.038929
GO:0046854	phosphatidylinositol phosphorylation	4	0.28	0.040163
GO:0009733	response to auxin	14	0.97	0.048619
GO:0019253	reductive pentose-phosphate cycle	3	0.21	0.048709

Table 15. Cellular Component of Gene Ontology (GO) enrichment analysis for 8266 DEGs in stMT-bd-36vs0

Term ID	Term Description	Gene Count	Gene (%)	*p* Value
Category of Cellular Component				
GO:0005634	nucleus	680	13.80	1.48E-09
GO:0005737	cytoplasm	405	8.22	9.98E-08
GO:0009535	chloroplast thylakoid membrane	59	1.20	3.15E-07
GO:0000786	nucleosome	33	0.67	6.28E-07
GO:0009538	photosystem I reaction center	9	0.18	7.78E-06
GO:0009523	photosystem II	27	0.55	1.92E-05
GO:0009522	photosystem I	23	0.47	2.42E-05
GO:0048046	apoplast	47	0.95	2.77E-05
GO:0009654	photosystem II oxygen evolving complex	14	0.28	0.000105
GO:0005886	plasma membrane	238	4.83	0.00047
GO:0005615	extracellular space	31	0.63	0.000591
GO:0005829	cytosol	134	2.72	0.000671
GO:0005730	nucleolus	47	0.95	0.000932
GO:0042555	MCM complex	6	0.12	0.001146
GO:0000347	THO complex	6	0.12	0.001146
GO:0022627	cytosolic small ribosomal subunit	26	0.53	0.001264
GO:0005770	late endosome	7	0.14	0.004329
GO:0031982	vesicle	10	0.20	0.005352
GO:0015629	actin cytoskeleton	12	0.24	0.006093
GO:0043231	intracellular membrane-bounded organelle	45	0.91	0.009848
GO:0005680	anaphase-promoting complex	8	0.16	0.015204
GO:0019898	extrinsic component of membrane	11	0.22	0.026784
GO:0005874	microtubule	32	0.65	0.034596
GO:0000812	Swr1 complex	4	0.08	0.045722
GO:0034663	endoplasmic reticulum chaperone complex	4	0.08	0.045722
GO:0009507	chloroplast	102	2.07	0.04586
GO:0000307	cyclin-dependent protein kinase holoenzyme complex	17	0.34	0.047461
GO:0032991	macromolecular complex	5	0.10	0.047881

Table 16. Cellular Component of Gene Ontology (GO) enrichment analysis for 2339 DEGs in stMT-bd-72vs0

Term ID	Term Description	Gene Count	Gene (%)	*p* Value
Category of Cellular Component				
GO:0009523	photosystem II	22	1.52	5.10E-12
GO:0000786	nucleosome	22	1.52	1.34E-10
GO:0009535	chloroplast thylakoid membrane	33	2.28	2.01E-10
GO:0005886	plasma membrane	106	7.33	4.49E-10
GO:0009538	photosystem I reaction center	9	0.62	4.82E-10
GO:0009522	photosystem I	17	1.18	3.12E-09
GO:0005634	nucleus	217	15.01	2.94E-06
GO:0005576	extracellular region	39	2.70	0.001707
GO:0019005	SCF ubiquitin ligase complex	9	0.62	0.002069
GO:0048046	apoplast	17	1.18	0.003018
GO:0000307	cyclin-dependent protein kinase holoenzyme complex	10	0.69	0.003037
GO:0009654	photosystem II oxygen evolving complex	5	0.35	0.034594

Table 17. Molecular Function of Gene Ontology (GO) enrichment analysis for 8266 unique DEGs in stMT-bd-36vs0

Term ID	Term Description	Gene Count	Gene (%)	*p* Value
Category of Molecular Function				
GO:0043621	protein self-association	26	0.53	2.44E-09
GO:0051082	unfolded protein binding	48	0.97	5.22E-09
GO:0000976	transcription regulatory region sequence-specific DNA binding	93	1.89	2.73E-06
GO:0008017	microtubule binding	41	0.83	6.68E-05
GO:0031072	heat shock protein binding	13	0.26	7.63E-05
GO:0097573	glutathione oxidoreductase activity	22	0.45	0.00017
GO:0003697	single-stranded DNA binding	19	0.39	0.000228
GO:0004364	glutathione transferase activity	25	0.51	0.000266
GO:0016762	xyloglucan:xyloglucosyl transferase activity	18	0.37	0.000269
GO:0004866	endopeptidase inhibitor activity	16	0.32	0.00048
GO:0051787	misfolded protein binding	11	0.22	0.000573
GO:0051015	actin filament binding	19	0.39	0.000587
GO:0003746	translation elongation factor activity	12	0.24	0.000793
GO:0003735	structural constituent of ribosome	90	1.83	0.000982
GO:0046982	protein heterodimerization activity	32	0.65	0.001032
GO:0003700	transcription factor activity, sequence-specific DNA binding	184	3.73	0.001197
GO:0003777	microtubule motor activity	13	0.26	0.001312
GO:0044183	protein binding involved in protein folding	12	0.24	0.001505
GO:0061631	ubiquitin conjugating enzyme activity	15	0.30	0.00199
GO:0004864	protein phosphatase inhibitor activity	15	0.30	0.002491
GO:0031492	nucleosomal DNA binding	7	0.14	0.002508
GO:0038023	signaling receptor activity	17	0.34	0.003032
GO:0010997	anaphase-promoting complex binding	6	0.12	0.003311
GO:0030145	manganese ion binding	18	0.37	0.004187
GO:0003678	DNA helicase activity	10	0.20	0.004835
GO:0016799	hydrolase activity, hydrolyzing N-glycosyl compounds	6	0.12	0.005899
GO:0043565	sequence-specific DNA binding	74	1.50	0.007636
GO:1990757	ubiquitin ligase activator activity	5	0.10	0.007879
GO:0003677	DNA binding	201	4.08	0.008665
GO:0005509	calcium ion binding	56	1.14	0.012347
GO:0046556	alpha-L-arabinofuranosidase activity	6	0.12	0.014729

Table 17. *Cont.*

GO:0034485	phosphatidylinositol-3,4,5-trisphosphate 5-phosphatase activity	6	0.12	0.014729
GO:0016717	oxidoreductase activity, acting on paired donors, with oxidation of a pair of donors resulting in the reduction of molecular oxygen to two molecules of water	8	0.16	0.020427
GO:0008080	N-acetyltransferase activity	14	0.28	0.022764
GO:0003727	single-stranded RNA binding	6	0.12	0.029642
GO:0016887	ATPase activity	54	1.10	0.029762
GO:0004439	phosphatidylinositol-4,5-bisphosphate 5-phosphatase activity	7	0.14	0.0323
GO:0003774	motor activity	7	0.14	0.0323
GO:0016881	acid-amino acid ligase activity	7	0.14	0.0323
GO:0051539	4 iron, 4 sulfur cluster binding	21	0.43	0.032839
GO:0003729	mRNA binding	64	1.30	0.033419
GO:0010427	abscisic acid binding	11	0.22	0.03369
GO:0003887	DNA-directed DNA polymerase activity	5	0.10	0.03397
GO:1990825	sequence-specific mRNA binding	4	0.08	0.034592
GO:0008194	UDP-glycosyltransferase activity	47	0.95	0.035548
GO:0070181	small ribosomal subunit rRNA binding	7	0.14	0.041089
GO:0005544	calcium-dependent phospholipid binding	5	0.10	0.047875
GO:0000234	phosphoethanolamine N-methyltransferase activity	3	0.06	0.048547

Table 18. Molecular Function of Gene Ontology (GO) enrichment analysis for 2339 unique DEGs in stMT-bd-72vs0

Term ID	Term Description	Gene Count	Gene (%)	*p* Value
Category of Molecular Function				
GO:0046982	protein heterodimerization activity	22	1.52	1.14E-07
GO:0016762	xyloglucan:xyloglucosyl transferase activity	11	0.76	4.55E-05
GO:0046872	metal ion binding	102	7.05	2.14E-04
GO:0000976	transcription regulatory region sequence-specific DNA binding	35	2.42	2.76E-04
GO:0043565	sequence-specific DNA binding	34	2.35	2.77E-04
GO:0003700	transcription factor activity, sequence-specific DNA binding	71	4.91	0.000305
GO:0003677	DNA binding	79	5.46	0.000415
GO:0004364	glutathione transferase activity	12	0.83	0.000822
GO:0030570	pectate lyase activity	7	0.48	0.001247
GO:0045551	cinnamyl-alcohol dehydrogenase activity	5	0.35	0.005593
GO:0043621	protein self-association	8	0.55	0.005943
GO:0031418	L-ascorbic acid binding	19	1.31	0.006817
GO:0016168	chlorophyll binding	14	0.97	0.007254
GO:0016538	cyclin-dependent protein serine/threonine kinase regulator activity	8	0.55	0.008847
GO:0016630	protochlorophyllide reductase activity	3	0.21	0.015722
GO:0016706	oxidoreductase activity, acting on paired donors, with incorporation or reduction of molecular oxygen, 2-oxoglutarate as one donor, and incorporation of one atom each of oxygen into both donors	16	1.11	0.015824
GO:0051119	sugar transmembrane transporter activity	7	0.48	0.01662
GO:0051082	unfolded protein binding	13	0.90	0.020109
GO:0097573	glutathione oxidoreductase activity	8	0.55	0.023661
GO:0015112	nitrate transmembrane transporter activity	4	0.28	0.0264
GO:0015250	water channel activity	5	0.35	0.030345
GO:1990757	ubiquitin ligase activator activity	3	0.21	0.031247
GO:0008422	beta-glucosidase activity	5	0.35	0.045975
GO:0042803	protein homodimerization activity	6	0.41	0.047378
GO:0016616	oxidoreductase activity, acting on the CH-OH group of donors, NAD or NADP as acceptor	7	0.48	0.048531

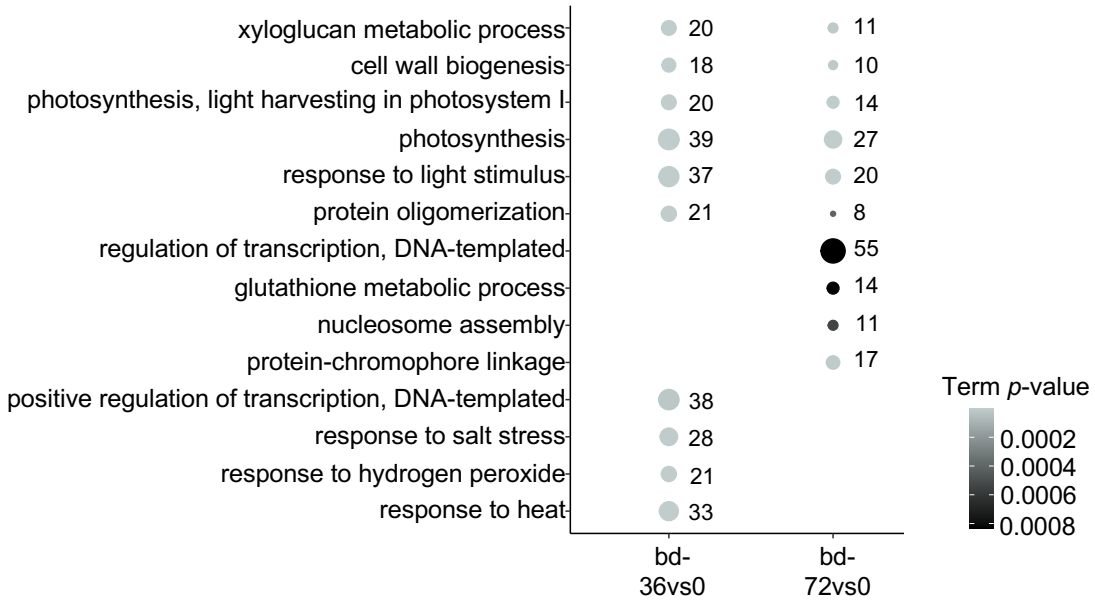


Figure 54. GO enrichment analysis of DEGs in the apical bud tissues (bd) on hour 36 and 72 of culture with exogenous GA, respectively.

A comparison of enriched GO terms (top 10) in biological processes between two comparisons of GA-treated 36 hours, 72 hours with 0 hour before treatment using DAVID (p value < 0.05).

Counts of DEGs included in each KEGG pathway are shown next to the plot.

4.3.5 Plant Hormone Signal Transduction Pathway Response to Nodal Stem Tissues

I first compared the differences in DEGs in nodal stem tissues between stMT-st-36vs0 and stMT-st-72vs0 (**Figure 55**). They shared 555 DEGs, of which 268 genes were upregulated, 191 were downregulated in both comparisons, 37 genes were downregulated in stMT-st-36vs0 but upregulated in stMT-st-72vs0, another 59 genes were upregulated in stMT-st-36vs0 but downregulated in stMT-st-72vs0 (**Figure 55A**). To reveal the molecular differences in sprouting response to the GA-treated period, I focused on all DEGs detected in stMT-st-36vs0 and stMT-st-72vs0. When stMTs were exposed to exogenous GA for 36 hours and 72 hours, the 12 and 9 most significant KEGG pathways ($p < 0.05$) were significantly enriched, respectively (**Figure 55B**). Five co-annotated metabolic pathways were found in both comparisons (**Figure 55B**), which were "Plant hormone signal transduction pathway", "Photosynthesis pathway", "Metabolic pathways", "MAPK signaling pathway-plant", and "Photosynthesis-antenna proteins pathway".

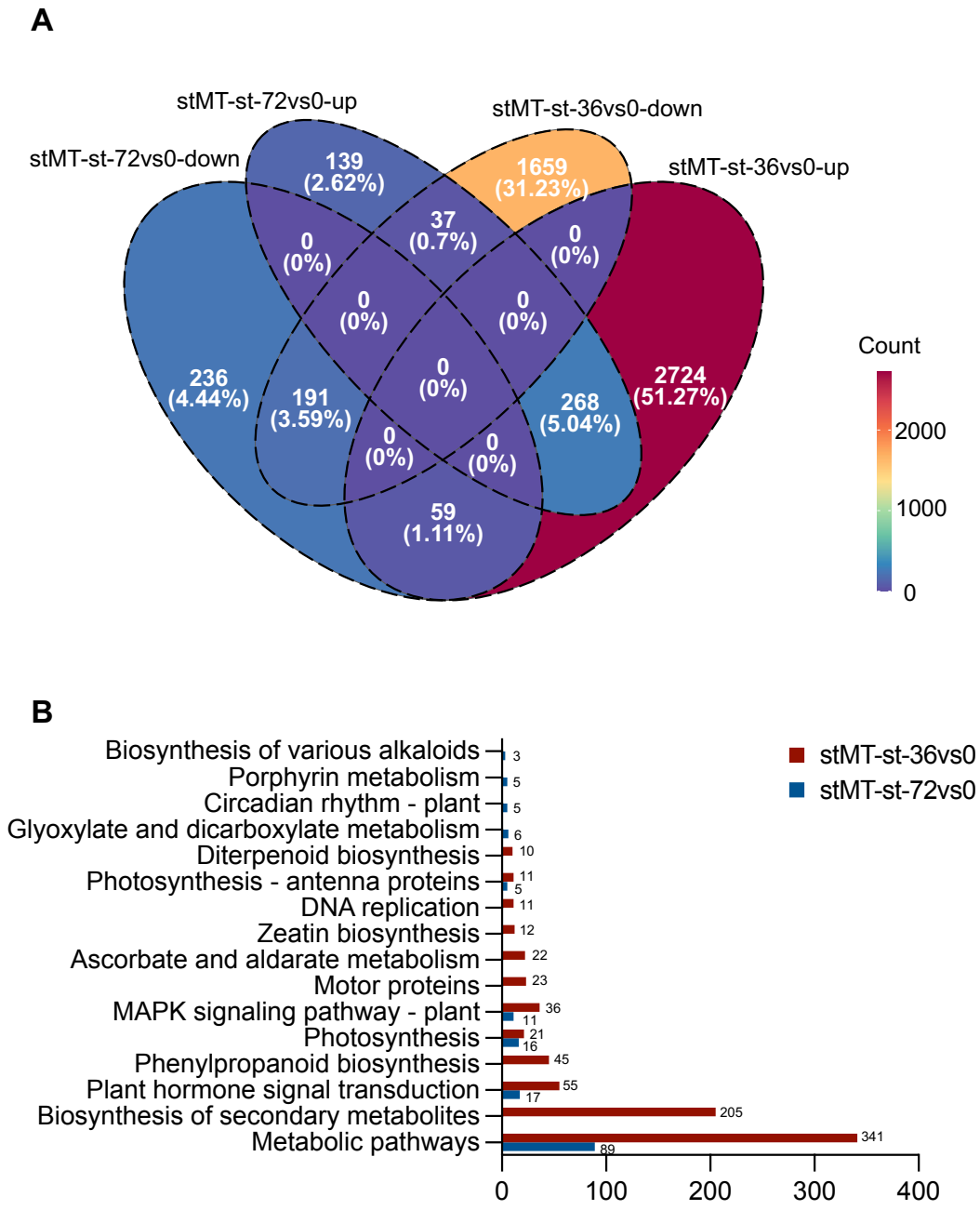


Figure 55. DEGs identified in the nodal stem tissues (st) of stemmed microtubers.

(**A**) A Venn diagram to visualize the similarities and differences of DEGs among four comparisons: stMT-st-36vs0-up, stMT-st-36vs0-down, stMT-st-72vs0-up, and stMT-st-72vs0-down.

(**B**) The comparison of enriched KEGG pathways for DEGs of stMT-st-36vs0 and stMT-st-72vs0 using DAVID ($p < 0.05$), visualized using GraphPad PRISM.

According to the analysis of the Plant hormone signal transduction pathway (**Figure 56, Figure 57**), the results showed that 55 DEGs were annotated in the comparison group of stMT-st-36vs0. Among them, 18 DEGs were upregulated and 37 DEGs were downregulated. In the comparison group of stMT-st-72vs0, 17 DEGs were annotated. Among them, 6 DEGs were upregulated and 11 DEGs were downregulated. In particular, there were 10 DEGs co-annotated to stMT-st-36vs0 and stMT-st-72vs0 comparison groups (**Figure 58**). Among these 62 (55+17-10) genes, the expression levels of genes involved in *PP2C*, and *PR-1* were downregulated when exogenous GA was applied for 36 hours, while upregulated when exogenous GA was applied for 72 hours. In contrast, the expression levels of the cytokinin response factor, *A-ARR*, *JAZ*, and *TGA* were the opposite (**Figure 56, Figure 57**). Suggesting that PGSC0003DMG400016742 (*PP2C*), PGSC0003DMG400009112 (*PP2C*), PGSC0003DMG400005117 (*PR-1*), PGSC0003DMG400027596 (*A-ARR17*), PGSC0003DMG400016643 (*A-ARR17*), PGSC0003DMG400002930 (*JAZ*), and PGSC0003DMG400012962 (*TGA*) were significant genes involved in the changes from dormancy breaking to sprouting of microtuber.

Remarkably, the expression levels of PGSC0003DMG400024997 (*GH3*) and PGSC0003DMG400015433 (*CYCD3*) were all upregulated, while PGSC0003DMG400003771 (*ARF5*), PGSC0003DMG400003849 (*GID1*), PGSC0003DMG400021991 (*GID1*), PGSC0003DMG400023897 (*ABF*), and PGSC0003DMG400005108 (*PR-1*) were all downregulated on hour 36 and 72 of culture (**Figure 58**). Moreover, a cytokinin-positive reporter, PGSC0003DMG400011980 (*B-ARR*) was found to downregulate response to GA treatment for 36 hours, indicating that CK involved in this growth process.

Therefore, these 15 DEGs above (**Figure 58**) are affected by exogenous GA addition, actively participate in dormancy breaking, and play an important role in the nodal stem tissues during the growth process.

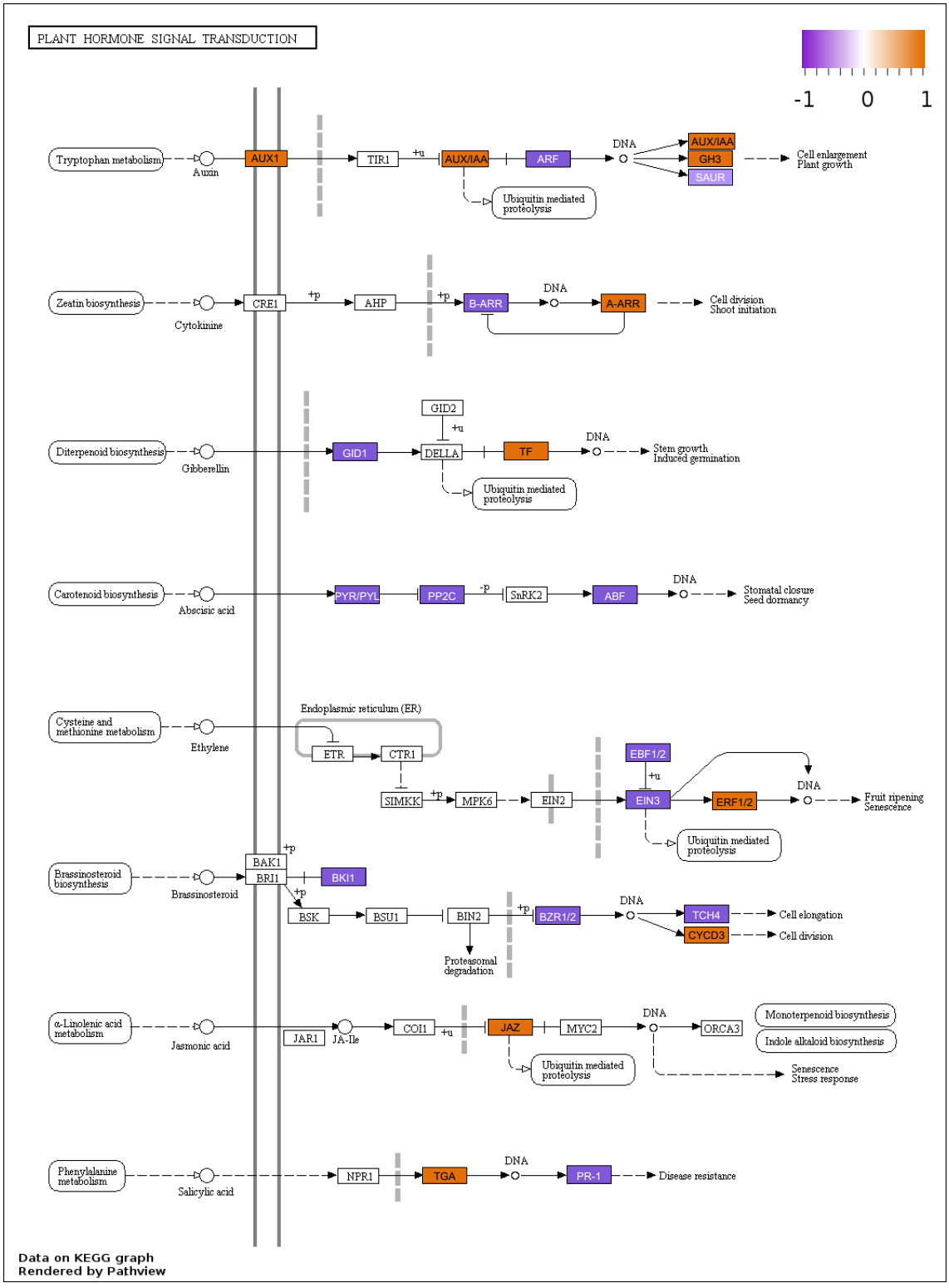


Figure 56. The differentially upregulated (orange) and downregulated (purple) DEGs involved in the pathway of "Plant hormone signal transduction" in the nodal stem tissues on hour 36 of culture.

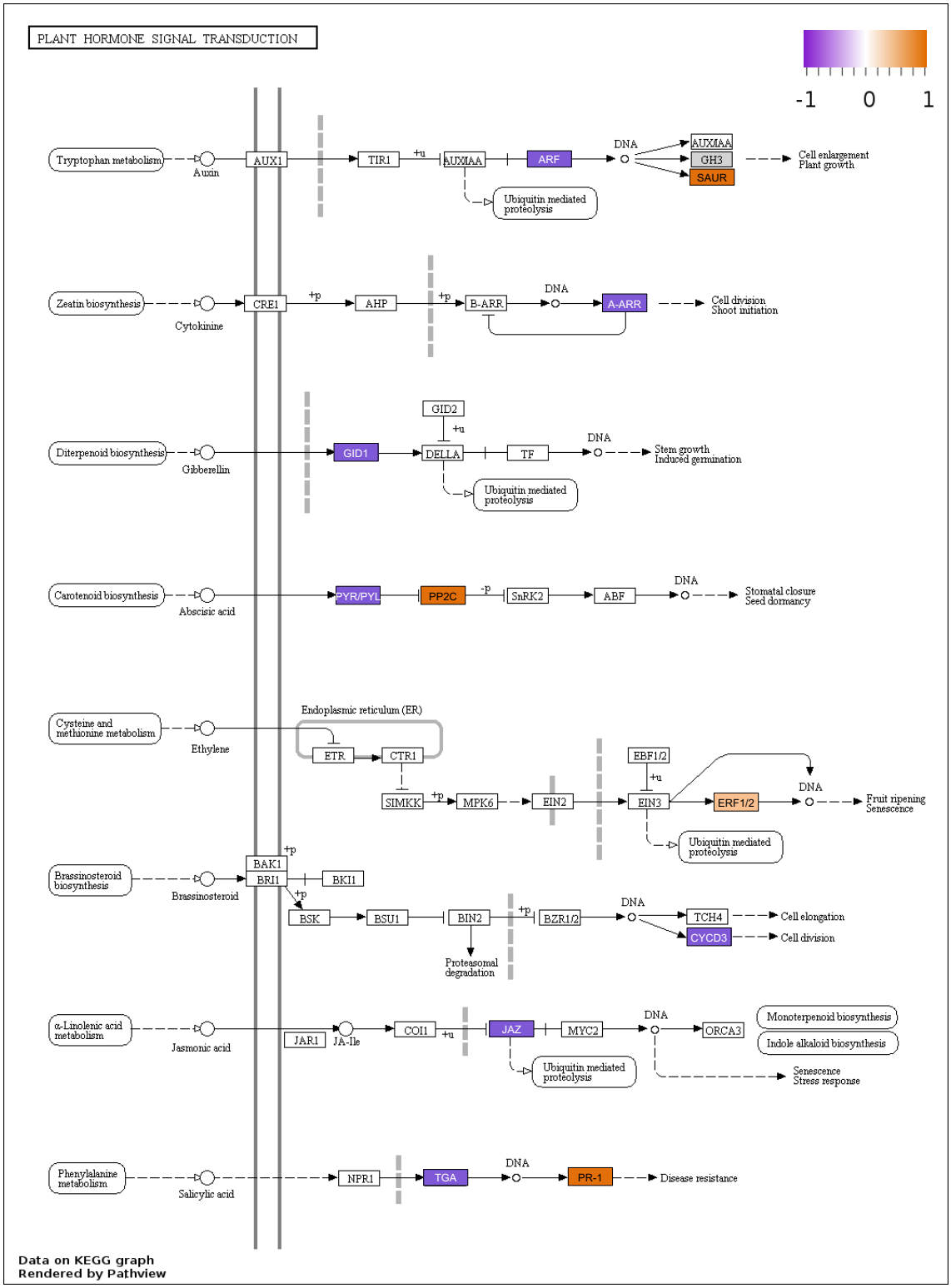


Figure 57. The differentially upregulated (orange) and downregulated (purple) DEGs involved in the pathway of "Plant hormone signal transduction" in the nodal stem tissues on hour 72 of culture.

Plant hormone signal transduction

Gene ID PGSC0003DMG	Gene Description	Function	stMT-st-36vs0	stMT-st-72vs0
400023205	AUX1	Auxin transporter-like protein 2	1.67	not DEG
402002635	IAA1	AUX/IAA gene family	-1.32	not DEG
400005338	IAA3	AUX/IAA gene family	1.50	not DEG
400029339	IAA13	AUX/IAA gene family	1.90	not DEG
400006093	IAA14	Auxin responsive protein	1.69	not DEG
400005327	IAA16	AUX/IAA gene family	2.21	not DEG
400020139	IAA22	AUX/IAA gene family	2.68	not DEG
400003771	ARF5	Auxin response factor 5	-1.05	-1.24
400025856	GH3	Auxin and ethylene responsive GH3	-1.17	not DEG
400024997	GH3	Indole-3-acetic acid-amido synthetase GH3.6	1.52	1.40
400021803	GH3	Indole-3-acetic acid-amido synthetase GH3.6	1.65	not DEG
400026186	GH3	Indole-3-acetic acid-amido synthetase GH3.6	not DEG	-1.34
400035783	SAUR	Auxin-responsive protein SAUR71	-1.86	not DEG
400029190	SAUR	Auxin-induced protein 15A	-1.55	not DEG
400026010	SAUR	Auxin-responsive protein SAUR36	-1.28	not DEG
400022233	SAUR	Auxin-responsive protein SAUR71	-1.56	not DEG
400020701	SAUR	Auxin-responsive protein SAUR71	-1.43	not DEG
400009168	SAUR	Auxin-responsive protein SAUR72	6.16	not DEG
400008950	SAUR	Auxin-induced protein 15A-like	-1.56	not DEG
400003773	SAUR	Auxin-induced protein 15A	-2.92	not DEG
400001668	SAUR	Auxin-induced protein 15A	1.58	not DEG
400001649	SAUR	Auxin-responsive protein SAUR21	5.97	not DEG
400001604	SAUR	Auxin-responsive protein SAUR21	2.17	not DEG
400029839	ARR9	Type-a response regulator	1.23	not DEG
400027597	ARR17	Type-a response regulator	1.55	not DEG
400011980	ARR11	Type-a response regulator	-1.43	not DEG
400016643	ARR17	Type-A response regulator	not DEG	-1.32
400021991	GID1	GID1-like gibberellin receptor	-1.84	-1.29
400003849	GID1	GID1-like gibberellin receptor	-2.29	-2.16
400029300	PLY2	Bet v I allergen family protein	-1.34	not DEG
400027118	PLY4	Abscisic acid receptor PYL4	2.79	not DEG

Figure 58. *Cont.*

Plant hormone signal transduction. Cont.

Gene ID PGSC0003DMG	Gene Description	Function	stMT-st-36vs0	stMT-st-72vs0
400011033	PLY4	Abscisic acid receptor PYL4	not DEG	-1.40
400012155	PLY9	Pathogenesis-induced protein	-1.51	not DEG
400000215	PLY7	Pathogenesis-induced protein	-1.78	not DEG
400030332	PP2C	Protein phosphatase 2C	-3.32	not DEG
400018004	PP2C	Abscisic insensitive 1B	-1.45	not DEG
400016742	PP2C	Protein phosphatase 2C AHG3 homolog	-1.71	1.05
400002573	PP2C	Protein phosphatase 2C ABI2 homolog	-1.07	not DEG
400009112	PP2C	Protein phosphatase 2C 8	not DEG	1.90
400025889	ABF	ABSCISIC ACID-INSENSITIVE 5-like protein 7	-1.64	not DEG
400023897	ABF	BZIP transcription factor 27	-3.64	-2.45
400008011	ABF	ABRE binding factor	-1.41	not DEG
400008712	EIN3	ETHYLENE INSENSITIVE 3-like, EIL2	-1.35	not DEG
400030928	EBF1/2	EIN3-binding F-box protein 1	-1.04	not DEG
400023619	ERF1/2	ERF transcription factor 5	-1.35	not DEG
400017231	ERF1/2	Ethylene-responsive transcription factor TSRF1	not DEG	-1.13
400013402	ERF1/2	Ethylene-responsive transcription factor TSRF1	not DEG	1.71
400015442	BKI1	BRI1 kinase inhibitor 1	-2.37	not DEG
400004501	BZR1/2	BRASSINAZOLE-RESISTANT 1 protein	-1.14	not DEG
401015433	CycD3	Cyclin-D3-3	2.09	1.38
400013975	TCH4	Xyloglucan endotransglycosylase/hydrolase XTH-6	1.50	not DEG
400002930	JAZ	Jasmonate ZIM-domain protein 1 TIFY 10A	2.25	-1.37
401015926	TGA	Isoform 2 of Transcription factor PIF5	1.37	not DEG
400012962	TGA	Transcription factor HBP-1b(C1)	1.63	-1.33
400005116	PR-1	Pathogenesis-related protein	-1.59	not DEG
400005112	PR-1	Pathogenesis-related protein	-1.48	not DEG
400005111	PR-1	Pathogenesis-related protein	-1.26	not DEG
400005108	PR-1	Pathogenesis-related protein	-2.29	-1.21
400005117	PR-1	Pathogenesis-related protein	not DEG	7.86
400002029	PR-1	Pathogenesis-related protein	-2.42	not DEG
400002028	PR-1	Pathogenesis-related protein	-2.77	not DEG
400002027	PR-1	Pathogenesis-related protein	-2.74	not DEG

-3.64 7.86

Figure 58. Functional annotations of DEGs in the nodal stem tissues (st) on hour 36 and 72 of culture with exogenous GA, respectively.

The table shows genes included in the pathways “Plant hormone signal transduction” for each comparison, with a heatmap showing gene expression levels as $\log_2$ FC.

Orange represents upregulation, and purple represents downregulation compared to Control (untreated).

4.3.6 Zeatin Biosynthesis Pathway Response to Nodal Stem Tissues

The CK-related pathway, "Zeatin biosynthesis", was suggested to significantly play an important role during microtuber sprouting in **Chapter 4**. Interestingly, the pathway of "Zeatin biosynthesis" was enriched only in stMTs exposed to exogenous GA for 36 hours (**Figure 55B**). Twelve DEGs were enriched in the "Zeatin biosynthesis" pathway, one was the adenosine phosphate-isopentenyltransferase 5 (*IPT5*) encoding a key enzyme in CK biosynthesis, which was downregulated during the GA-treated 36-hour-period, suggesting that cytokinin biosynthesis was involved in the nodal stem. Three were UDP-glycosyltransferase, *UGT85A1*, associated with the process of CK homeostasis; and eight were is-zeatin (cis- CK) O-glucosyltransferase (*CISZOG*) involved in the synthesis of cis-zeatin riboside. This suggests that the expression of genes related to CK homeostasis and signaling is enhanced in dormancy breaking in the nodal stem tissues.

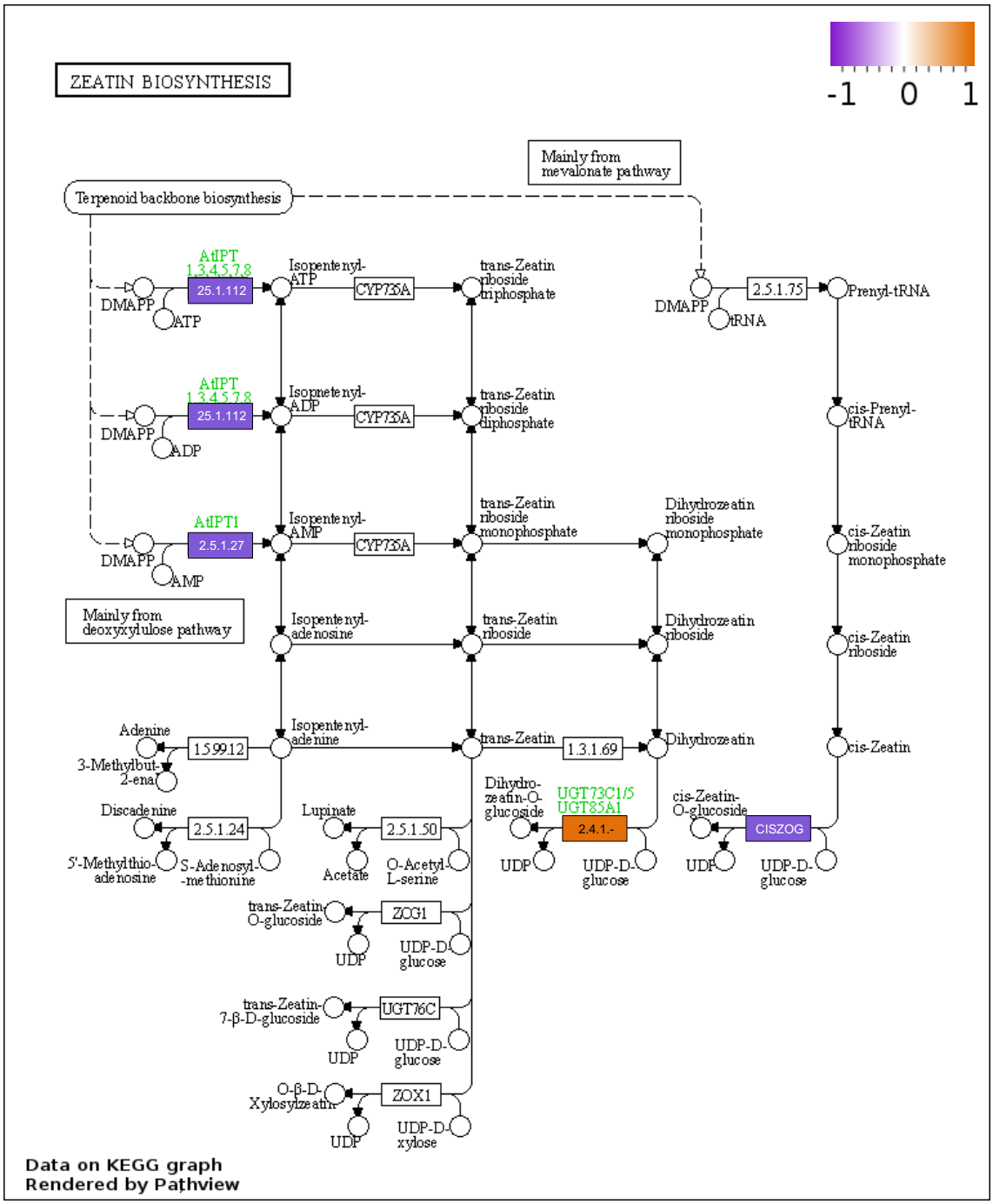


Figure 59. The differentially upregulated (orange) and downregulated (purple) DEGs involved in the pathway of "Zeatin biosynthesis" in the nodal stem tissues on hour 36 of culture.

Zeatin biosynthesis

Gene ID PGSC0003DMG	Gene Description	Function	stMT-st-36vs0	stMT-st-72vs0
400033116	IPT5	Adenylate isopentenyltransferase	-1.70	
400008593	UGT73C	Flavonoid glucoyltransferase	2.83	
400017603	UGT73C	Flavonoid glucoyltransferase	-1.38	
400028632	UGT73C	Flavonoid glucoyltransferase	1.17	
400035573	CISZOG	Zeatin O-glucosyltransferase	-1.77	
400011935	CISZOG	Zeatin O-glucosyltransferase	6.13	not enriched pathway
400029489	CISZOG	Zeatin O-glucosyltransferase	-2.81	
400023732	CISZOG	Zeatin O-glucosyltransferase	-1.59	
400018754	CISZOG	Zeatin O-glucosyltransferase	-1.48	
400007909	CISZOG	Zeatin O-glucosyltransferase	-1.56	
400044152	CISZOG	Zeatin O-xylosyltransferase	-1.43	
400029491	CISZOG	Zeatin O-xylosyltransferase	-2.34	

-2.81 6.13

Figure 60. Functional annotations of DEGs in the nodal stem tissues (st) on hour 36 and 72 of culture with exogenous GA, respectively.

The table shows genes included in the pathways "Zeatin biosynthesis" for each comparison, with a heatmap showing gene expression levels as $\log_2$ FC.

Orange represents upregulation, and purple represents downregulation compared to Control (untreated).

4.3.7 Gene Ontology (GO) Terms Response to Nodal Stem Tissues

When stMTs were exposed to exogenous GA for 36 hours and 72 hours, the 40 and 17 most significant biological processes (BP) terms (**Table 19, Table 20**), 18 and 12 cellular components (CC) terms (**Table 21, Table 22**), 32 and 11 molecular functions (MF) terms (**Table 23, Table 24**) were significantly enriched ($p < 0.05$), respectively. Two co-annotated GO terms in the top 10 BP terms were found in both comparisons (**Figure 61**), which were "photosynthesis" and "response to light stimulus". For stMT exposed to exogenous GA for 36 hours, "lignin catabolic process", "exocytosis", "chlorophyll biosynthetic process", "plant-type secondary cell wall biogenesis", "glyoxylate cycle", "photosynthesis, light harvesting in photosystem I", "response to molecule of fungal origin", and "coumarin biosynthetic process" played the essential role in response to the dormancy breaking. For stMT exposed to exogenous GA for 72 hours, "cell wall organization", "protein oligomerization", "double-strand break repair via break-induced replication", "microtubule-based movement", "positive regulation of transcription, DNA-templated", "cell wall biogenesis", "hydrogen peroxide catabolic process", and "xyloglucan metabolic process" played the essential role in response to microtuber sprouting.

Table 19. Biological Processes of Gene Ontology (GO) enrichment analysis for 4938 DEGs in stMT-st-36vs0

Term ID	Term Description	Gene Count	Gene (%)	*p* Value
Category of Biological Processes				
GO:0010411	xyloglucan metabolic process	20	0.68	1.68E-10
GO:0042744	hydrogen peroxide catabolic process	36	1.22	3.20E-10
GO:0042546	cell wall biogenesis	17	0.58	2.05E-09
GO:0045893	positive regulation of transcription, DNA-templated	30	1.02	5.01E-07
GO:0015979	photosynthesis	26	0.88	6.85E-07
GO:0007018	microtubule-based movement	18	0.61	1.79E-06
GO:0000727	double-strand break repair via break-induced replication	8	0.27	3.06E-06
GO:0009416	response to light stimulus	21	0.71	2.29E-05
GO:0051259	protein oligomerization	12	0.41	2.82E-05
GO:0071555	cell wall organization	28	0.95	3.05E-05
GO:0006270	DNA replication initiation	8	0.27	6.44E-05
GO:0009408	response to heat	17	0.58	0.000147
GO:0009834	plant-type secondary cell wall biogenesis	13	0.44	0.000177
GO:0042542	response to hydrogen peroxide	13	0.44	0.000224
GO:0006979	response to oxidative stress	33	1.12	0.000383
GO:0009768	photosynthesis, light harvesting in photosystem I	11	0.37	0.000494
GO:0030154	cell differentiation	15	0.51	0.001784
GO:0046274	lignin catabolic process	9	0.31	0.001797
GO:0009805	coumarin biosynthetic process	26	0.88	0.002628
GO:0002238	response to molecule of fungal origin	26	0.88	0.002628
GO:0009631	cold acclimation	6	0.20	0.003204
GO:0000302	response to reactive oxygen species	6	0.20	0.004638
GO:0051603	proteolysis involved in cellular protein catabolic process	11	0.37	0.007417
GO:0016567	protein ubiquitination	42	1.43	0.008135
GO:0009638	phototropism	4	0.14	0.010135
GO:0042545	cell wall modification	16	0.54	0.014185
GO:0009664	plant-type cell wall organization	9	0.31	0.015419
GO:0007043	cell-cell junction assembly	4	0.14	0.016621
GO:0006268	DNA unwinding involved in DNA replication	5	0.17	0.020068
GO:0044772	mitotic cell cycle phase transition	9	0.31	0.0206
GO:0009651	response to salt stress	13	0.44	0.021889
GO:0019941	modification-dependent protein catabolic process	6	0.20	0.023405
GO:0009414	response to water deprivation	10	0.34	0.030125
GO:0009607	response to biotic stimulus	11	0.37	0.035728
GO:0000079	regulation of cyclin-dependent protein serine/threonine kinase activity	10	0.34	0.037438
GO:0019419	sulfate reduction	3	0.10	0.038731
GO:1902975	mitotic DNA replication initiation	3	0.10	0.038731
GO:0010167	response to nitrate	4	0.14	0.046987
GO:0045490	pectin catabolic process	17	0.58	0.048252
GO:0071712	ER-associated misfolded protein catabolic process	6	0.20	0.04842

Table 20. Biological Processes of Gene Ontology (GO) enrichment analysis for 930 DEGs in stMT-st-72vs0

Term ID	Term Description	Gene Count	Gene (%)	*p* Value
Category of Biological Processes				
GO:0015979	photosynthesis	20	3.26	1.71E-14
GO:0009805	coumarin biosynthetic process	10	1.63	2.86E-03
GO:0002238	response to molecule of fungal origin	10	1.63	2.86E-03
GO:0009768	photosynthesis, light harvesting in photosystem I	5	0.81	3.57E-03
GO:0009416	response to light stimulus	7	1.14	4.48E-03
GO:0006097	glyoxylate cycle	3	0.49	0.006488
GO:0009834	plant-type secondary cell wall biogenesis	5	0.81	0.007523
GO:0015995	chlorophyll biosynthetic process	4	0.65	0.011295
GO:0006887	exocytosis	5	0.81	0.01187
GO:0046274	lignin catabolic process	4	0.65	0.013858
GO:0006334	nucleosome assembly	5	0.81	0.027438
GO:0051260	protein homooligomerization	3	0.49	0.029486
GO:0097753	membrane bending	2	0.33	0.035957
GO:0016567	protein ubiquitination	12	1.95	0.036743
GO:0006749	glutathione metabolic process	6	0.98	0.039586
GO:0006970	response to osmotic stress	3	0.49	0.041466
GO:0009773	photosynthetic electron transport in photosystem I	3	0.49	0.041466

Table 21. Cellular Component of Gene Ontology (GO) enrichment analysis for 4938 DEGs in stMT-st-36vs0

Term ID	Term Description	Gene Count	Gene (%)	*p* Value
Category of Cellular Component				
GO:0005576	extracellular region	98	3.33	3.65E-13
GO:0048046	apoplast	43	1.46	2.14E-10
GO:0005886	plasma membrane	178	6.05	2.23E-10
GO:0005615	extracellular space	31	1.05	7.40E-09
GO:0009538	photosystem I reaction center	8	0.27	3.00E-06
GO:0000347	THO complex	6	0.20	7.98E-05
GO:0042555	MCM complex	6	0.20	7.98E-05
GO:0009535	chloroplast thylakoid membrane	34	1.16	0.000222
GO:0009505	plant-type cell wall	16	0.54	0.000482
GO:0046658	anchored component of plasma membrane	26	0.88	0.001127
GO:0005634	nucleus	370	12.59	0.001252
GO:0009522	photosystem I	14	0.48	0.001339
GO:0009654	photosystem II oxygen evolving complex	9	0.31	0.002259
GO:0005764	lysosome	10	0.34	0.002573
GO:0005737	cytoplasm	220	7.48	0.002694
GO:0000786	nucleosome	17	0.58	0.003151
GO:0005794	Golgi apparatus	46	1.56	0.003213
GO:0005874	microtubule	24	0.82	0.004347

Table 22. Cellular Component of Gene Ontology (GO) enrichment analysis for 930 DEGs in stMT-st-72vs0

Term ID	Term Description	Gene Count	Gene (%)	*p* Value
Category of Cellular Component				
GO:0009538	photosystem I reaction center	9	1.47	4.74E-13
GO:0000786	nucleosome	15	2.44	7.24E-10
GO:0009535	chloroplast thylakoid membrane	20	3.26	5.88E-09
GO:0009523	photosystem II	8	1.30	4.56E-04
GO:0005886	plasma membrane	42	6.84	4.82E-04
GO:0009522	photosystem I	7	1.14	0.000751
GO:0009654	photosystem II oxygen evolving complex	5	0.81	0.001769
GO:0048046	apoplast	10	1.63	0.004103
GO:0009514	glyoxysome	3	0.49	0.004693
GO:0016021	integral component of membrane	165	26.87	0.017116
GO:0019898	extrinsic component of membrane	4	0.65	0.02526
GO:0000145	exocyst	4	0.65	0.033462

Table 23. Molecular Function of Gene Ontology (GO) enrichment analysis for 4938 unique DEGs in stMT-st-36vs0

Term ID	Term Description	Gene Count	Gene (%)	*p* Value
Category of Molecular Function				
GO:0008017	microtubule binding	37	1.26	2.39E-08
GO:0016762	xyloglucan:xyloglucosyl transferase activity	18	0.61	3.96E-07
GO:0004601	peroxidase activity	36	1.22	1.13E-06
GO:0005507	copper ion binding	23	0.78	1.43E-05
GO:0016413	O-acetyltransferase activity	16	0.54	4.51E-05
GO:0043621	protein self-association	14	0.48	0.000254
GO:0003777	microtubule motor activity	11	0.37	0.000347
GO:0016717	oxidoreductase activity, acting on paired donors, with oxidation of a pair of donors resulting in the reduction of molecular oxygen to two molecules of water	8	0.27	0.001344
GO:0052716	hydroquinone:oxygen oxidoreductase activity	9	0.31	0.00135
GO:0003700	transcription factor activity, sequence-specific DNA binding	118	4.01	0.002265
GO:0016788	hydrolase activity, acting on ester bonds	23	0.78	0.00235
GO:0043565	sequence-specific DNA binding	51	1.73	0.00341
GO:0008422	beta-glucosidase activity	9	0.31	0.004187
GO:0016491	oxidoreductase activity	64	2.18	0.006267
GO:0015250	water channel activity	8	0.27	0.007438
GO:0097573	glutathione oxidoreductase activity	13	0.44	0.009331
GO:0004866	endopeptidase inhibitor activity	10	0.34	0.009382
GO:0034485	phosphatidylinositol-3,4,5-trisphosphate 5-phosphatase activity	5	0.17	0.012765
GO:0071916	dipeptide transmembrane transporter activity	4	0.14	0.014713
GO:0008574	ATP-dependent microtubule motor activity, plus-end-directed	4	0.14	0.014713
GO:0031386	protein tag	7	0.24	0.019369
GO:0046872	metal ion binding	164	5.58	0.020057
GO:0004197	cysteine-type endopeptidase activity	12	0.41	0.025452
GO:0008194	UDP-glycosyltransferase activity	32	1.09	0.026495
GO:0015098	molybdate ion transmembrane transporter activity	4	0.14	0.031214
GO:0016759	cellulose synthase activity	4	0.14	0.031214
GO:0042937	tripeptide transporter activity	4	0.14	0.031214
GO:0031418	L-ascorbic acid binding	28	0.95	0.031856
GO:0046910	pectinesterase inhibitor activity	12	0.41	0.033565
GO:0008447	L-ascorbate oxidase activity	3	0.10	0.035611
GO:0044390	ubiquitin-like protein conjugating enzyme binding	5	0.17	0.036152
GO:0005504	fatty acid binding	5	0.17	0.036152

Table 24. Molecular Function of Gene Ontology (GO) enrichment analysis for 930 unique DEGs in stMT-st-72vs0

Term ID	Term Description	Gene Count	Gene (%)	*p* Value
Category of Molecular Function				
GO:0046982	protein heterodimerization activity	16	2.61	9.29E-09
GO:0016717	oxidoreductase activity, acting on paired donors, with oxidation of a pair of donors resulting in the reduction of molecular oxygen to two molecules of water	5	0.81	4.97E-04
GO:0003677	DNA binding	38	6.19	1.60E-03
GO:0009055	electron carrier activity	8	1.30	2.83E-03
GO:0043565	sequence-specific DNA binding	16	2.61	5.94E-03
GO:0005507	copper ion binding	7	1.14	0.007725
GO:0052716	hydroquinone:oxygen oxidoreductase activity	4	0.65	0.012085
GO:0004364	glutathione transferase activity	6	0.98	0.016535
GO:0031418	L-ascorbic acid binding	10	1.63	0.017928
GO:0004866	endopeptidase inhibitor activity	4	0.65	0.042301
GO:0003700	transcription factor activity, sequence-specific DNA binding	28	4.56	0.045819

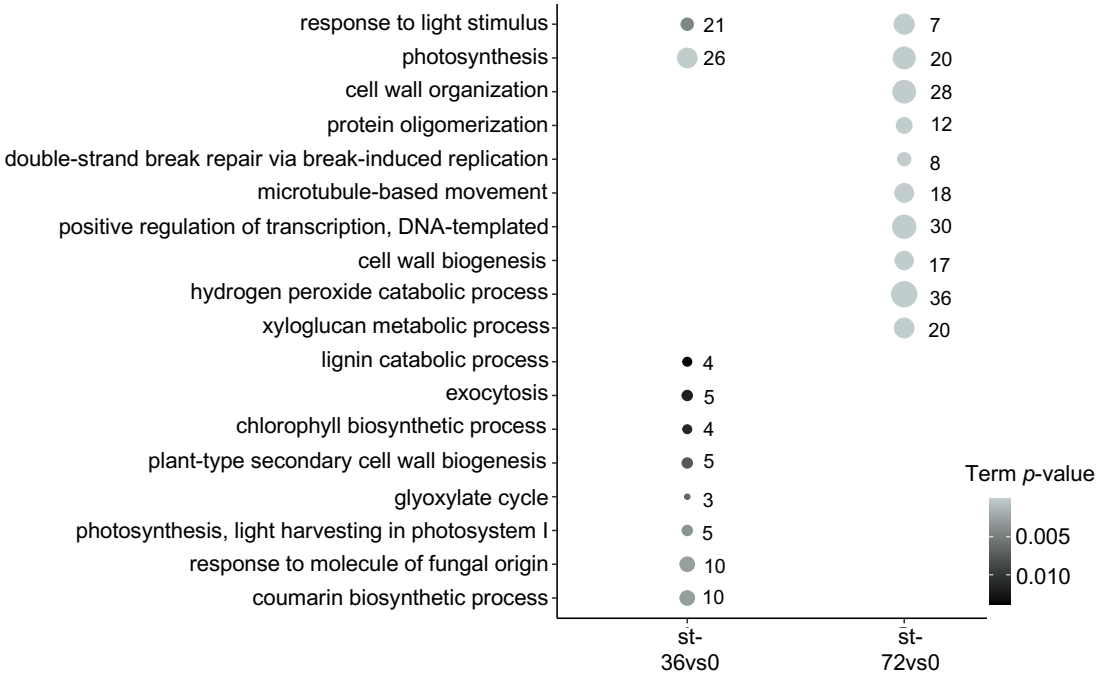


Figure 61. GO enrichment analysis of DEGs in the nodal stem tissues (st) on hour 36 and 72 of culture with exogenous GA, respectively.

A comparison of enriched GO terms (top 10) in biological processes between two comparisons of GA-treated 36 hours, 72 hours with 0 hour before treatment using DAVID (p value < 0.05).

Counts of DEGs included in each KEGG pathway are shown next to the plot.

4.4 Discussion

Given that genes involved in ABA, *PYL4*, *PP2C*, and SnRK2 were downregulated and only detected as DEGs in apical bud tissues on hour 36 of culture in this RNA-seq analysis (**Figure 51**, **Figure 52**, and **Figure 53**), *PYL4* likely interacted with *PP2C* to reduce the ABA level, due to the fact that *PYL*s interact with *PP2C* and inhibit *PP2C* by repressing phosphatase activity upon binding with ABA; in turn, the inhibition of *PP2C* results in the inactivation of ABA. With genes involved in GA, *GID1*, downregulated, indicating a change in the balance of ABA/GA levels response to dormancy-releasing and sprouting of microtubers. I speculate that it is possible that the reduction in ABA level was initiated before hour 36 of culture. In addition, *SlARF5*, closely related with *SlARF7* in molecular phylogenetic trees, was reported to play an important role in regulating both the auxin- and GA-signaling pathways during fruit set and development in tomato (Liu et al., 2018). *SlARF7* (de Jong et al., 2011) and *SlARF9* (De Jong et al., 2015) have effects on tomato fruit initiation and development through the interaction of the auxin- and GA-signaling pathways. My results showed that three auxin-responsive transcription factors, *ARF*s were upregulated on hour 36 of culture (*ARF7* and *ARF9*), while downregulated on hour 72 of culture (*ARF5*) (**Figure 51**, **Figure 52**, and **Figure 53**), suggesting that the changes in expression of *ARFs* from hour 36 to hour 72 of culture may reveal the change in mediating the crosstalk between auxin and GA during microtuber sprouting development.

Interestingly, genes involved in the pathway of "Zeatin biosynthesis" were not enriched in apical bud tissues either on hour 36 or 72 of culture (**Figure 59**, and **Figure 60**), when compared with apical bud tissues on hour 0 of culture, which was enriched in 3-stMT-bd-GA/Con in the result of **Chapter 3**, in response to microtuber sprouting. In contrast, genes involved in the pathway of "Zeatin biosynthesis" were only enriched in nodal stem tissues on hour 36 of culture, when compared with nodal stem tissues on hour 0 of culture. Twelve DEGs were found in response to CK (**Figure 60**), *IPT5* involved in cytokinin biosynthesis, three *UGT85A1*, associated with the process of CK homeostasis, and eight *CISZOG* involved in the synthesis of cis-zeatin riboside. Since genes associated with the pathway of "Zeatin biosynthesis" play a key role during sprouting in apical bud tissues in sprouting-induced conditions (**Chapter 3**), this suggests that the change in gene expression related to CK homeostasis and signaling is dynamic in nodal stem tissues and

apical bud tissues to respond to the dormancy breaking and sprouting form hour 36 of culture to hour 72 of culture.

General Discussion

In this study, I used tissue culture technology to build the system of microtubers and microtuber chains. Ancymidol, an inhibitor of gibberellin biosynthesis, was very effective in altering the development of bud meristems from shoot formation to tuber formation. 20 μM ancymidol of Sigma-Aldrich Co. LLC (A9431) was a more suitable concentration to form microtubers and microtuber chains at 20 °C in the dark. The results also showed that the adjusted medium supplemented with a high concentration of ancymidol had a very serious impact on the formation of microtubers (**Figure 8**), mainly resulting in a large reduction in size. Whether this implies that ancymidol has a greater impact on cell growth than on cell division needs further cytological study. In ssp. *andigena*, for microtubers, its formation can be observed on day 3 of culture, while for microtuber chains, its formation was not observed until day 21 of culture, and a MS medium with 10% sucrose co-applied with a higher level of ancymidol after treatments of GA, CK, NAA for 12, 24, 36, and 48 hours did not help to shorten the formation period into 14 days although previous reports have shown that > 8% sucrose in a MS medium was sufficient to induce this process and cause tuberization (Chen *et al.*, 2007; Cheng *et al.*, 2018), while microtubers in cv. May Queen had microtuber chains formed in the same condition. Suggesting that the dormancy of microtubers in ssp. *andigena* is deeper than that in cv. May Queen. There is still a lot to discover about dormancy-breaking timing in ssp. *andigena*, such as the role of exogenous GA and sucrose levels supplemented within MS medium and other incubation temperatures and periods.

In addition, to understand the role of CK and the nodal stem in GA-induced sprouting, I investigated the profiling of gene expression change at the transcriptome level using MTs (stMTs and hMTs) with the treatment of GA, CK, GACK, or the untreated control. In my observation experiments, GA alone was sufficient to induce stMT sprouting but failed to induce hMT sprouting, However, CK co-application could compensate for the absence of the nodal stem, supporting GA-induced sprouting. RNA-seq analyses showed that DEGs associated with “Plant hormone biosynthesis and signal transduction” were detected as the hub genes in this study. In sprouting buds, genes related to the “CK-activated signaling pathway” and “CK biosynthesis process” were downregulated. However, genes related to “Zeatin biosynthesis”, such as *CYP735A* and *CISZOG*, were

upregulated in apical bud tissues on day 3 culture in sprouting conditions during sprouting growth in **Chapter 3**. In contrast, in **Chapter 4,** genes involved in the pathway of "Zeatin biosynthesis" were only enriched in nodal stem tissues on hour 36 of culture, while not enriched in apical bud tissues either on hour 36 or 72 of culture, when compared with nodal stem tissues on hour 0 of culture. Twelve DEGs were found in response to CK (**Figure 60**), *IPT5* involved in cytokinin biosynthesis, three *UGT85A1*, associated with the process of CK homeostasis, and eight *CISZOG* involved in the synthesis of cis-zeatin riboside. Suggesting that the change in gene expression related to CK homeostasis and signaling is dynamic in nodal stem tissues and apical bud tissues to respond to the microtuber sprouting during sprouting growth.

Although GA treatment activated genes related to auxin, as was evident from genes related to the "auxin-activated signaling pathway" in response to sprouting, and even in sprouting-failed conditions, the lack of regulation of *IAA15*, *IAA22*, and *SAUR50* in GA-treated hMTs made the nodal stem or CK co-application very important for GA-induced sprouting in **Chapter 3**. My results in **Chapter 4** showed that three auxin-responsive transcription factors, *ARF*s were upregulated on hour 36 of culture (*ARF7* and *ARF9*), while downregulated on hour 72 of culture (*ARF5*) (**Figure 53**). Given that *SlARF5, closely related to SlARF7* in molecular phylogenetic trees, was reported to play an important role in regulating both the auxin- and GA-signaling pathways during fruit set and development in tomato (Liu *et al.*, 2018). *SlARF7* (de Jong *et al.*, 2011) and *SlARF9* (De Jong *et al.*, 2015) have effects on tomato fruit initiation and development through the interaction of the auxin- and GA-signaling pathways. These results reveal the change in mediating the crosstalk between auxin and GA during microtuber sprouting development.

Furthermore, the ABA negative regulators, *PYL4* and *PP2C*, were only detected in sprouting conditions on day 3 of culture. Moreover, it is possible that the reduction in ABA level was initiated before hour 36 of culture, since genes involved in ABA, *PYL4*, *PP2C*, and SnRK2 were downregulated and only detected as DEGs in apical bud tissues on hour 36 of culture in this RNA-seq analysis (**Figure 53**), *PYL4* likely interacted with *PP2C* to reduce the ABA level, due to the fact that *PYL*s interact with *PP2C* and inhibit *PP2C* by repressing phosphatase activity upon binding with ABA. With genes involved in GA, *GID1*, downregulated, indicating a change in the balance of ABA/GA levels response to dormancy-releasing and sprouting of microtubers from hour 36 to hour 72 of

culture.

These results made me conclude that the endogenous CK is involved in the nodal stem and plays a vital role in GA-induced sprouting by maintaining CK homeostasis to sustain the developmental processes in sprouting, which impacts the expression of these key genes related to ABA, auxin, GA, and CK. More effort is required to be devoted to these critical genes relevant to the crosstalk among GA, CK, and auxin regarding the control of sprouting to effectively control tuber sprouting. More research on the mechanisms and the verification of genes involved in this sprouting process using overexpression, RNAi, or CRISPR/Cas9 systems needs to be conducted with both apical buds and nodal stems with a detailed time course design, especially the timing of dormancy break. In addition, other factors, such as environmental factors, nitrogen supply, growth regulators, temperature, potato cultivar, and sucrose concentration, should be investigated with reasonable orthogonal experimental designs, given that global warming has become a significant issue for potato tuber secondary growth. This study provides further insight into the potential molecular mechanisms initiating and motivating tuber sprouting and sheds light on avoiding and reducing tuber sprouting, allowing me to address and optimize the methods for breeding and cultivating potatoes.

Summary

Potatoes are a representative crop of Hokkaido and are of global agricultural importance. The edible part of potatoes is the tubers enlarged from underground stolon. An increase in temperature may cause a temporary release of tuber dormancy, resulting in sprouting called "secondary growth". Once the secondary growth sprouts go dormant again, "secondary hypertrophy" occurs, forming a hump-shaped, malformed tubers. Which diminishes tuber starch content and significantly lowers the commercial value of potatoes as well as morphological characteristics. Moreover, climate change due to global warming tends to increase secondary growth and secondary hypertrophy in the field and increase tuber sprouting during storage. Tuber sprouting is induced by signal substances, such as gibberellin (GA), which are transported to the tuber from the plant body during tuber development. Here, I recreated secondary growth and secondary hypertrophy using *in vitro* microtubers (MTs) and studied the effect on the induction of secondary growth with plant hormone treatment. In addition, I employed transcriptomic analysis using RNA-seq to find out genes involved in sprouting and study the changes in gene expression during the development of tuber sprouting.

Chapter 1. *in vitro* Induction of Secondary Growth and Secondary Hypertrophy

in vitro plant tissue culture affords a useful tool for studying potatoes. In this study, I developed a protocol for MT and MT chain induction and obtained optimal parameters for forming MTs and MT chains, using *Solanum tuberosum* L ssp. *andigena*, cv. May Queen, and cv. Irish Cobbler. I optimized the incubated period to break the dormancy of lateral buds in single-node cuttings and buds in MTs, the way to induce secondary growth and secondary hypertrophy of MTs, and the amount of GA_3 (GA) or ancymidol added. The results suggest that 10 μM GA is more suitable for breaking the dormancy of lateral buds in single-node cuttings and the buds of MTs at 25 °C in the dark for 36 hours, and 20 μM ancymidol is more favorable for forming MTs and MT chains at 20 °C in the dark. In addition, the dormancy of buds of MTs in ssp. *andigena* is deeper than that in cv. May Queen. In ssp. *andigena*, for MT chains, its formation was not observed until day 21 of culture, while MT chains in cv. May Queen could form in 14 days.

Chapter 2. *in vitro* Induction of Secondary Growth and Microtuber Sprouting

Since the MTs mentioned above are all attached to the nodal stem, I hypothesized that things related to CK in the nodal stem played an important role during the development of induction of sprouting (secondary growth) based on the study of Hartmann et al., (2011), which showed that GA has a dormancy-terminating capacity but requires CK to induce sprouting growth in potato tubers. I investigated the role the nodal stem played in plant hormone-induced secondary growth using stemmed MTs (stMTs, MT attached to a nodal stem), destemmed MTs (deMTs, detaching the nodal stem from the stMT, but the junction part remains attached to the MT), and MT halves (hMTs, cutting the MT in half along the equatorial plane to completely remove the nodal stem, including the junction part with the MT) prepared from single-node cuttings. Meanwhile, I observed the effect on the induction of secondary growth in three treatments of MTs using GA, CK, or GACK. In observation experiments, GA alone was sufficient to induce stMTs and deMTs sprouting but failed to induce hMTs sprouting, and CK alone did not initiate any sprouting in either stMTs, deMTs, or hMTs. But CK co-application could compensate for the absence of the nodal stem, supporting GA-induced sprouting. I infer that GA alone or CK alone is inadequate to initiate MTs sprouting. GA and CK are both essential for secondary growth in this study.

Chapter 3. Transcriptomic Analyses of Microtuber Sprouting Response to Phytohormone Treatments

The results above showed that exogenous CK co-application and the nodal stem were necessary for supporting GA to promote sprouting and bud growth, so I presented the investigation to study the regulatory mechanisms of GA-induced secondary growth and the role of the nodal stem during this process at the transcriptome sequencing level. To identify genes involved in the process, apical bud tissues (bd) of stMTs and hMTs and nodal stem tissues (st) of stMTs, which were treated by GA, CK, and GACK for 3 days (3), or the untreated control, were sampled for RNA-Seq analysis. Differentially expressed gene (DEG) analysis was performed using HISAT2, mapping to the potato genome sequence of doubled monoploid S. tuberosum (PGSC_DM_v4.03) and using R packages (DEseq2, ClusterProfiler 4.0, ggplot2, and WGCNA, etc.) to visualize the results. Results showed that a total of 6515 DEGs were detected in 9 comparisons: 3-

stMT-bd-GA vs (/) Con, 3-stMT-bd-CK/Con, 3-stMT-bd-GACK/Con, 3-hMT-bd-GA/Con, 3-hMT-bd-CK/Con, 3-hMT-bd-GACK/Con, 3-stMT-st-GA/Con, 3-stMT-st-CK/Con, and 3-stMT-st-GACK/Con. DEGs associated with the enriched pathway of "Plant hormone biosynthesis and signal transduction" were enriched as the hub genes in this study. WGCNA results for 6515 DEGs show that genes related to CK in the "plant hormone signaling pathway" were positively regulated in the nodal stem of stMTs with GA alone treatment.

In sprouting apical bud tissues of GA-treated stMTs, GACK-treated stMTs, and GACK-treated hMTs, they shared 1064 DEGs, among them, 15 DEGs were detected in the pathway of "Plant hormone biosynthesis and signal transduction", *RR9* (type-A response regular) was the only CK-responsive gene and was upregulated. Gene Ontology (GO) enrichment analysis for 1064 DEGs showed that 4 genes related to the "CK-activated signaling pathway" and "CK biosynthesis process" were downregulated. However, genes related to the enriched pathway of "Zeatin biosynthesis," such as *CYP735A* (a CK biosynthesis gene) and *CISZOG* and *UGT85A1* (related to CK homeostasis and signaling), were upregulated in apical bud tissues on day 3 of culture in sprouting conditions. These findings suggest that the role of the nodal stem is synonymous with CK during sprouting growth, and CK signaling and homeostasis are critical to supporting GA-induced sprouting.

Chapter 4. Transcriptomic Analyses of Microtuber Sprouting Response to Incubation Periods with Gibberellin Treatment

Since GA can induce stMTs sprouting, I want to figure out the difference in DEGs of apical bud tissues and nodal stem tissues between 36-hour-GA treatment with 72-hour-GA treatment at the transcriptome sequencing level, especially genes involved in CK. This time, apical bud tissues and nodal stem tissues of stMTs treated by GA for 36 hours and 72 hours, stMTs before incubation with GA (i.e., on hour 0 of culture) were set as control. The ways to visualize the RNA-Seq results were the same as described above. I only focused on the pathways of "Plant hormone biosynthesis and signal transduction" and "Zeatin biosynthesis" because of their significance during the development of secondary growth and microtuber sprouting, as suggested in the results above. In the pathway of "Plant hormone biosynthesis and signal transduction", 72 and 30 DEGs were

enriched in stMT-bd-36vs0 and stMT-bd-72vs0, respectively; 55 and 17 DEGs were enriched in stMT-st-36vs0 and stMT-st-72vs0, respectively. In addition, in the pathway of "Zeatin biosynthesis", 12 DEGs were enriched only in stMT-st-36vs0, while not enriched in either stMT-st-36vs0 or stMT-st-72vs0. Among them, *IPT5* (encoding a key enzyme in CK biosynthesis) was downregulated, and *UGT85A1* and *CISZOG* were upregulated. Proving again that cytokinin biosynthesis was involved in the nodal stem tissues and indicating that the expression of genes related to CK homeostasis and signaling is dynamic from the nodal stem tissues to the apical bud tissues from 36-hour culture to 72-hour culture, during the development of secondary growth inducted by GA treatment.

Although GA and CK are both required for microtuber sprouting, GA alone can induce sprouting in microtubers attached to the nodal stem tissues. In addition, GA was shown to regulate genes related to CK in the nodal stem tissues. In this study, I established a model system for secondary growth, one important tool for elucidating the physiological mechanisms of potato secondary growth and tuber sprouting during storage, which is becoming an issue due to climate change, such as global warming, as well as a comprehensive gene expression analysis using this system. I believe that my results are useful as a means to further elucidate the mechanisms of potato secondary growth and tuber sprouting in detail.

References

Ahloowalia, B. (1994). Production and performance of potato mini-tubers. Euphytica *75*, 163-172.

Akoumianakis, K.A., Aivalakis, G., Alexopoulos, A., Karapanos, I., Skarmoutsos, K., and Passam, H. (2008). Bromoethane-induced changes in respiration rate, ethylene synthesis, and enzyme activities in potato tubers in relation to dormancy breakage. The Journal of Horticultural Science and Biotechnology *83*, 441-446.

Alamar, M.C., Tosetti, R., Landahl, S., Bermejo, A., and Terry, L.A. (2017). Assuring Potato Tuber Quality during Storage: A Future Perspective. Front Plant Sci *8*, 2034. 10.3389/fpls.2017.02034.

Barbier, F., Péron, T., Lecerf, M., Perez-Garcia, M.D., Barrière, Q., Rolčík, J., Boutet-Mercey, S., Citerne, S., Lemoine, R., Porcheron, B., et al. (2015). Sucrose is an early modulator of the key hormonal mechanisms controlling bud outgrowth in Rosa hybrida. J Exp Bot *66*, 2569-2582. 10.1093/jxb/erv047.

Bhogale, S., Mahajan, A.S., Natarajan, B., Rajabhoj, M., Thulasiram, H.V., and Banerjee, A.K. (2014). MicroRNA156: a potential graft-transmissible microRNA that modulates plant architecture and tuberization in Solanum tuberosum ssp. andigena. Plant physiology *164*, 1011-1027.

Biemelt, S., Hajirezaei, M., Hentschel, E., and Sonnewald, U. (2000). Comparative analysis of abscisic acid content and starch degradation during storage of tubers harvested from different potato varieties. Potato Research *43*, 371-382.

Bindea, G., Galon, J., and Mlecnik, B. (2013). CluePedia Cytoscape plugin: pathway insights using integrated experimental and in silico data. Bioinformatics *29*, 661-663.

Bolger, A.M., Lohse, M., and Usadel, B. (2014). Trimmomatic: a flexible trimmer for Illumina sequence data. Bioinformatics *30*, 2114-2120.

Burton, W.G. (1948). The potato. The potato.

Buskila, Y., Sela, N., Teper-Bamnolker, P., Tal, I., Shani, E., Weinstain, R., Gaba, V.,

Tam, Y., Lers, A., and Eshel, D. (2016). Stronger sink demand for metabolites supports dominance of the apical bud in etiolated growth. J Exp Bot *67*, 5495-5508. 10.1093/jxb/erw315.

Cardenas, J. (2021). Elucidate the Role of PUX1 in GA Signaling through Its Interaction with the GA Receptor GID1 to Control Cell Growth and Development (The University of Wisconsin-Madison).

Celik, H.K., Cinar, R., Yilmaz, D., Ulmeanu, M.E., Rennie, A.E., and Akinci, I. (2019). Mechanical collision simulation of potato tubers. Journal of Food Process Engineering *42*, e13078.

Chen, F.-Q., Fu, Y., Wang, D.-L., Gao, X., and Wang, L. (2007). The effect of plant growth regulators and sucrose on the micropropagation and microtuberization of Dioscorea nipponica Makino. Journal of plant growth regulation *26*, 38-45.

Chen, L., Xue, X., Yang, Y., Chen, F., Zhao, J., Wang, X., Khan, A.T., and Hu, Y. (2018). Effects of red and blue LEDs on in vitro growth and microtuberization of potato single-node cuttings. Frontiers of Agricultural Science and Engineering *5*, 197-205.

Cheng, L., Wang, Y., Liu, Y., Zhang, Q., Gao, H., and Zhang, F. (2018). Comparative proteomics illustrates the molecular mechanism of potato (Solanum tuberosum L.) tuberization inhibited by exogenous gibberellins in vitro. Physiologia plantarum *163*, 103-123.

Claassens, M.M., and Vreugdenhil, D. (2000). Is dormancy breaking of potato tubers the reverse of tuber initiation? Potato Research *43*, 347-369.

Coolbaugh, R.C., Hirano, S.S., and West, C.A. (1978). Studies on the specificity and site of action of α-cyclopropyl-α-[p-methoxyphenyl]-5-pyrimidine methyl alcohol (ancymidol), a plant growth regulator. Plant Physiology *62*, 571-576.

Dai, H., Fu, M., Yang, X., and Chen, Q. (2016). Ethylene inhibited sprouting of potato tubers by influencing the carbohydrate metabolism pathway. J Food Sci Technol *53*, 3166-3174. 10.1007/s13197-016-2290-0.

de Jong, M., Wolters-Arts, M., García-Martínez, J.L., Mariani, C., and Vriezen, W.H.

(2011). The Solanum lycopersicum AUXIN RESPONSE FACTOR 7 (SlARF7) mediates cross-talk between auxin and gibberellin signalling during tomato fruit set and development. Journal of Experimental Botany *62*, 617-626.

De Jong, M., Wolters-Arts, M., Schimmel, B.C., Stultiens, C.L., de Groot, P.F., Powers, S.J., Tikunov, Y.M., Bovy, A.G., Mariani, C., and Vriezen, W.H. (2015). Solanum lycopersicum AUXIN RESPONSE FACTOR 9 regulates cell division activity during early tomato fruit development. Journal of experimental botany *66*, 3405-3416.

Delgado-Paredes, G.E., Vásquez-Díaz, C., Esquerre-Ibañez, B., Bazán-Sernaqué, P., and Rojas-Idrogo, C. (2021). In vitro tissue culture in plants propagation and germplasm conservation of economically important species in Peru. Scientia Agropecuaria *12*, 337-349.

Denoeud, F., Aury, J.-M., Da Silva, C., Noel, B., Rogier, O., Delledonne, M., Morgante, M., Valle, G., Wincker, P., and Scarpelli, C. (2008). Annotating genomes with massive-scale RNA sequencing. Genome biology *9*, 1-12.

Destefano-Beltrán, L., Knauber, D., Huckle, L., and Suttle, J.C. (2006). Effects of postharvest storage and dormancy status on ABA content, metabolism, and expression of genes involved in ABA biosynthesis and metabolism in potato tuber tissues. Plant molecular biology *61*, 687-697.

Donnelly, D.J., Coleman, W.K., and Coleman, S.E. (2003). Potato microtuber production and performance: A review. American journal of potato research *80*, 103-115.

Dun, E.A., de Saint Germain, A., Rameau, C., and Beveridge, C.A. (2012). Antagonistic action of strigolactone and cytokinin in bud outgrowth control. Plant Physiol *158*, 487-498. 10.1104/pp.111.186783.

El-Sawy, A., Matter, M., and Girgis, N.D. (2015). Effect of Gelling Agent on in vitro tuberization of potato. Am Eur J Agric Environ Sci *15*, 1934-1939.

Ewing, E.E. (1985). Cuttings as simplified models of the potato plant. Potato physiology, 153-207.

Ezekiel, R., Singh, N., Sharma, S., and Kaur, A. (2013). Beneficial phytochemicals in potato—a review. Food Research International *50*, 487-496.

Finch-Savage, W.E., and Leubner-Metzger, G. (2006). Seed dormancy and the control of germination. New Phytol *171*, 501-523. 10.1111/j.1469-8137.2006.01787.x.

Fischer, L., Lipavska, H., Hausman, J.-F., and Opatrny, Z. (2008). Morphological and molecular characterization of a spontaneously tuberizing potato mutant: an insight into the regulatory mechanisms of tuber induction. BMC plant biology *8*, 1-13.

Flores, R., Navarro, B., Delgado, S., Serra, P., and Di Serio, F. (2020). Viroid pathogenesis: a critical appraisal of the role of RNA silencing in triggering the initial molecular lesion. FEMS Microbiol Rev *44*, 386-398. 10.1093/femsre/fuaa011.

Francis, D., and Sorrell, D.A. (2001). The interface between the cell cycle and plant growth regulators: a mini review. Plant Growth Regulation *33*, 1-12. 10.1023/A:1010762111585.

Gajdosová, S., Spíchal, L., Kamínek, M., Hoyerová, K., Novák, O., Dobrev, P.I., Galuszka, P., Klíma, P., Gaudinová, A., Zizková, E., et al. (2011). Distribution, biological activities, metabolism, and the conceivable function of cis-zeatin-type cytokinins in plants. J Exp Bot *62*, 2827-2840. 10.1093/jxb/erq457.

Gao, J., Cao, X., Shi, S., Ma, Y., Wang, K., Liu, S., Chen, D., Chen, Q., and Ma, H. (2016). Genome-wide survey of Aux/IAA gene family members in potato (Solanum tuberosum): Identification, expression analysis, and evaluation of their roles in tuber development. Biochem Biophys Res Commun *471*, 320-327. 10.1016/j.bbrc.2016.02.013.

Garcia, J.A., Azofeifa-Bolaños, J.B., Solano-Campos, F., and Orozco Rodríguez, R. (2019). Effect of two cytokinins and a growth inhibitor on the in vitro tuberization of two genotypes of Solanum tuberosum L. cvs. Atlantic and Alpha.

Gixhari, B. (2018). In vitro micropropagation of potato (Solanum tuberosum L). cultivars. Poljoprivreda i Sumarstvo *64*, 105.

Haas, B.J., Kamoun, S., Zody, M.C., Jiang, R.H., Handsaker, R.E., Cano, L.M.,

Grabherr, M., Kodira, C.D., Raffaele, S., and Torto-Alalibo, T. (2009). Genome sequence and analysis of the Irish potato famine pathogen Phytophthora infestans. Nature *461*, 393-398.

Haider, M.W., Nafeesa, M., Amina, M., Asadb, H.U., and Ahmad, I. (2021). Physiology of tuber dormancy and its mechanism of release in potato. J Hortic Sci Technol *4*, 13-21.

Hammond, R.W. (2022). Detection and characterization of viroids via biological assays on herbaceous hosts. Viroids: Methods and Protocols, 23-28.

Han, B., Paek, K., and Choi, J. (1994). Prevention of vitrification of Gypsophila paniculata regenerated in vitro.

Hardigan, M.A., Crisovan, E., Hamilton, J.P., Kim, J., Laimbeer, P., Leisner, C.P., Manrique-Carpintero, N.C., Newton, L., Pham, G.M., and Vaillancourt, B. (2016). Genome reduction uncovers a large dispensable genome and adaptive role for copy number variation in asexually propagated Solanum tuberosum. The Plant Cell *28*, 388-405.

Hartmann, A., Senning, M., Hedden, P., Sonnewald, U., and Sonnewald, S. (2011). Reactivation of meristem activity and sprout growth in potato tubers require both cytokinin and gibberellin. Plant physiology *155*, 776-796.

Hemberg, T. (1970). The action of some cytokinins on the rest-period and the content of acid growth-inhibiting substances in potato. Physiologia Plantarum *23*, 850-858.

Hemberg, T. (1985). Potato rest. Potato physiology, 353-388.

Jefferies, R., and Mackerron, D. (1987). Effect of second growth on the quality of tubers as seed in the cultivar Record. Potato Research *30*, 337-340.

Joshi, M., Fogelman, E., Belausov, E., and Ginzberg, I. (2016). Potato root system development and factors that determine its architecture. Journal of plant physiology *205*, 113-123.

Kefi, S., Meagher, M., Read, P., and Pavlista, A. (1997). Effects of Different Cytokinin-like Compounds on Invertase Activity during Potato in Vitro Tuberization. HortScience

32, 515B-515.

Kim, D., Paggi, J.M., Park, C., Bennett, C., and Salzberg, S.L. (2019). Graph-based genome alignment and genotyping with HISAT2 and HISAT-genotype. Nat Biotechnol *37*, 907-915. 10.1038/s41587-019-0201-4.

Kolachevskaya, O., Lomin, S.N., Kojima, M., Getman, I.A., Sergeeva, L., Sakakibara, H., and Romanov, G. (2019a). Tuber-specific expression of two gibberellin oxidase transgenes from Arabidopsis regulates over wide ranges the potato tuber formation. Russian journal of plant physiology *66*, 984-991.

Kolachevskaya, O.O., Lomin, S.N., Arkhipov, D.V., and Romanov, G.A. (2019b). Auxins in potato: molecular aspects and emerging roles in tuber formation and stress resistance. Plant Cell Rep *38*, 681-698. 10.1007/s00299-019-02395-0.

Kolachevskaya, O.O., Sergeeva, L.I., Floková, K., Getman, I.A., Lomin, S.N., Alekseeva, V.V., Rukavtsova, E.B., Buryanov, Y.I., and Romanov, G.A. (2017). Auxin synthesis gene tms1 driven by tuber-specific promoter alters hormonal status of transgenic potato plants and their responses to exogenous phytohormones. Plant Cell Rep *36*, 419-435. 10.1007/s00299-016-2091-y.

Kumar, G.N.M., and Knowles, N.R. (1993). Involvement of auxin in the loss of apical dominance and plant growth potential accompanying aging of potato seed tubers. Canadian Journal of Botany *71*, 541-550. 10.1139/b93-060.

Langfelder, P., and Horvath, S. (2008). WGCNA: an R package for weighted correlation network analysis. BMC Bioinformatics *9*, 559. 10.1186/1471-2105-9-559.

Leclerc, Y. (1993). The production and utilization of potato microtubers.

Liu, H., Zhang, Y., Yang, F., Qi, X., Ahmad, H., Wu, C., and Cheng, Z. (2019). Effect of the mode and time of gibberellic acid treatment on plant architecture and bulb structure in garlic (Allium sativum L.). Scientia Horticulturae *257*, 108723.

Liu, S., Zhang, Y., Feng, Q., Qin, L., Pan, C., Lamin-Samu, A.T., and Lu, G. (2018). Tomato AUXIN RESPONSE FACTOR 5 regulates fruit set and development via the mediation of auxin and gibberellin signaling. Scientific Reports *8*, 2971.

10.1038/s41598-018-21315-y.

Livak, K.J., and Schmittgen, T.D. (2001). Analysis of relative gene expression data using real-time quantitative PCR and the 2(-Delta Delta C(T)) Method. Methods *25*, 402-408. 10.1006/meth.2001.1262.

Lomin, S.N., Myakushina, Y.A., Kolachevskaya, O.O., Getman, I.A., Savelieva, E.M., Arkhipov, D.V., Deigraf, S.V., and Romanov, G.A. (2020). Global View on the Cytokinin Regulatory System in Potato. Front Plant Sci *11*, 613624. 10.3389/fpls.2020.613624.

Love, M.I., Huber, W., and Anders, S. (2014). Moderated estimation of fold change and dispersion for RNA-seq data with DESeq2. Genome Biol *15*, 550. 10.1186/s13059-014-0550-8.

Mardis, E.R. (2008). Next-generation DNA sequencing methods. Annu. Rev. Genomics Hum. Genet. *9*, 387-402.

Marguerat, S., and Bähler, J. (2010). RNA-seq: from technology to biology. Cellular and molecular life sciences *67*, 569-579.

Martin, M. (2011). Cutadapt removes adapter sequences from high-throughput sequencing reads. EMBnet. journal *17*, 10-12.

Martin, R.C., Mok, M.C., Habben, J.E., and Mok, D.W. (2001). A maize cytokinin gene encoding an O-glucosyltransferase specific to cis-zeatin. Proc Natl Acad Sci U S A *98*, 5922-5926. 10.1073/pnas.101128798.

Menzel, C. (1980). Tuberization in potato at high temperatures: responses to gibberellin and growth inhibitors. Annals of Botany *46*, 259-265.

Metzker, M.L. (2010). Sequencing technologies—the next generation. Nature reviews genetics *11*, 31-46.

Morais, T., Asmar, S., Silva, H., Luz, J., and Melo, B. (2018). Application of tissue culture techniques in Potato. Bioscience Journal *34*, 952-969. 10.14393/BJ-v34n1a2018-38775.

Morozova, O., and Marra, M.A. (2008). Applications of next-generation sequencing technologies in functional genomics. Genomics *92*, 255-264.

Murashige, T., and Skoog, F. (1962). A revised medium for rapid growth and bio assays with tobacco tissue cultures. Physiologia plantarum *15*, 473-497.

Natarajan, B., Kalsi, H.S., Godbole, P., Malankar, N., Thiagarayaselvam, A., Siddappa, S., Thulasiram, H.V., Chakrabarti, S.K., and Banerjee, A.K. (2018). MiRNA160 is associated with local defense and systemic acquired resistance against Phytophthora infestans infection in potato. J Exp Bot *69*, 2023-2036. 10.1093/jxb/ery025.

Née, G., Kramer, K., Nakabayashi, K., Yuan, B., Xiang, Y., Miatton, E., Finkemeier, I., and Soppe, W.J.J. (2017). DELAY OF GERMINATION1 requires PP2C phosphatases of the ABA signalling pathway to control seed dormancy. Nat Commun *8*, 72. 10.1038/s41467-017-00113-6.

Nikitin, M., Statsyuk, N., Frantsuzov, P., Dzhavakhiya, V., and Golikov, A. (2018). Matrix approach to the simultaneous detection of multiple potato pathogens by real-time PCR. Journal of applied microbiology *124*, 797-809.

Nishimura, N., Yoshida, T., Kitahata, N., Asami, T., Shinozaki, K., and Hirayama, T. (2007). ABA-Hypersensitive Germination1 encodes a protein phosphatase 2C, an essential component of abscisic acid signaling in Arabidopsis seed. Plant J *50*, 935-949. 10.1111/j.1365-313X.2007.03107.x.

Nuraini, A., Mubarok, S., and Hamdani, J. (2018). Effects of application time and concentration of paclobutrazol on the growth and yield of potato seed of G2 cultivar medians at medium altitude. Journal of Agronomy *17*, 169-173.

Park, S.Y., Fung, P., Nishimura, N., Jensen, D.R., Fujii, H., Zhao, Y., Lumba, S., Santiago, J., Rodrigues, A., Chow, T.F., et al. (2009). Abscisic acid inhibits type 2C protein phosphatases via the PYR/PYL family of START proteins. Science *324*, 1068-1071. 10.1126/science.1173041.

Peivastegan, B., Hadizadeh, I., Nykyri, J., Nielsen, K.L., Somervuo, P., Sipari, N., Tran, C., and Pirhonen, M. (2019). Effect of wet storage conditions on potato tuber transcriptome, phytohormones and growth. BMC plant biology *19*, 1-18.

Rappaport, L. (1956). Growth regulating metabolites: gibberellin compounds derived from rice disease-producing fungus exhibit powerful plant growth regulating properties. California Agriculture *10*, 4-11.

Raudvere, U., Kolberg, L., Kuzmin, I., Arak, T., Adler, P., Peterson, H., and Vilo, J. (2019). g: Profiler: a web server for functional enrichment analysis and conversions of gene lists (2019 update). Nucleic acids research *47*, W191-W198.

Sachs, T., and Thimann, K.V. (1967). The Role of Auxins and Cytokinins in the Release of Buds From Dominance. American Journal of Botany *54*, 136-144. 10.2307/2440896.

Salam, B.B., Barbier, F., Danieli, R., Teper-Bamnolker, P., Ziv, C., Spíchal, L., Aruchamy, K., Shnaider, Y., Leibman, D., Shaya, F., et al. (2021). Sucrose promotes stem branching through cytokinin. Plant Physiol *185*, 1708-1721. 10.1093/plphys/kiab003.

Sharma, S.K., Bolser, D., de Boer, J., Sønderkær, M., Amoros, W., Carboni, M.F., D'Ambrosio, J.M., de la Cruz, G., Di Genova, A., Douches, D.S., et al. (2013). Construction of Reference Chromosome-Scale Pseudomolecules for Potato: Integrating the Potato Genome with Genetic and Physical Maps. G3 Genes|Genomes|Genetics *3*, 2031-2047. 10.1534/g3.113.007153.

Sherman, B.T., Hao, M., Qiu, J., Jiao, X., Baseler, M.W., Lane, H.C., Imamichi, T., and Chang, W. (2022). DAVID: a web server for functional enrichment analysis and functional annotation of gene lists (2021 update). Nucleic acids research *50*, W216-W221.

Shive Jr, J.B., and Sisler, H.D. (1976). Effects of ancymidol (a growth retardant) and triarimol (a fungicide) on the growth, sterols, and gibberellins of Phaseolus vulgaris (L.). Plant physiology *57*, 640-644.

Shumate, A., Wong, B., Pertea, G., and Pertea, M. (2022). Improved transcriptome assembly using a hybrid of long and short reads with StringTie. PLoS Comput Biol *18*, e1009730. 10.1371/journal.pcbi.1009730.

Siregar, L.A.M., Turnip, L., and Damanik, I.R. (2021). Immersion in 6-Benzylaminopurine for Dormancy Release and Initiation of Potato Sprouts at Various

Tuber Weight and Storage Duration. Indonesian Journal of Agronomy *49*, 60-67.

Skalický, V., Kubeš, M., Napier, R., and Novák, O. (2018). Auxins and Cytokinins-The Role of Subcellular Organization on Homeostasis. Int J Mol Sci *19*. 10.3390/ijms19103115.

Šmehilová, M., Dobrůšková, J., Novák, O., Takáč, T., and Galuszka, P. (2016). Cytokinin-Specific Glycosyltransferases Possess Different Roles in Cytokinin Homeostasis Maintenance. Front Plant Sci *7*, 1264. 10.3389/fpls.2016.01264.

Soma, F., Takahashi, F., Suzuki, T., Shinozaki, K., and Yamaguchi-Shinozaki, K. (2020). Plant Raf-like kinases regulate the mRNA population upstream of ABA-unresponsive SnRK2 kinases under drought stress. Nat Commun *11*, 1373. 10.1038/s41467-020-15239-3.

Sonnewald, S., and Sonnewald, U. (2014). Regulation of potato tuber sprouting. Planta *239*, 27-38. 10.1007/s00425-013-1968-z.

Sorce, C., Lombardi, L., Giorgetti, L., Parisi, B., Ranalli, P., and Lorenzi, R. (2009). Indoleacetic acid concentration and metabolism changes during bud development in tubers of two potato (Solanum tuberosum) cultivars. Journal of Plant Physiology *166*, 1023-1033. https://doi.org/10.1016/j.jplph.2008.12.003.

Stark, R., Grzelak, M., and Hadfield, J. (2019). RNA sequencing: the teenage years. Nature Reviews Genetics *20*, 631-656. 10.1038/s41576-019-0150-2.

Struik, P.C. (2007). Above-ground and below-ground plant development. In Potato biology and biotechnology, (Elsevier), pp. 219-236.

Suttle, J.C. (2003). Auxin-induced sprout growth inhibition: Role of endogenous ethylene. American Journal of Potato Research *80*, 303-309. 10.1007/BF02854314.

Suttle, J.C. (2004a). Involvement of endogenous gibberellins in potato tuber dormancy and early sprout growth: a critical assessment. J Plant Physiol *161*, 157-164. 10.1078/0176-1617-01222.

Suttle, J.C. (2004b). Physiological regulation of potato tuber dormancy. American Journal of Potato Research *81*, 253-262.

Suttle, J.C. (2007). Dormancy and sprouting. Potato biology and biotechnology, 287-309.

Suttle, J.C. (2008). Effects of Synthetic Phenylurea and Nitroguanidine Cytokinins on Dormancy Break and Sprout Growth in Russet Burbank Minitubers. American Journal of Potato Research *85*, 121-128. 10.1007/s12230-008-9002-x.

Suttle, J.C., and Banowetz, G. (2000). Changes in cis-zeatin and cis-zeatin riboside levels and biological activity during potato tuber dormancy. Physiologia Plantarum *109*, 68-74.

Takei, K., Sakakibara, H., and Sugiyama, T. (2001). Identification of genes encoding adenylate isopentenyltransferase, a cytokinin biosynthesis enzyme, in Arabidopsis thaliana. J Biol Chem *276*, 26405-26410. 10.1074/jbc.M102130200.

Takei, K., Yamaya, T., and Sakakibara, H. (2004). Arabidopsis CYP735A1 and CYP735A2 encode cytokinin hydroxylases that catalyze the biosynthesis of trans-Zeatin. J Biol Chem *279*, 41866-41872. 10.1074/jbc.M406337200.

Tanaka, M., Takei, K., Kojima, M., Sakakibara, H., and Mori, H. (2006). Auxin controls local cytokinin biosynthesis in the nodal stem in apical dominance. Plant J *45*, 1028-1036. 10.1111/j.1365-313X.2006.02656.x.

Tovar, P. (1985). Induction and use of in vitro potato tubers. CIP circular *13*, 1-5.

Tuan, P.A., Kumar, R., Rehal, P.K., Toora, P.K., and Ayele, B.T. (2018). Molecular Mechanisms Underlying Abscisic Acid/Gibberellin Balance in the Control of Seed Dormancy and Germination in Cereals. Front Plant Sci *9*, 668. 10.3389/fpls.2018.00668.

Turnbull, C., and Hanke, D. (1985a). The control of bud dormancy in potato tubers. Measurement of the seasonal pattern of changing concentrations of zeatin-cytokinins. Planta *165*, 366-376.

Turnbull, C.G.N., and Hanke, D.E. (1985b). The control of bud dormancy in potato tubers. Planta *165*, 359-365. 10.1007/BF00392233.

Valencia-Lozano, E., Herrera-Isidrón, L., Flores-López, J.A., Recoder-Meléndez, O.S.,

Barraza, A., and Cabrera-Ponce, J.L. (2022). Solanum tuberosum Microtuber Development under Darkness Unveiled through RNAseq Transcriptomic Analysis. International Journal of Molecular Sciences *23*, 13835.

Vennapusa, A.R., Somayanda, I.M., Doherty, C.J., and Jagadish, S.V.K. (2020). A universal method for high-quality RNA extraction from plant tissues rich in starch, proteins and fiber. Sci Rep *10*, 16887. 10.1038/s41598-020-73958-5.

Voelkerding, K.V., Dames, S.A., and Durtschi, J.D. (2009). Next-generation sequencing: from basic research to diagnostics. Clinical chemistry *55*, 641-658.

Wang, J., Ma, X.M., Kojima, M., Sakakibara, H., and Hou, B.K. (2011). N-glucosyltransferase UGT76C2 is involved in cytokinin homeostasis and cytokinin response in Arabidopsis thaliana. Plant Cell Physiol *52*, 2200-2213. 10.1093/pcp/pcr152.

Wang, K., Zhang, N., Fu, X., Zhang, H., Liu, S., Pu, X., Wang, X., and Si, H. (2022). StTCP15 regulates potato tuber sprouting by modulating the dynamic balance between abscisic acid and gibberellic acid. Front Plant Sci *13*, 1009552. 10.3389/fpls.2022.1009552.

Wang, P.-j., and Hu, C.-y. (1985). Potato tissue culture and its applications in agriculture. Potato physiology, 503-577.

Wang, R.L., Biales, A., Bencic, D., Lattier, D., Kostich, M., Villeneuve, D., Ankley, G.T., Lazorchak, J., and Toth, G. (2008). DNA microarray application in ecotoxicology: experimental design, microarray scanning, and factors affecting transcriptional profiles in a small fish species. Environmental Toxicology and Chemistry: An International Journal *27*, 652-663.

Wang, X., Lin, S., Liu, D., Gan, L., McAvoy, R., Ding, J., and Li, Y. (2020). Evolution and roles of cytokinin genes in angiosperms 1: Do ancient IPTs play housekeeping while non-ancient IPTs play regulatory roles? Horticulture Research *7*, 28. 10.1038/s41438-019-0211-x.

Werner, T., Köllmer, I., Bartrina, I., Holst, K., and Schmülling, T. (2006). New insights into the biology of cytokinin degradation. Plant Biol (Stuttg) *8*, 371-381. 10.1055/s-

2006-923928.

Woolley, D., and Wareing, P. (1972). The interaction between growth promoters in apical dominance. New phytologist *71*, 781-793.

Wu, T., Hu, E., Xu, S., Chen, M., Guo, P., Dai, Z., Feng, T., Zhou, L., Tang, W., and Zhan, L. (2021). clusterProfiler 4.0: A universal enrichment tool for interpreting omics data. The Innovation *2*, 100141.

Xu, X., Pan, S., Cheng, S., Zhang, B., Mu, D., Ni, P., Zhang, G., Yang, S., Li, R., and Wang, J. (2011a). B., de Boer. J., Borm, T., Kloosterman, B., van Eck, H., Datema, E., Hekkert, BTL, Goverse, A., van Ham, RCHJ, & Visser, RGF, 189-195.

Xu, X., Pan, S., Cheng, S., Zhang, B., Mu, D., Ni, P., Zhang, G., Yang, S., Li, R., Wang, J., et al. (2011b). Genome sequence and analysis of the tuber crop potato. Nature *475*, 189-195. 10.1038/nature10158.

Xu, X., van Lammeren, A.A., Vermeer, E., and Vreugdenhil, D. (1998a). The role of gibberellin, abscisic acid, and sucrose in the regulation of potato tuber formation in vitro. Plant Physiol *117*, 575-584. 10.1104/pp.117.2.575.

Xu, X., Vreugdenhil, D., and Lammeren, A.A.v. (1998b). Cell division and cell enlargement during potato tuber formation. Journal of Experimental Botany *49*, 573-582.

Yu, W.-C. (1998). Production of potato microtubers in bioreactors (The University of Wisconsin-Madison).

Zhang, H., Fen, X., Yu, W., Hu, H.-h., and Dai, X.-f. (2017). Progress of potato staple food research and industry development in China. Journal of integrative agriculture *16*, 2924-2932.

Zhang, X., Campbell, R., Ducreux, L.J., Morris, J., Hedley, P.E., Mellado-Ortega, E., Roberts, A.G., Stephens, J., Bryan, G.J., and Torrance, L. (2020). TERMINAL FLOWER-1/CENTRORADIALIS inhibits tuberisation via protein interaction with the tuberigen activation complex. The Plant Journal *103*, 2263-2278.

Zhang, X., Fujino, K., and Shimura, H. (2023). Transcriptomic Analyses Reveal the

Role of Cytokinin and the Nodal Stem in Microtuber Sprouting in Potato (Solanum tuberosum L.). Int J Mol Sci *24*. 10.3390/ijms242417534.

Zhao, H., Nie, K., Zhou, H., Yan, X., Zhan, Q., Zheng, Y., and Song, C.P. (2020). ABI5 modulates seed germination via feedback regulation of the expression of the PYR/PYL/RCAR ABA receptor genes. New Phytol *228*, 596-608. 10.1111/nph.16713.

Zhuang, L., Ge, Y., Wang, J., Yu, J., Yang, Z., and Huang, B. (2019). Gibberellic acid inhibition of tillering in tall fescue involving crosstalks with cytokinins and transcriptional regulation of genes controlling axillary bud outgrowth. Plant Sci *287*, 110168. 10.1016/j.plantsci.2019.110168.